

Electron Emissive Devices

A materials science approach to photocathodes and secondary emitters
(with a bit of diamond thrown in at the end for fun)

John Smedley

Brookhaven National Laboratory

Feb. 24, 2016

Overview

Brief intro to 3-step model as it applies to semiconductors

In situ materials analysis during cathode formation

How better diagnostics might lead to better cathodes

How to grow smoother cathodes (and why you might want to)

Secondary electron emission: Diamond, SiN and Topsy

Diamond as a sensing material for detectors and beam diagnostics

Reference Material

Some of this talk comes from a course on Cathode Physics Matt Poelker and I taught at the US Particle Accelerator School

http://uspas.fnal.gov/materials/12UTA/UTA_Cathode.shtml

Modern Theory and Applications of Photocathodes

W.E. Spicer & A. Herrera-Gómez

SAC-PUB-6306 (1993)

Great Surface Science Resource:

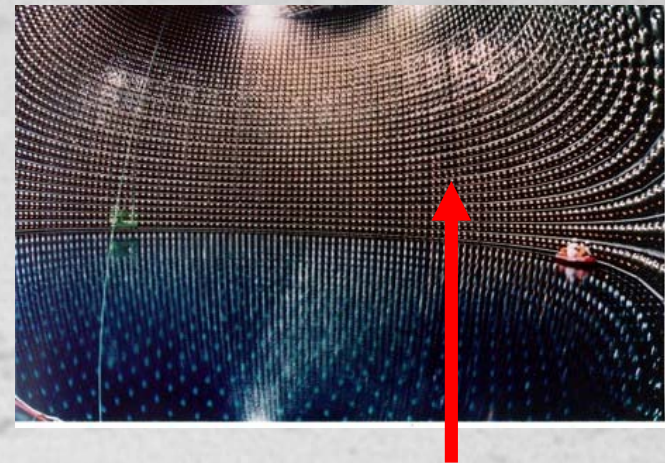
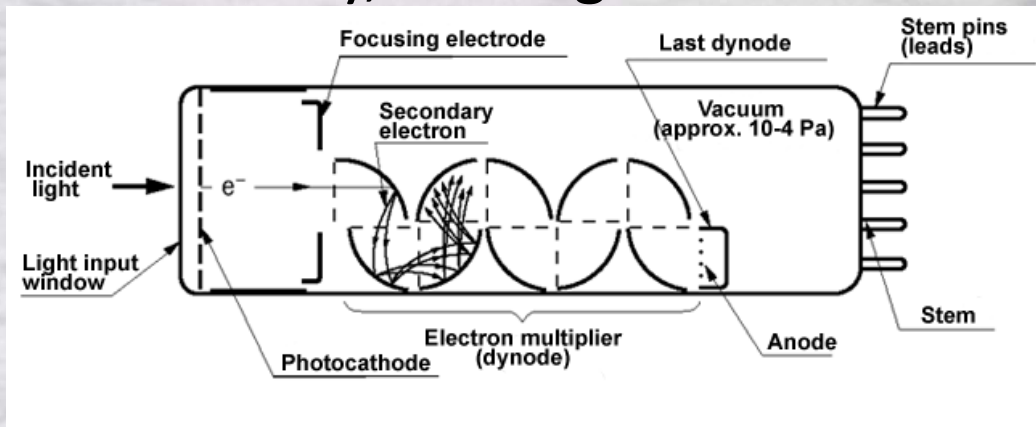
<http://www.philiphofmann.net/surflec3/index.html>

What is a photocathode?

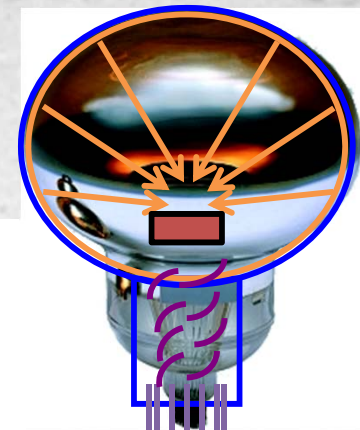
A surface that emits electrons when illuminated (Go Einstein!)

What are they used for?

Traditionally, in image intensifiers and photodetectors/PMT



Super-Kamiokande
Neutrino Detector
11,200 20"
 K_2CsSb PMTs



What is a photocathode?

A surface that emits electrons when illuminated (Go Einstein!)

What are they used for?

Traditionally, in image intensifiers and photodetectors/PMT

More recently also as electron sources for accelerators

- Allow control of the spatial and temporal profile of the beam

- Produce a “Brighter” electron beam than can be achieved from other sources

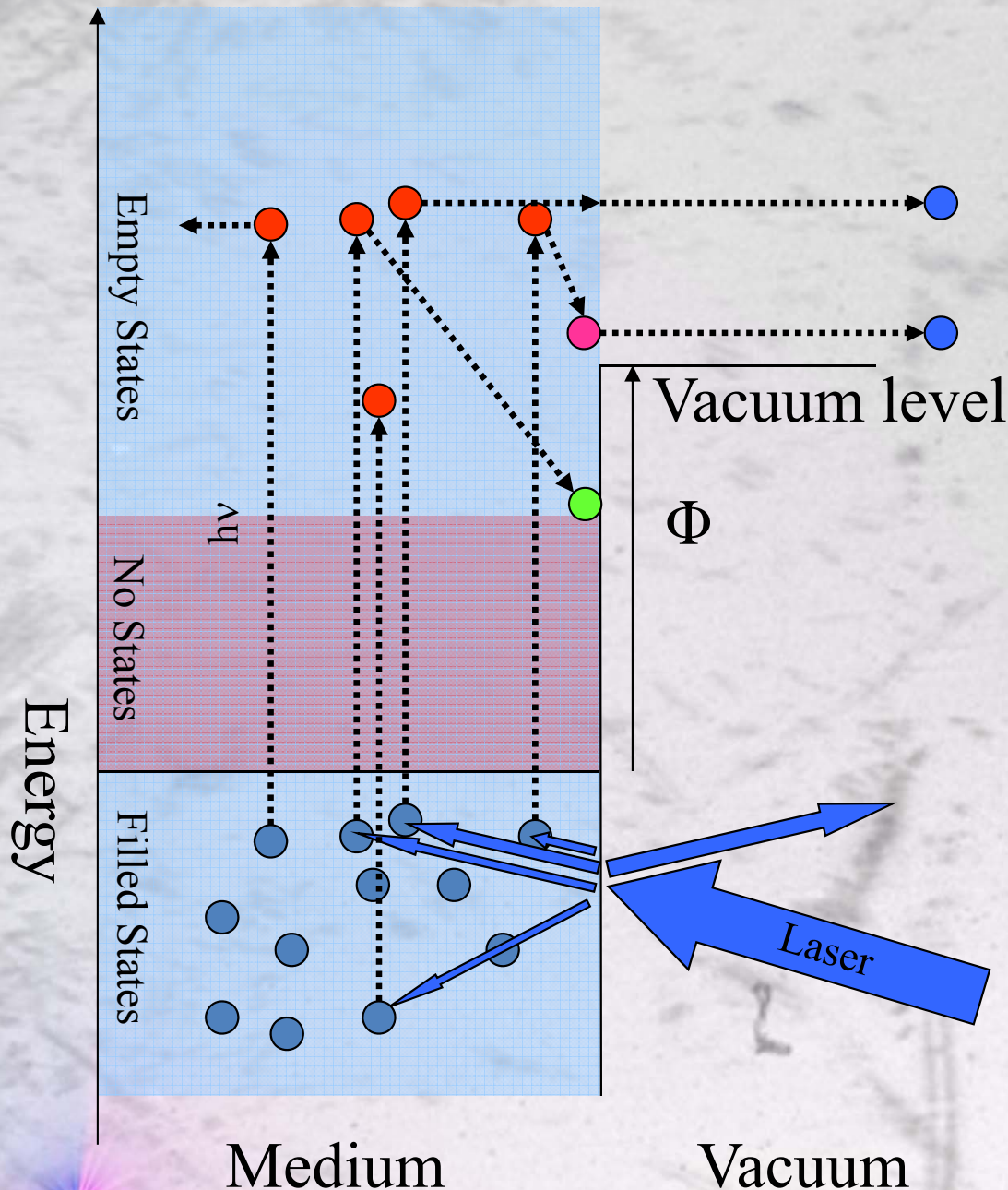
What makes a good photocathode?

- Quantum Efficiency, lifetime, fast temporal response

- Correlation of emitted electrons (low beam “temperature”, or emittance), high current, low dark current, spin polarization

Important applications to other fields – Photovoltaics, PET imaging

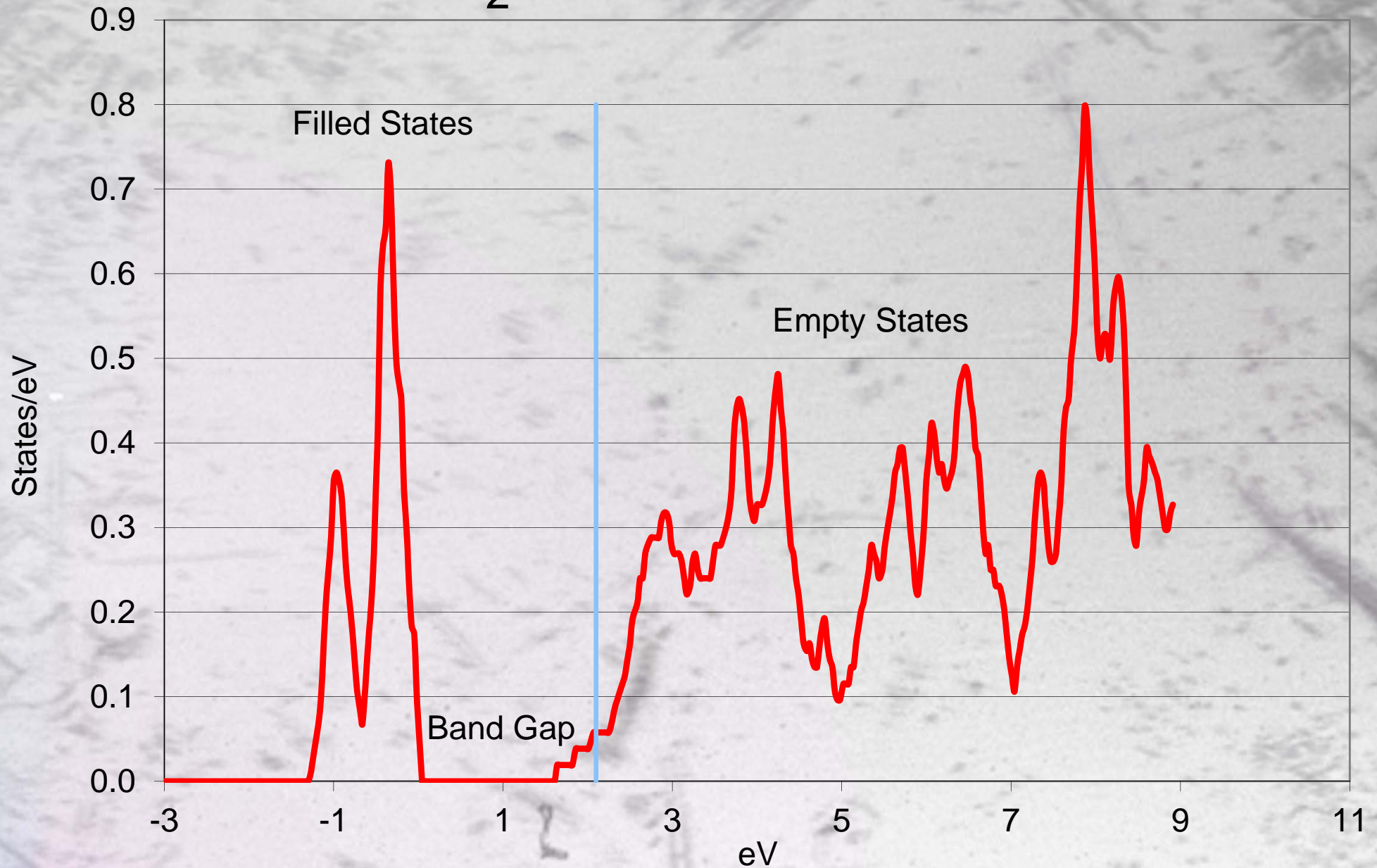
Three Step Model of Photoemission - Semiconductors



- 1) Excitation of e^-
Reflection, Transmission
Energy distribution of excited e^-
- 2) Transit to the Surface
 e^- -phonon scattering
 e^- -defect scattering
 e^-e^- scattering
Random Walk
- 3) Escape surface
Overcome Workfunction
Multiple tries

Need to account for Random Walk in cathode suggests Monte Carlo modeling

K_2CsSb DOS



A.R.H.F. Ettema and R.A. de Groot, Phys. Rev. B **66**, 115102 (2002)

Parameters, and how to affect them

Increasing the electron MFP will improve the QE. Phonon scattering cannot be removed, but a more perfect crystal can reduce defect and impurity scattering:

$$\frac{1}{\lambda_{MFP}} = \frac{1}{\lambda_{el-el}} + \frac{1}{\lambda_{ap}} + \frac{1}{\lambda_{ap,ems}} - \frac{1}{\lambda_{ap,abs}} + \frac{1}{\lambda_{impurity}} + \frac{1}{\lambda_{defect}} + \frac{1}{\lambda_{boundary}}$$

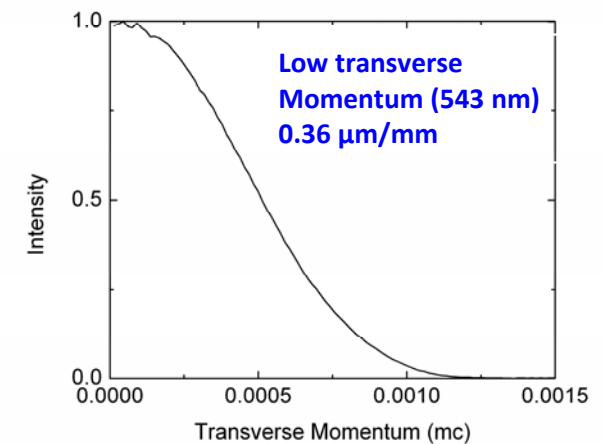
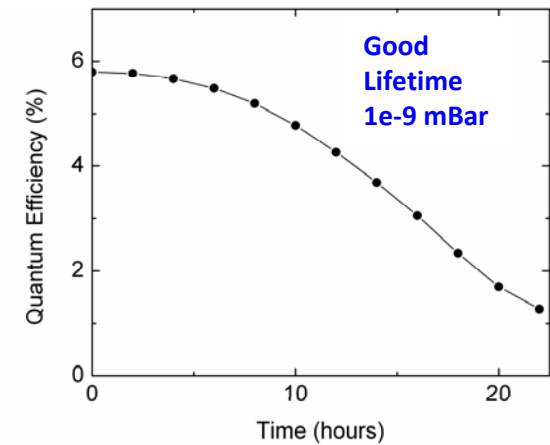
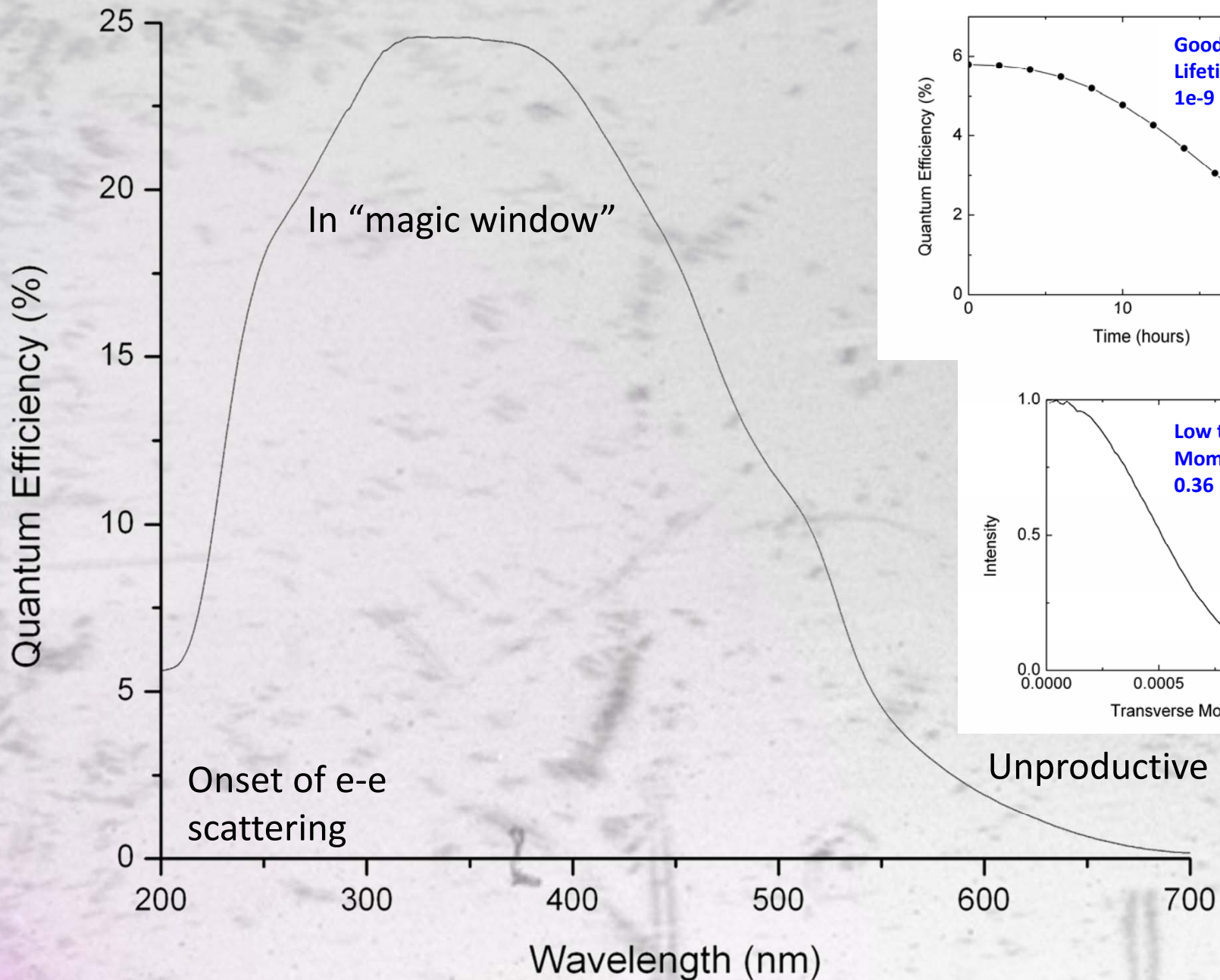
Control of surface roughness is critical to minimizing the intrinsic emittance – epitaxial growth?

A question to consider: Why can CsI (another ionic crystal, PEA cathode) achieve QE>80%?

T.H. Di Stefano and W.E. Spicer, Phys. Rev. B **7**, 1554 (1973)

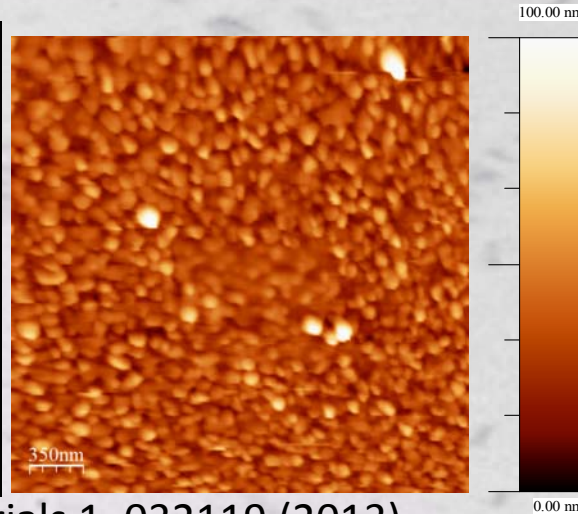
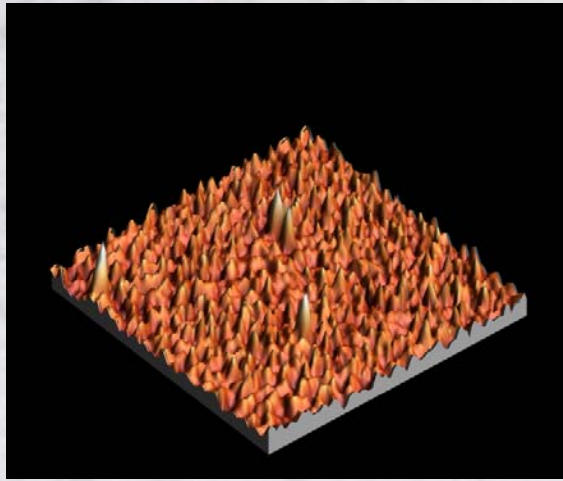
Large band gap and small electron affinity play a role, but, so does crystal quality.

K_2CsSb : A cathode with excellent characteristics for accelerators



Traditional Sequential Deposition of K_2CsSb

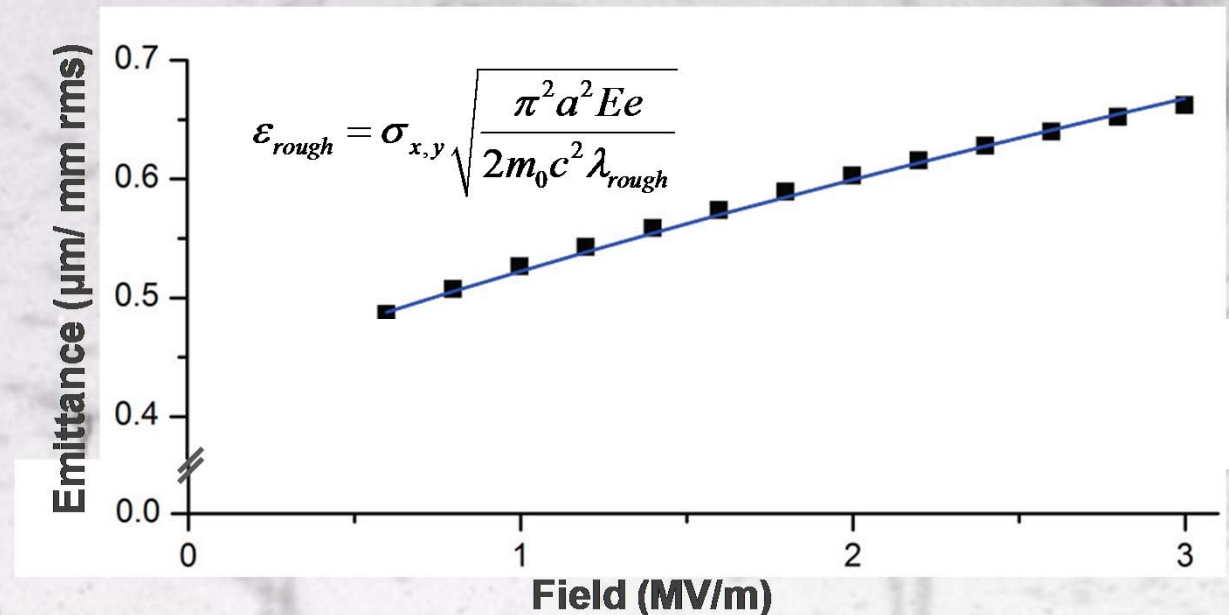
High QE and Rough Surface



25 nm roughness,
100 nm spatial period

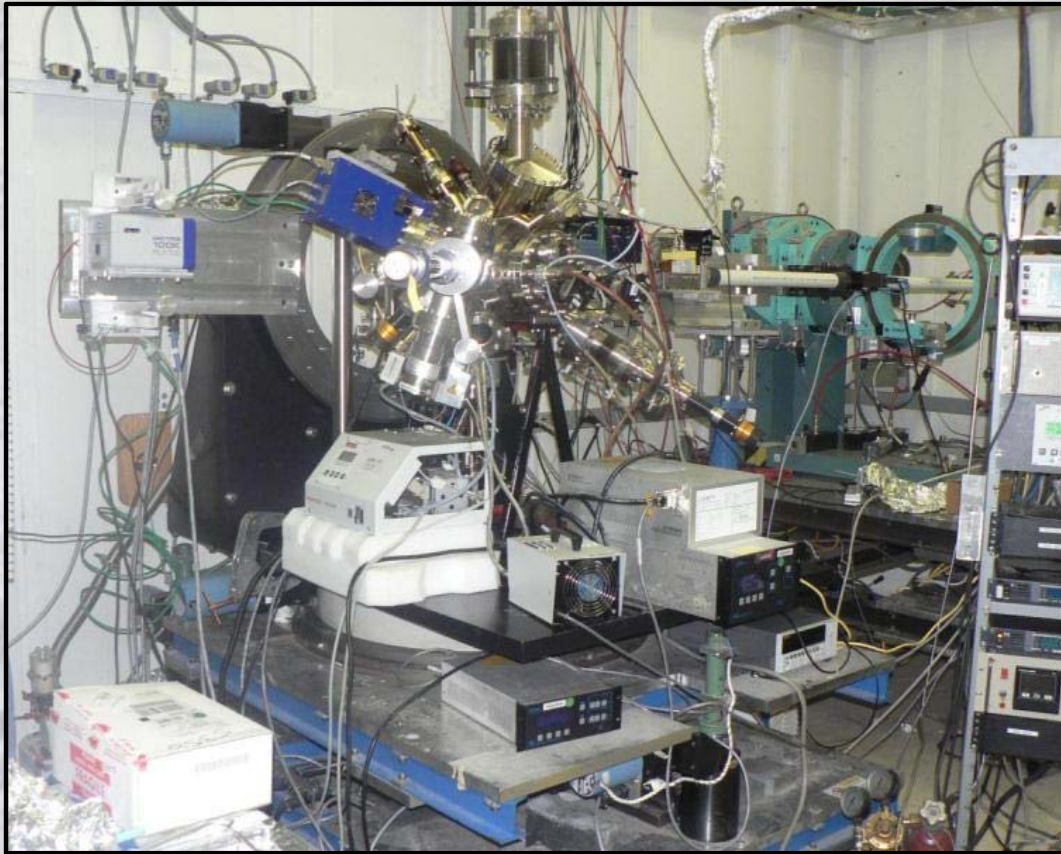
S. Schubert et al., APL Materials 1, 032119 (2013)

Emittance vs field
measured with
Momentatron, 532 nm light



T. Vecchione, et al, Proc. of IPAC12, 655 (2012)

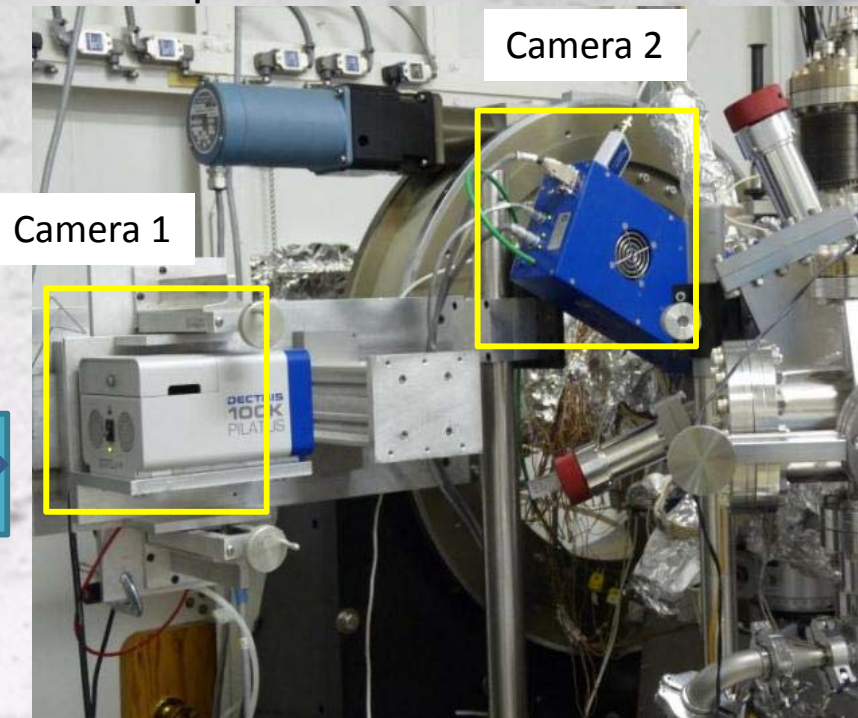
In operando analysis during growth (setup at NSLS/X21 & CHESS G3)



- UHV system (0.2 nTorr base pressure)
- Residual Gas Analyzer (RGA)
- Heating/cooling substrate/cathode
- Load lock
 - fast exchange of substrates
 - gun transfer
- Horizontal deposition of Sb, K and Cs.
- Sputter Deposition!

Two 2D detectors (Pilatus 100K) ➡

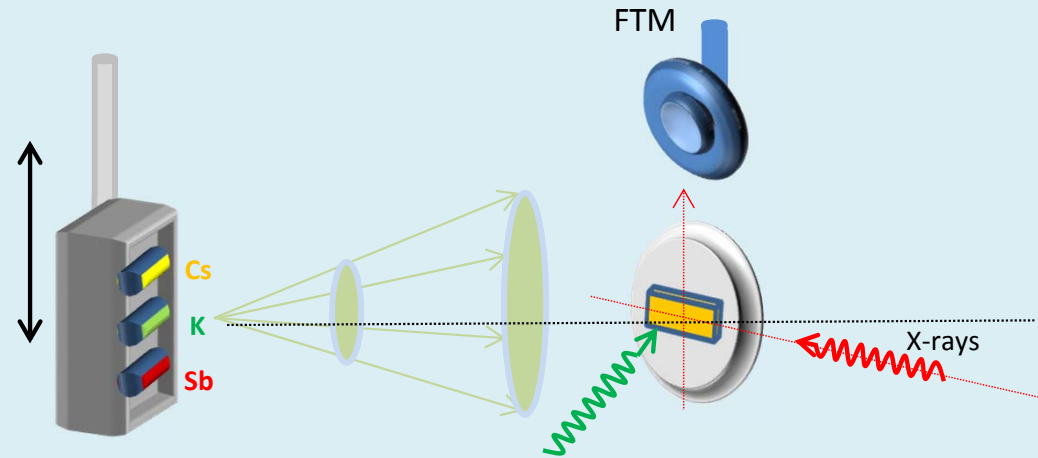
XRF, XRD, XRR, GISAXS, QE



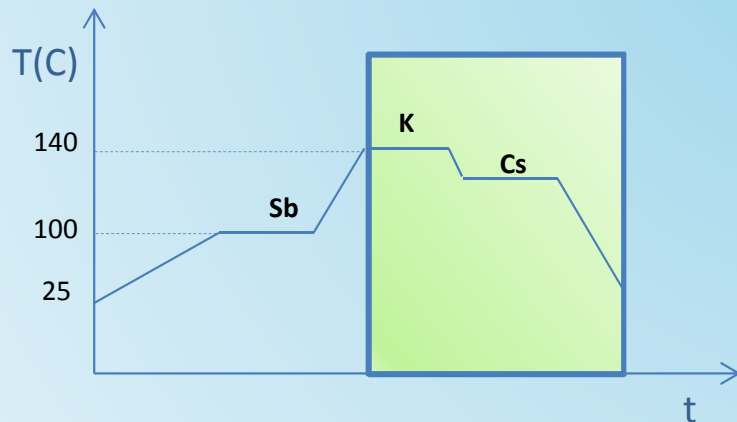
Experimental set up: K_2CsSb cathode growth

Horizontal evaporation of three sources:

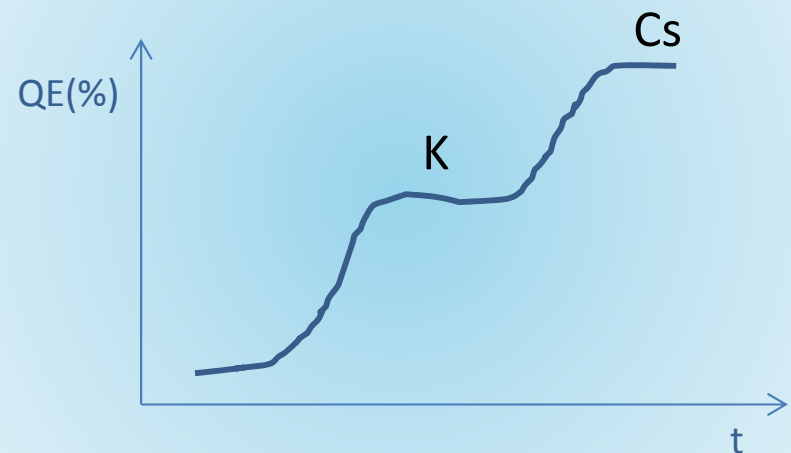
$P=1 \times 10^{-10}$ mbar



Recipe:



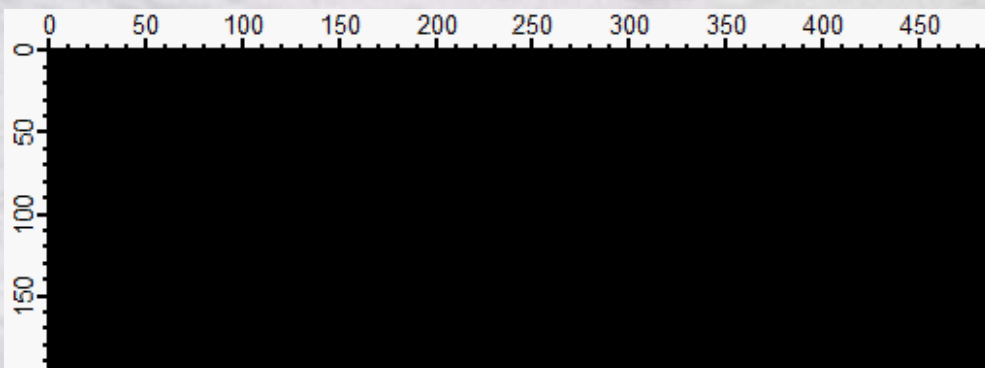
QE during growth (532 nm laser)



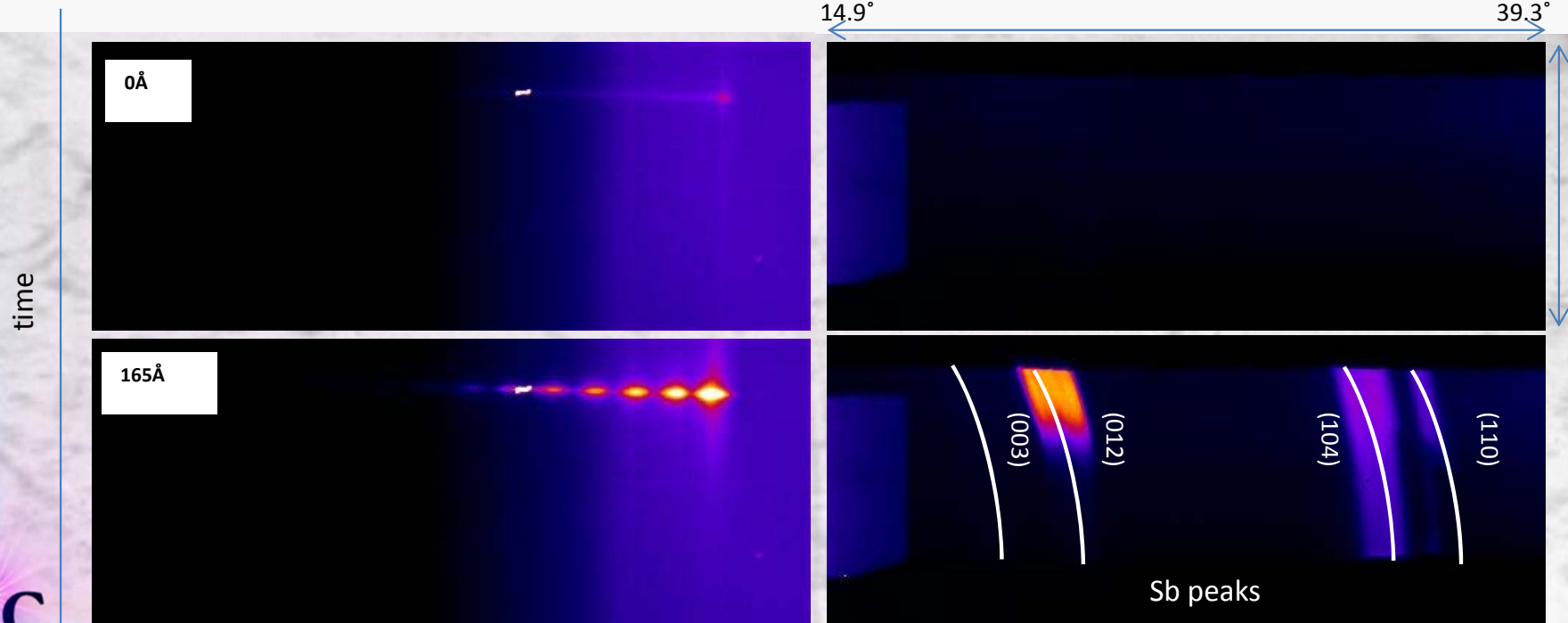
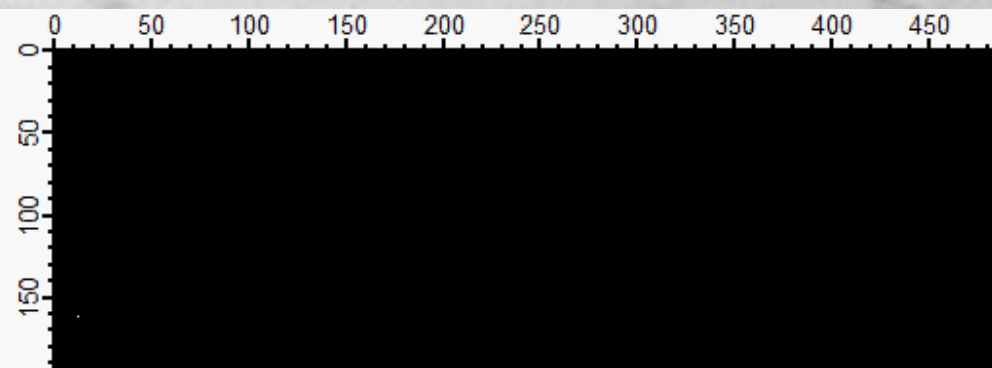
Simultaneously Acquire XRD and GISAXS

- Understanding reaction dynamics through crystalline phase evolution
- Map the thickness and roughness evolution of the cathode
- Is there a correlation between reactivity, QE and roughness?

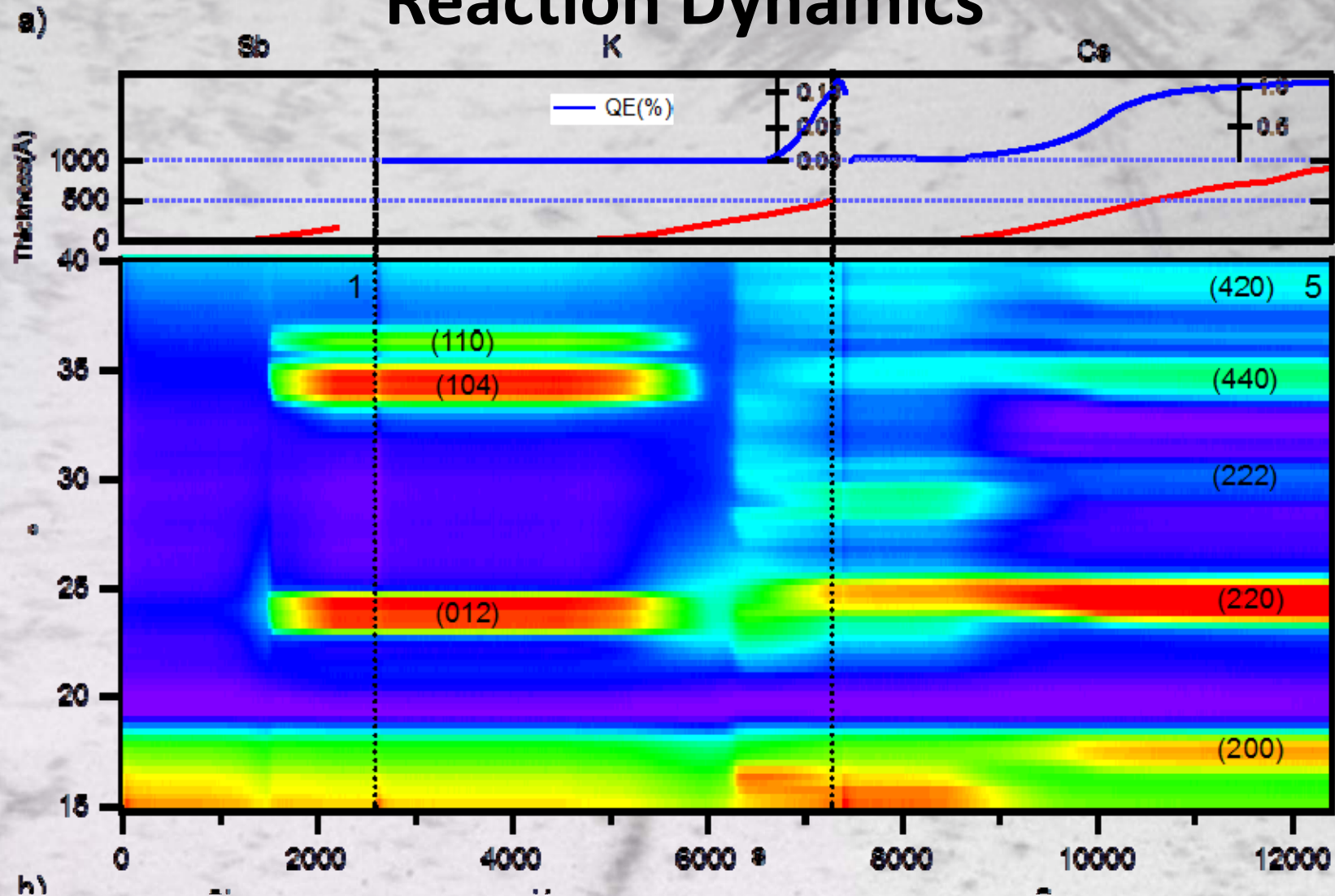
Camera 1: GISAXS & XRR



Camera 2: WAXS



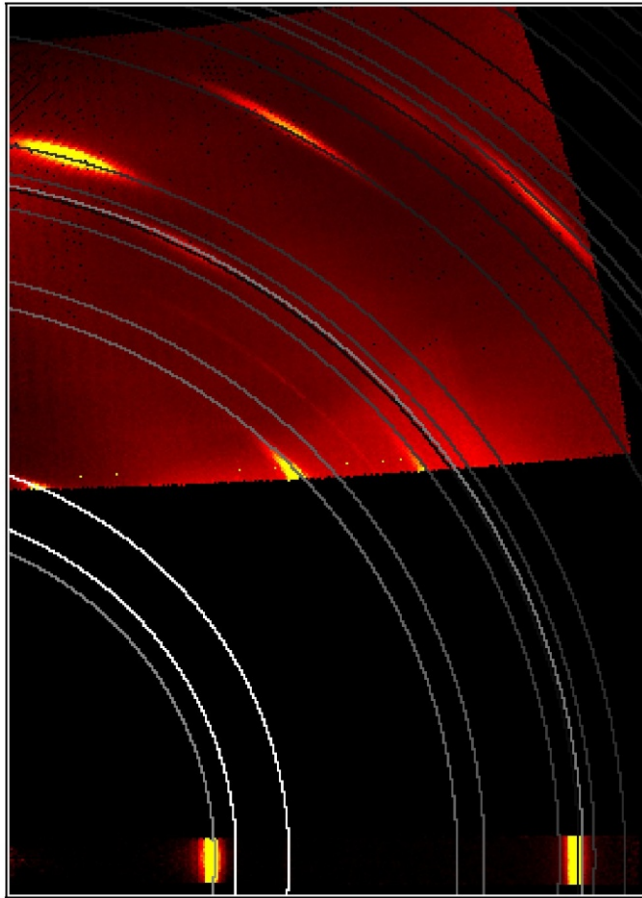
Reaction Dynamics



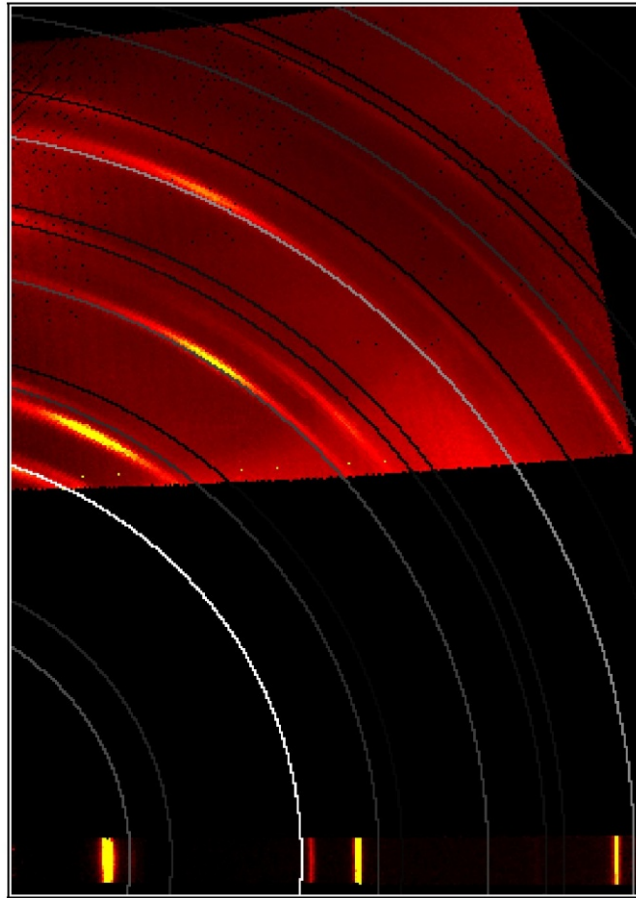
Antimony evaporated on Si, 0.2 Å/s ; crystallize at 4nm
 K deposition dissolves Sb layer - This is where roughening occurs!
 QE increase corresponds with $K_x\text{Sb}$ crystallization
 Cs increases lattice constant and reduces defects

M. Ruiz-Osés et al., APL Mat. 2, 121101 (2014)

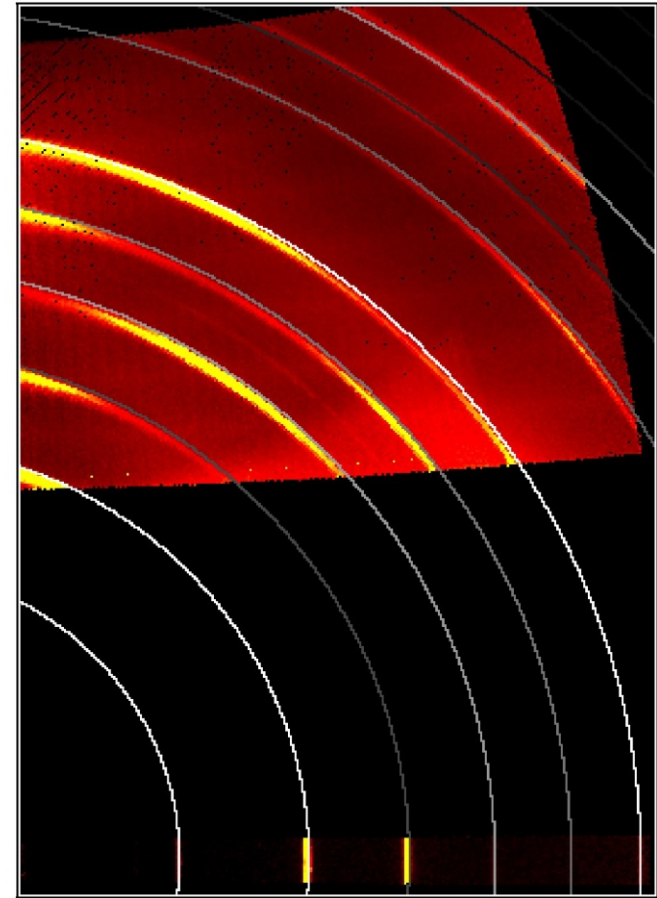
Cathode Texture



Sb evaporated at RT
Clear [003] texture

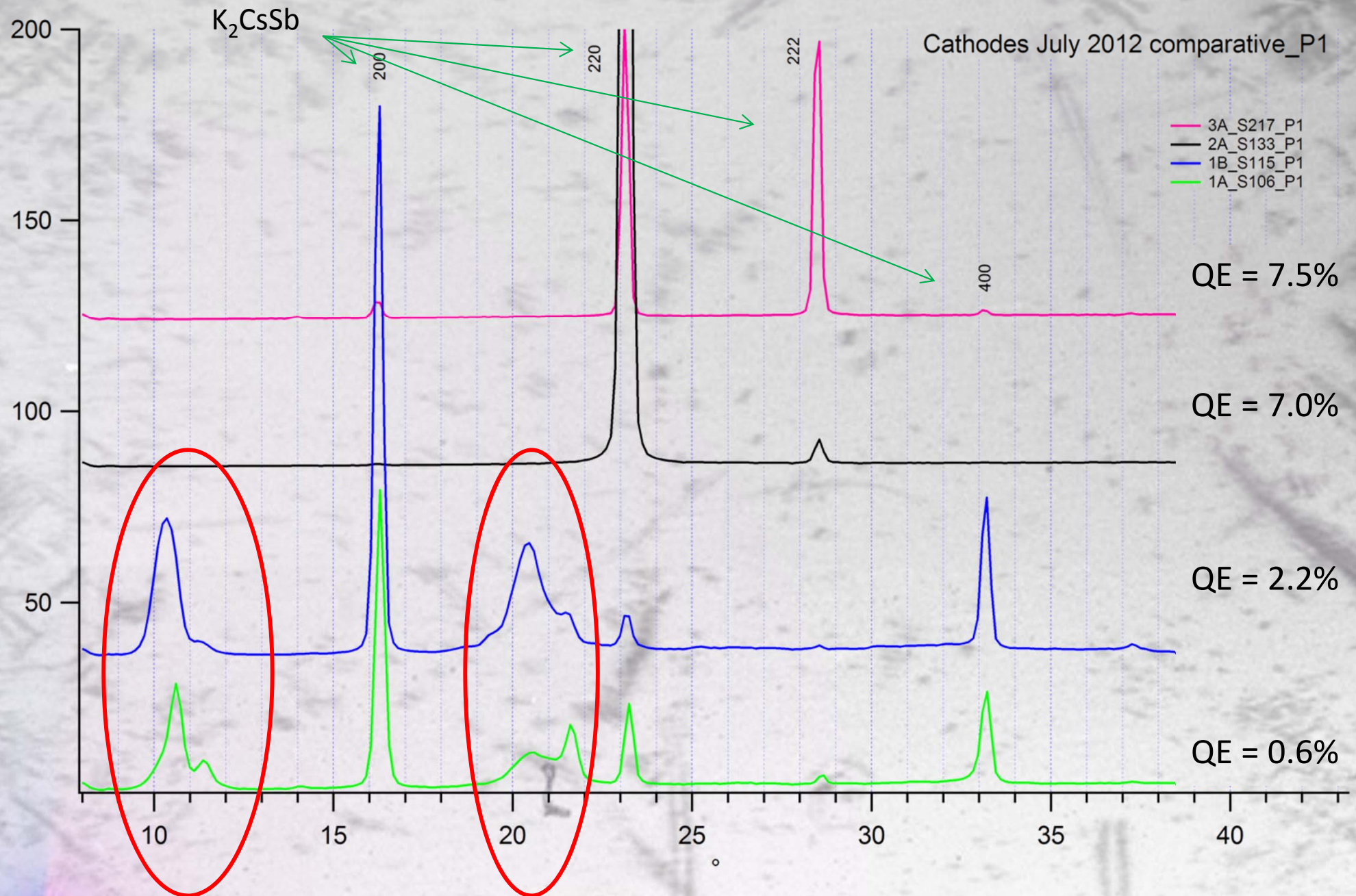


Add Potassium at 140C
Textured final film
But not K₃Sb



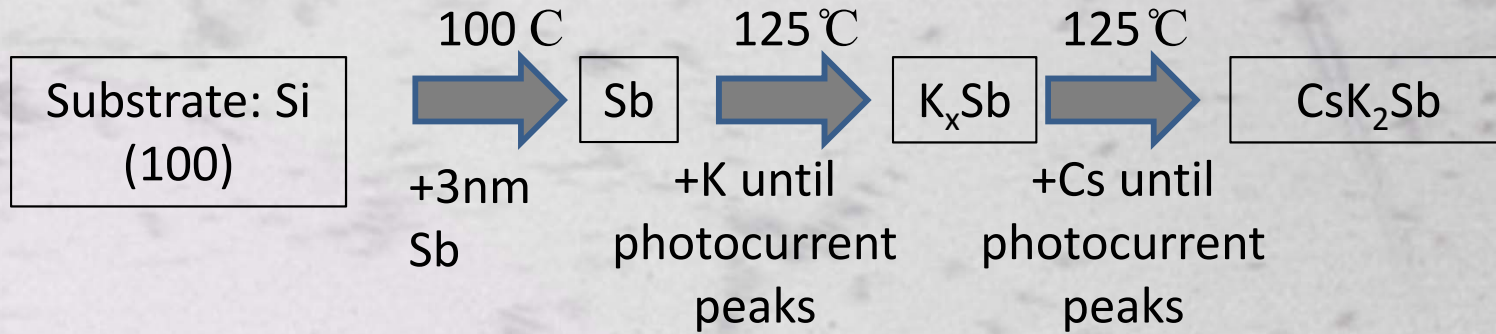
Add Cesium at 140C
Textured final film
Both [220] & [222]
(domains?)
Final QE 7.5% @ 532nm

Comparison of Crystal structure and Final QE



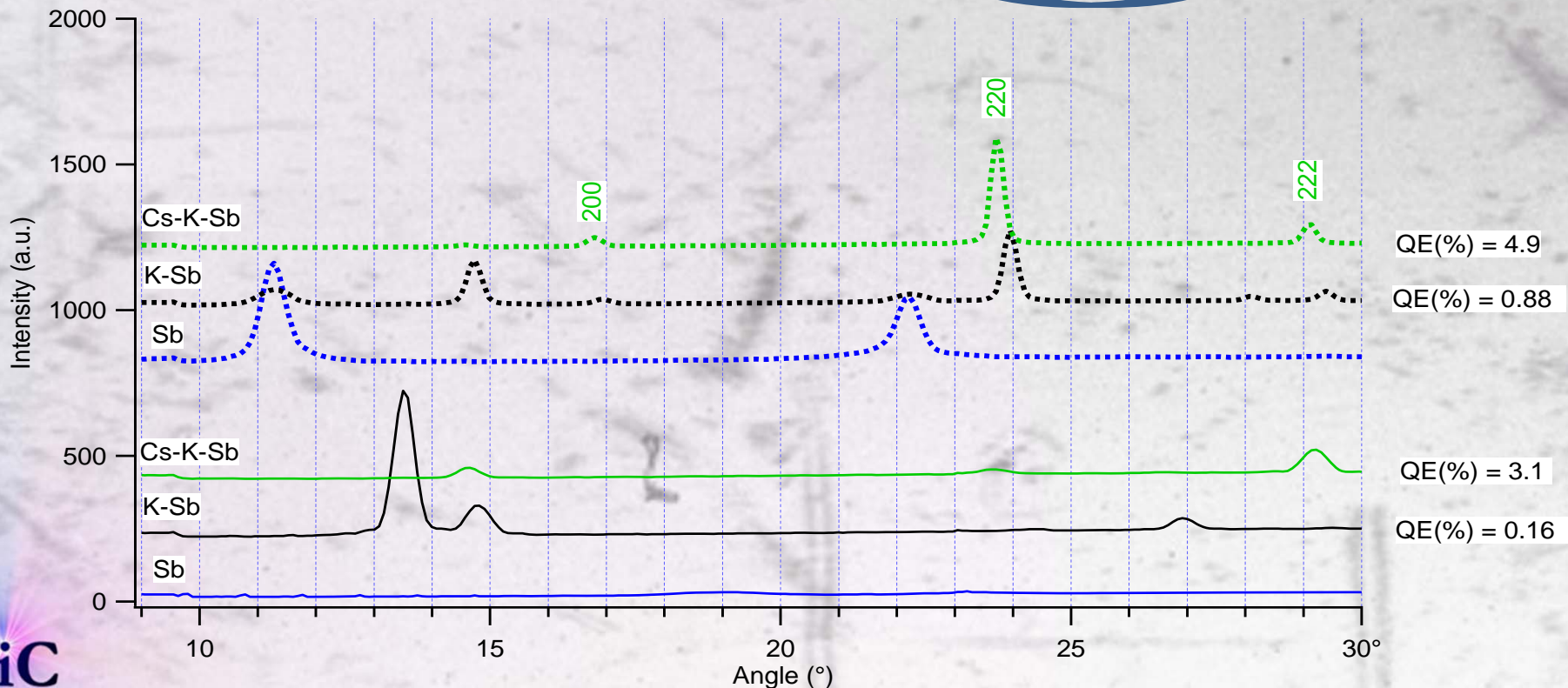
Engineering a Smoother Cathode

Idea: Never let Sb crystalize

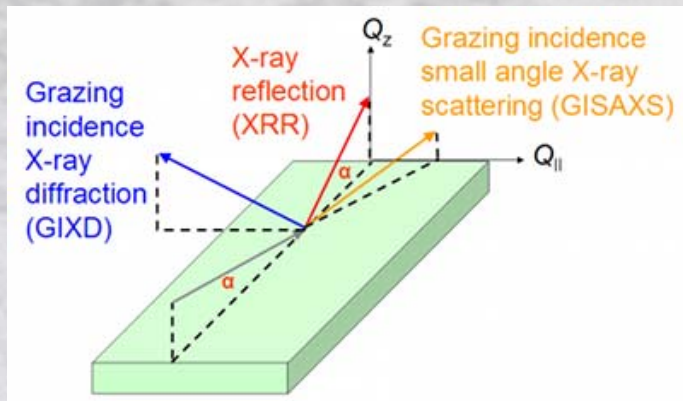


M. Ruiz-Osés et al., APL Mat. 2, 121101 (2014)

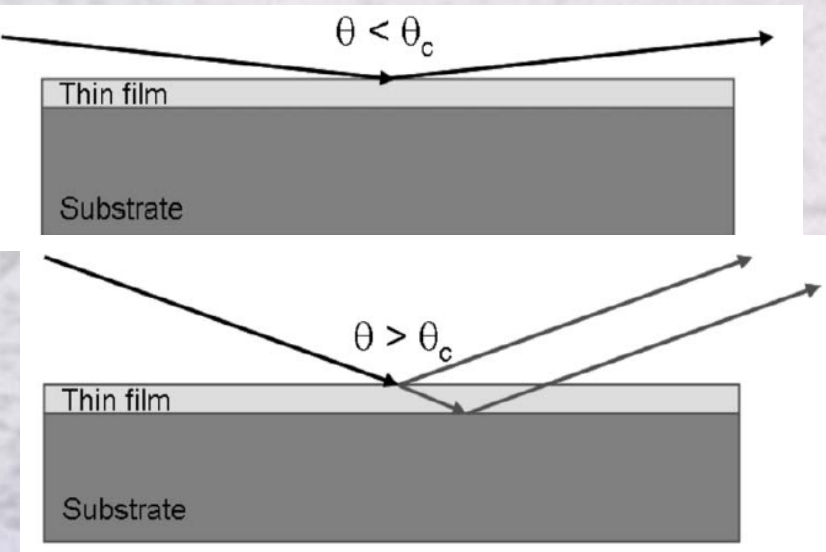
2nd layer: +5nm Sb



X-ray reflectometry (XRR) provides in-situ thickness monitoring



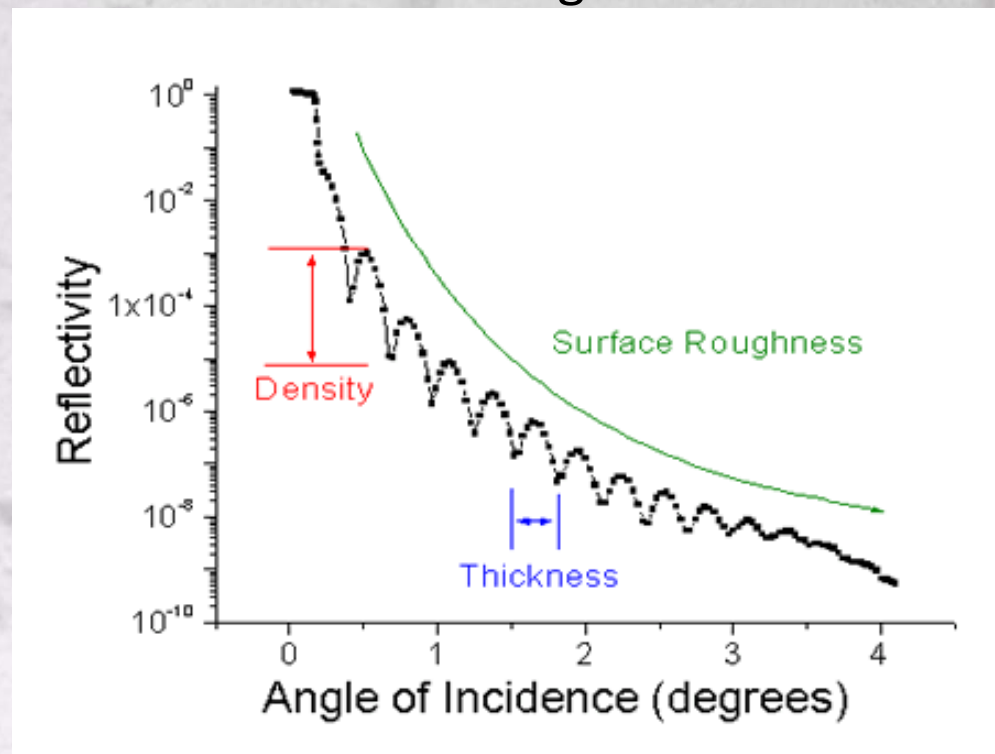
$$\theta_c = \arccos(n_{\text{medium}} / n_{\text{air}})$$



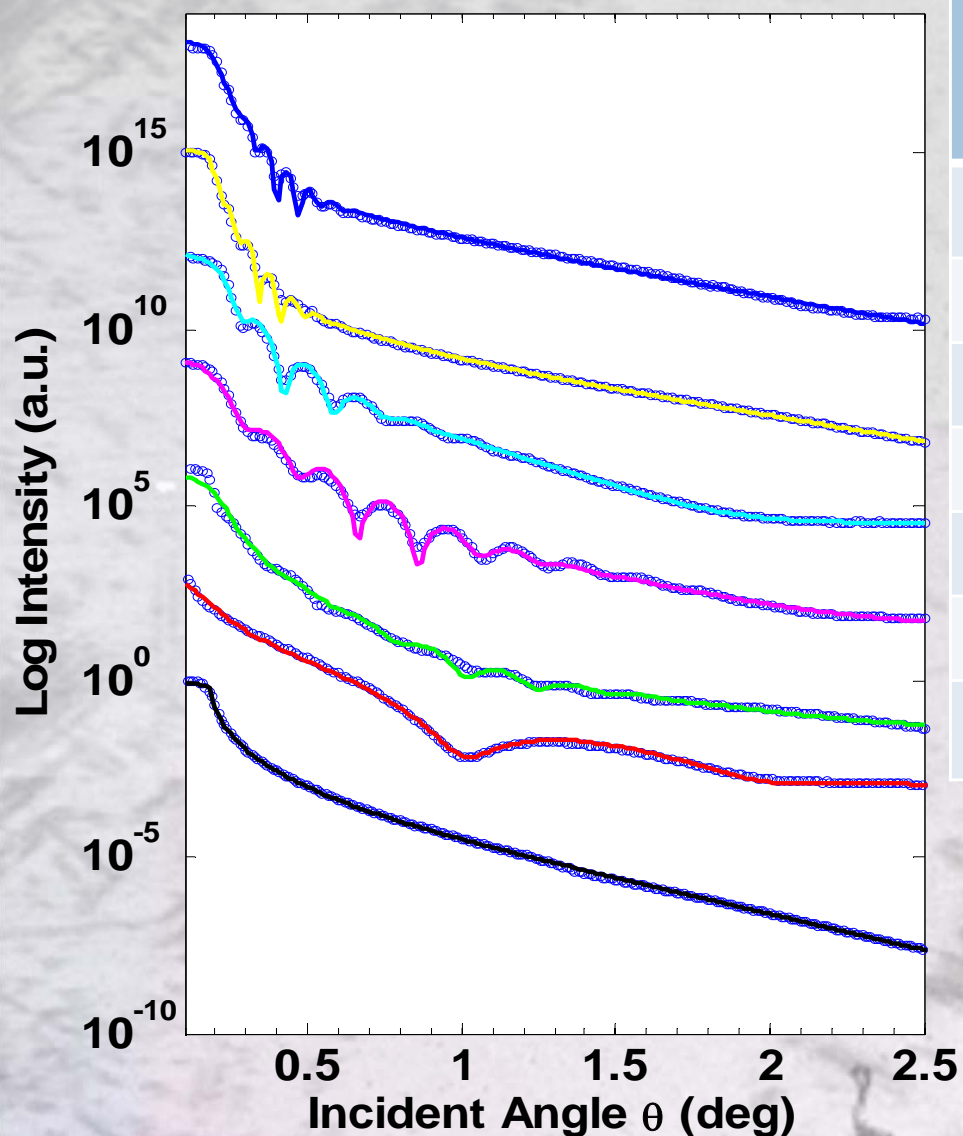
Understand 'sticking' coefficient of materials to substrates at various temperatures

Observe the intermixing vs layering of materials

Observe the onset of roughness



XRR shows roughness evolution



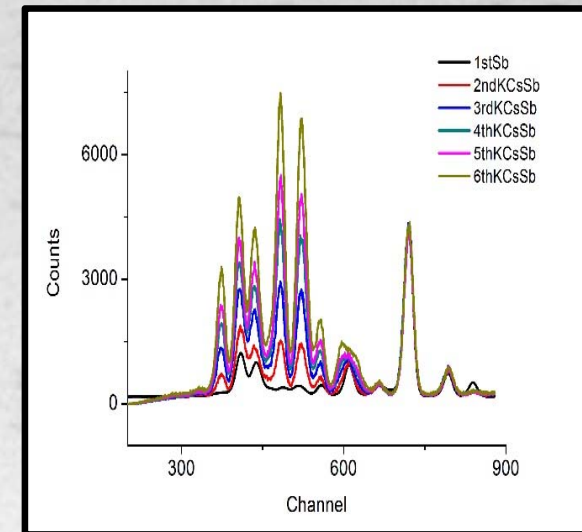
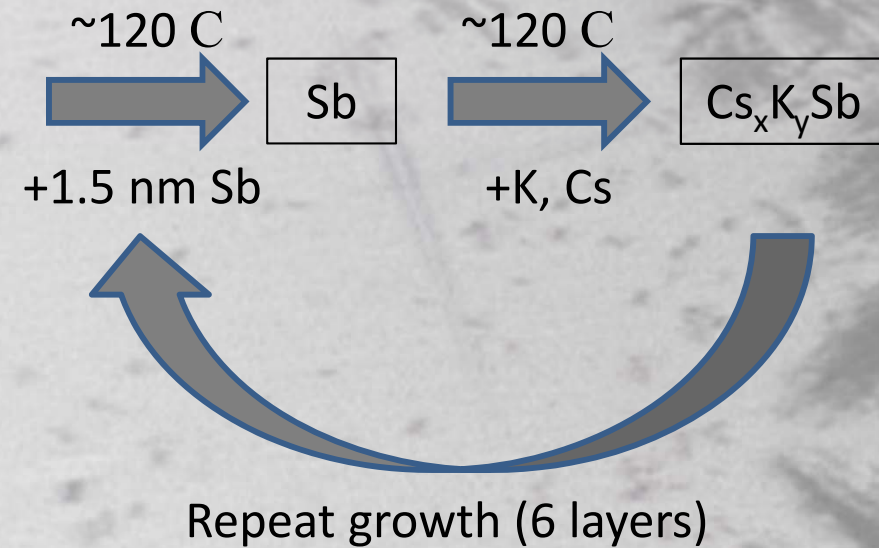
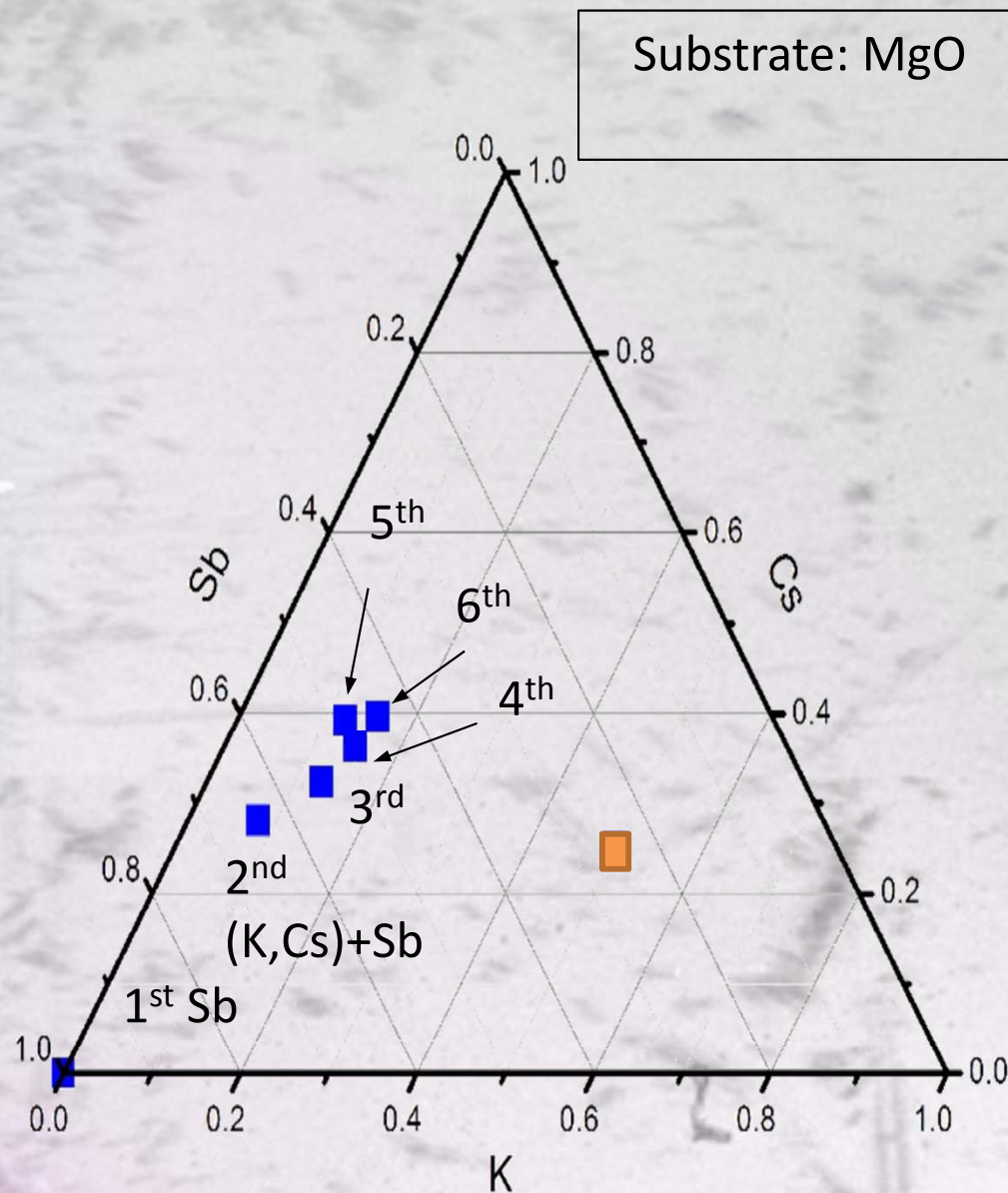
Deposited Layers	Total Thickness (Å)	Roughness (Å)
Cs-K-Sb-Cs-K-Sb/Si	469	32
K-Sb-Cs-K-Sb/Si	449	36
Sb-Cs-K-Sb/Si	200	21.3
Cs-K-Sb/Si	174	13.2
K-Sb/Si	141	10.5
Sb/Si	35	2.9
Si Substrate	-	3.1

The substrate fit includes 1.5 nm of SiO_2

Multi-layer subcrystalline film is smoother,
At slight loss of QE

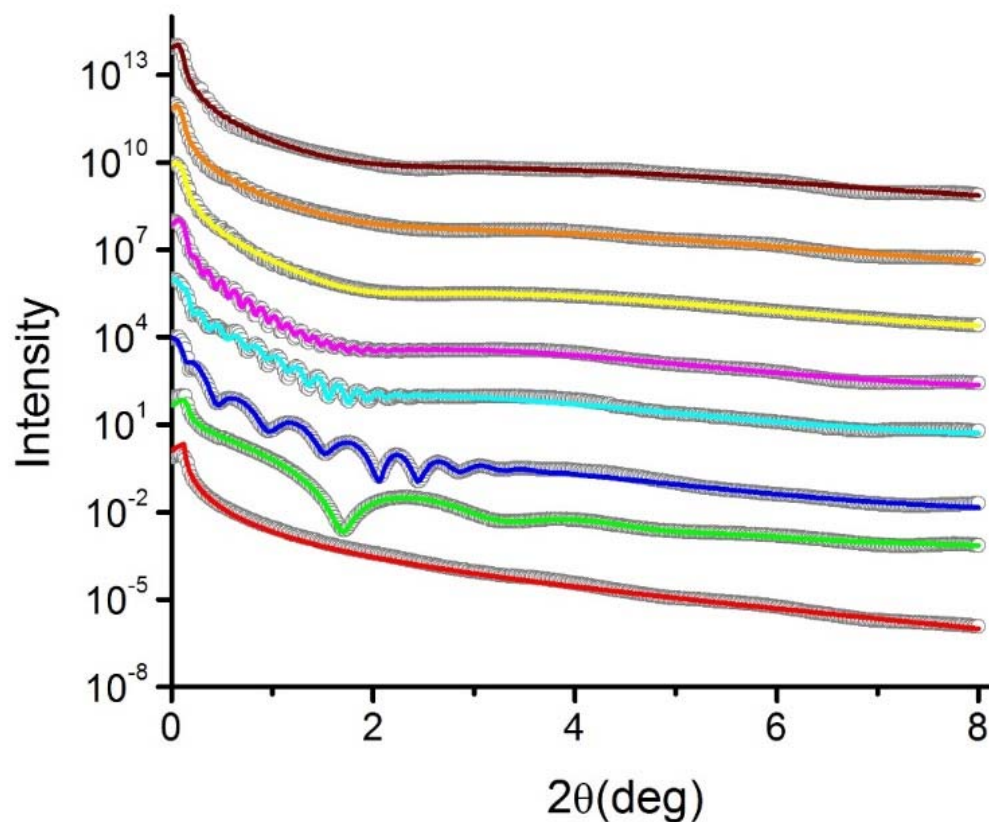
What if we co-deposit the alkalis?

Yo-yo deposition



XRF analysis results of co-dep sample.
→ Calculated stoichiometry shows
Sb, Cs - excess, K-deficient

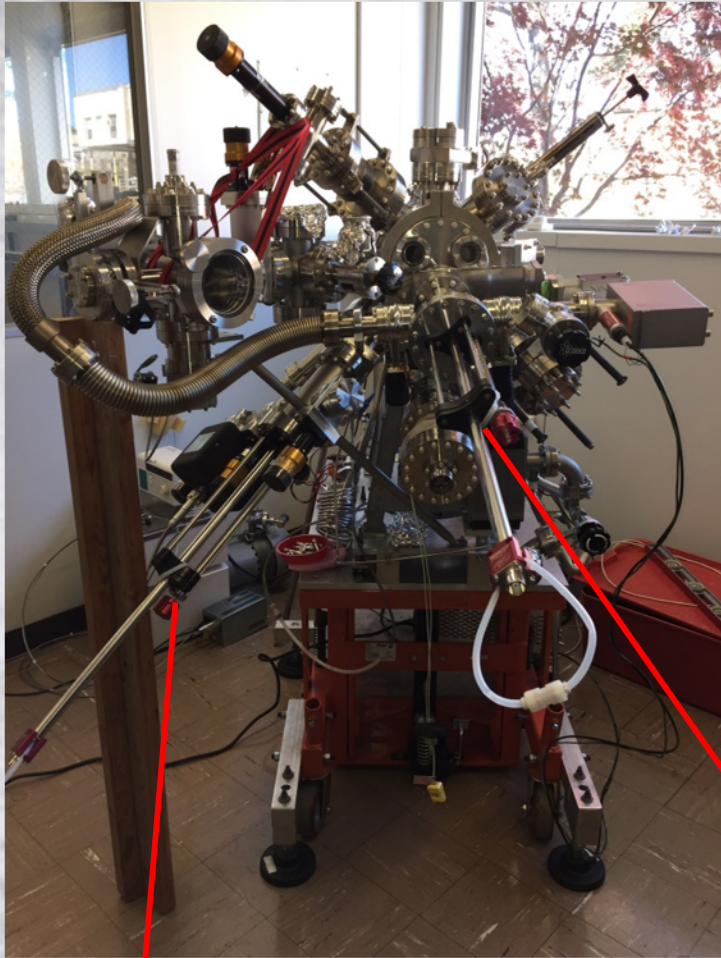
Yo-yo deposition



layer	Roughness (Å)	Thickness(Å)	QE
6 th (K,Cs)+Sb	23.6 (-3.9, 1.4)	806.7 (-25.3, 98.9)	4.5 %
5 th (K,Cs)+Sb	24.9 (-17.2, 1.0)	725.5 (-46.5, 24.6)	4.9 %
4 th (K,Cs)+Sb	14.5 (-2.1, 0.40)	609.3 (-70.5, 9.5)	3.7 %
3 rd (K,Cs)+Sb	9.92 (-1.5, 1.5)	489.09 (-6.8, 18.7)	4.2 %
2 nd (K,Cs)+Sb	9.73 (-0.30, 0.86)	334.3 (-1.8, 2.1)	1.7 %
1 st (K,Cs)+Sb	9.22 (-2.9, 0.78)	159.3 (-1.6, 0.9)	1.2 %
Sb	5.2 (-0.11, 0.35)	36.74 (-0.26, 0.13)	
Substrate (MgO)	1.5 (-, -)		

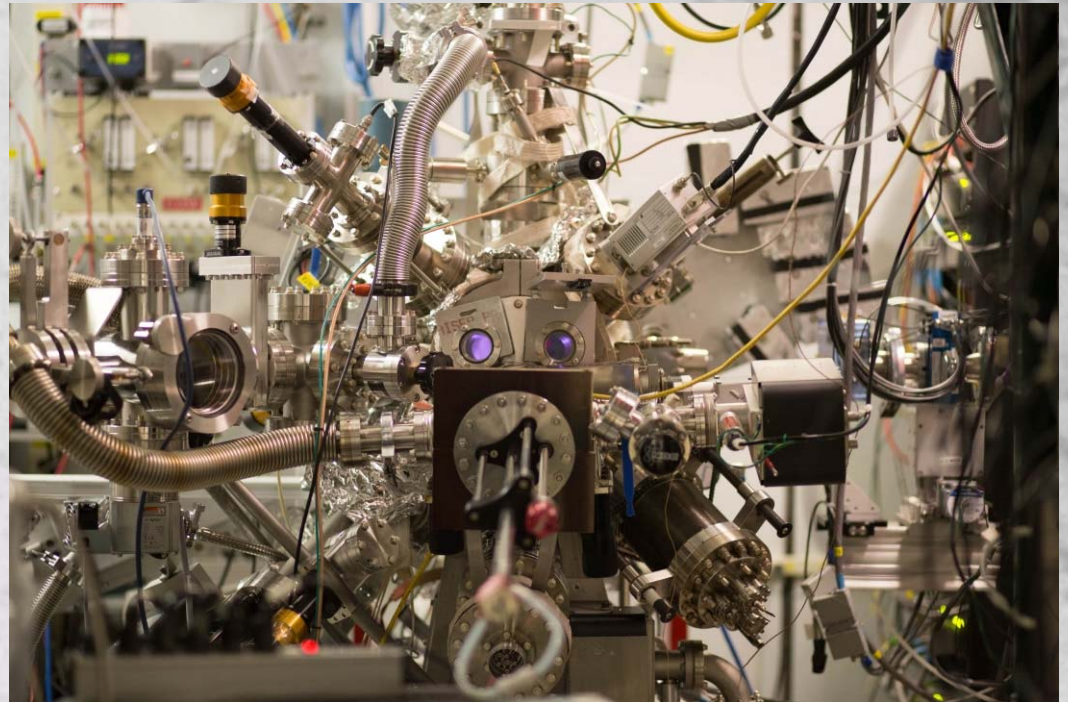
XRR simulation result of K/Cs co-dep sample.
 Colored solid lines: simulation; Open circle:
 measured data. Error noted is 5% of change in
 logarithm FOM function

Sputter Growth

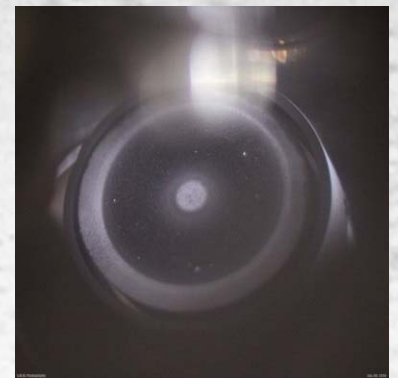


Cs_3Sb
sputter gun

K_2CsSb
sputter gun



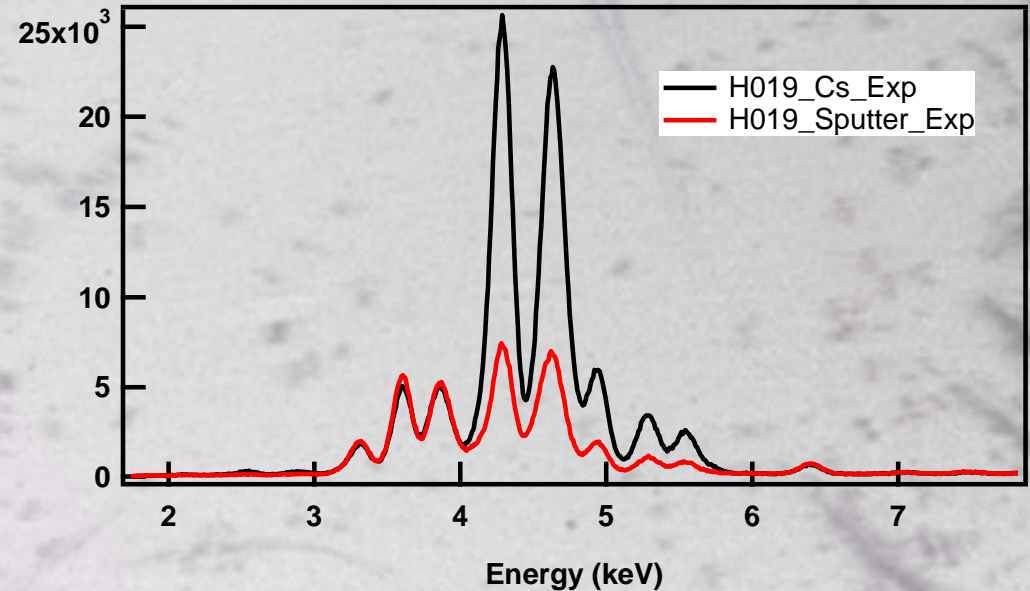
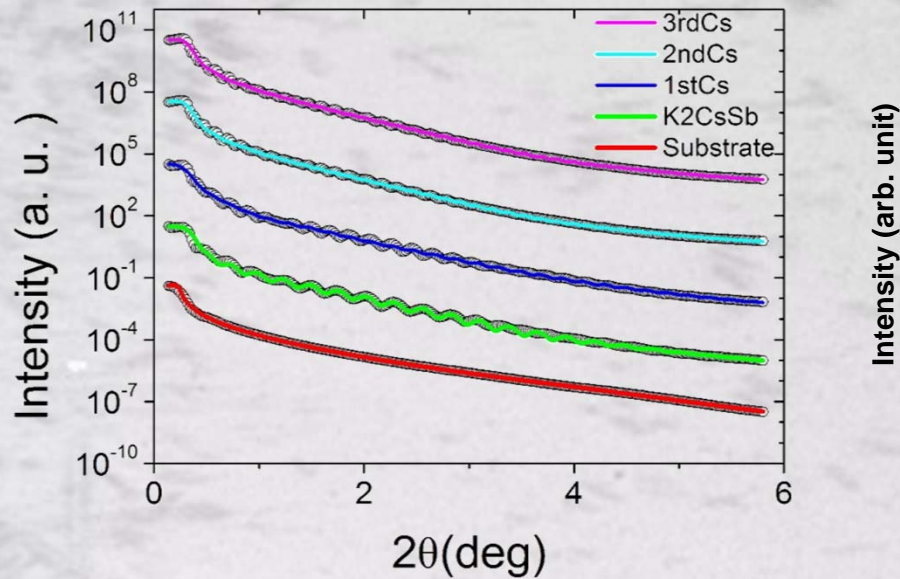
In situ, In operando XRR, XRF, XRD & Quantum efficiency (QE) measurement



Sputter targets grown by RMD, Inc

Sputter Growth

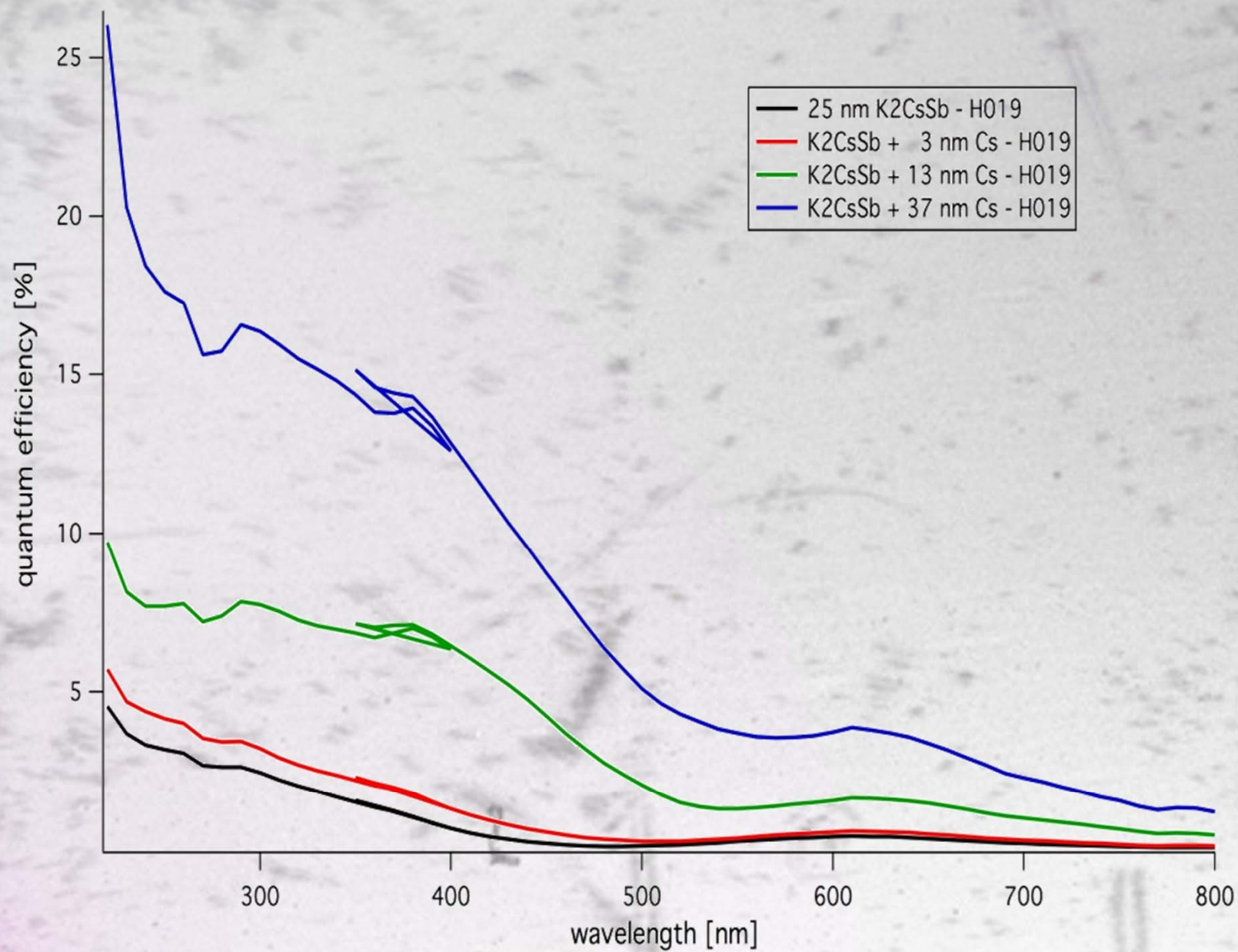
25 nm K₂CsSb + layers of (total 30 nm) Cs evap.
Silicon substrate at 90 C, layer barely crystalline



	Thickness (Å)	Roughness (Å)
3 rd Cs	416.0	5.67
2 nd Cs	341.3	4.94
1 st Cs	249.5	4.91
sputter K ₂ CsSb	234.2	5.17
SiO ₂	10.24	3.27
Substrate (Si)	---	3.75

layer	K (±0.1)	Sb (±0.05)	Cs (±0.05)	K/Cs
K ₂ CsSb sputter	0.85	1.00	0.41	2.08
Cs	0.84	1.00	1.75	0.48

Sputter Growth

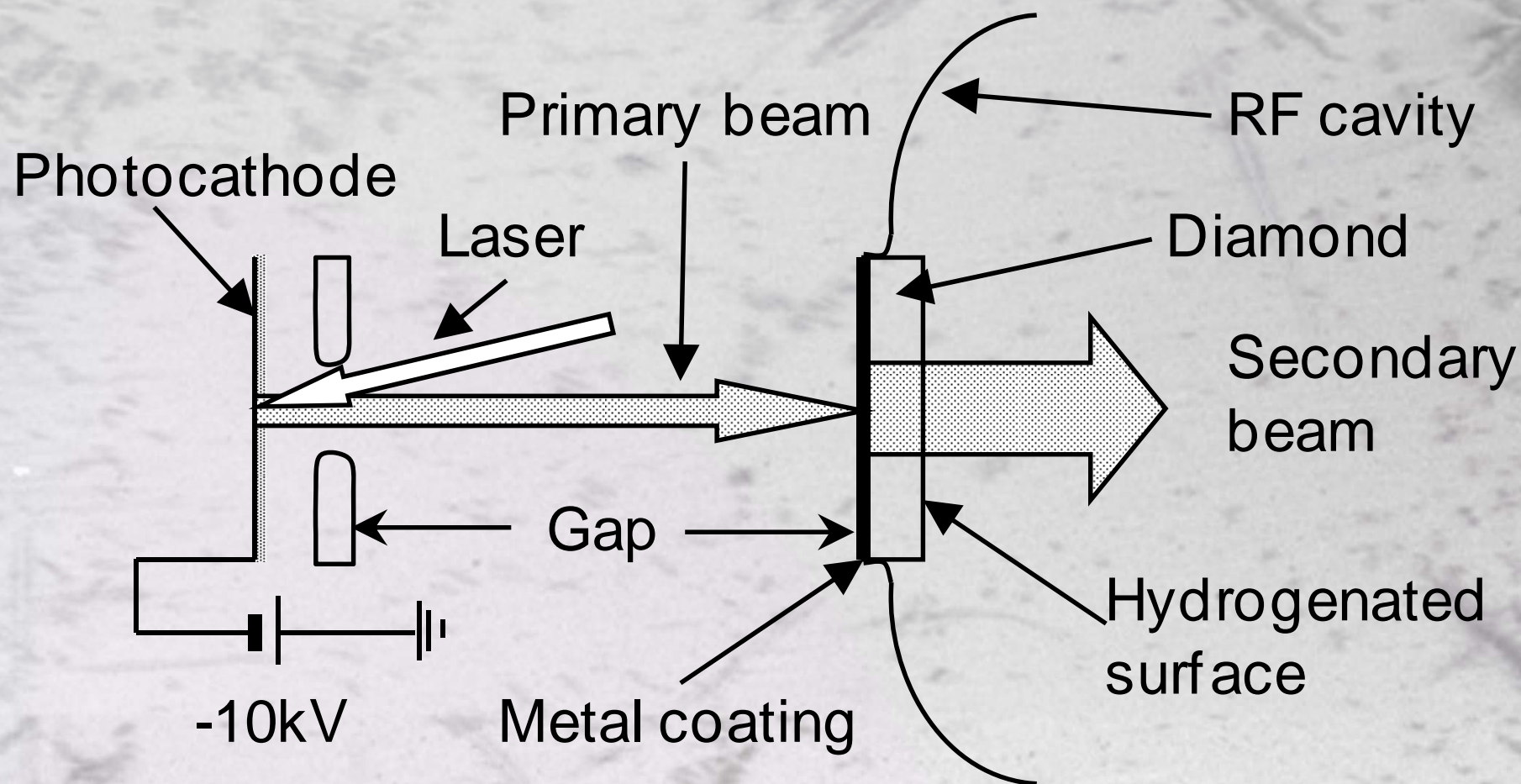


Alkali Antimonide Cathodes

What we've learned

- We now have a tool which is capable of optimizing growth parameters for figures of merit other than Quantum Efficiency
- We understand the formation chemistry of these materials, and why traditional deposition results in rough cathodes
- Avoiding crystalline Sb helps, as does co-evaporating alkali
- Sputter deposition is best – easy to do, covers large area, almost atomically smooth even for thick films
- Can now consider heterojunctions and doping of alkali antimonides (following a similar development path to the III-V materials)

Diamond Amplifier



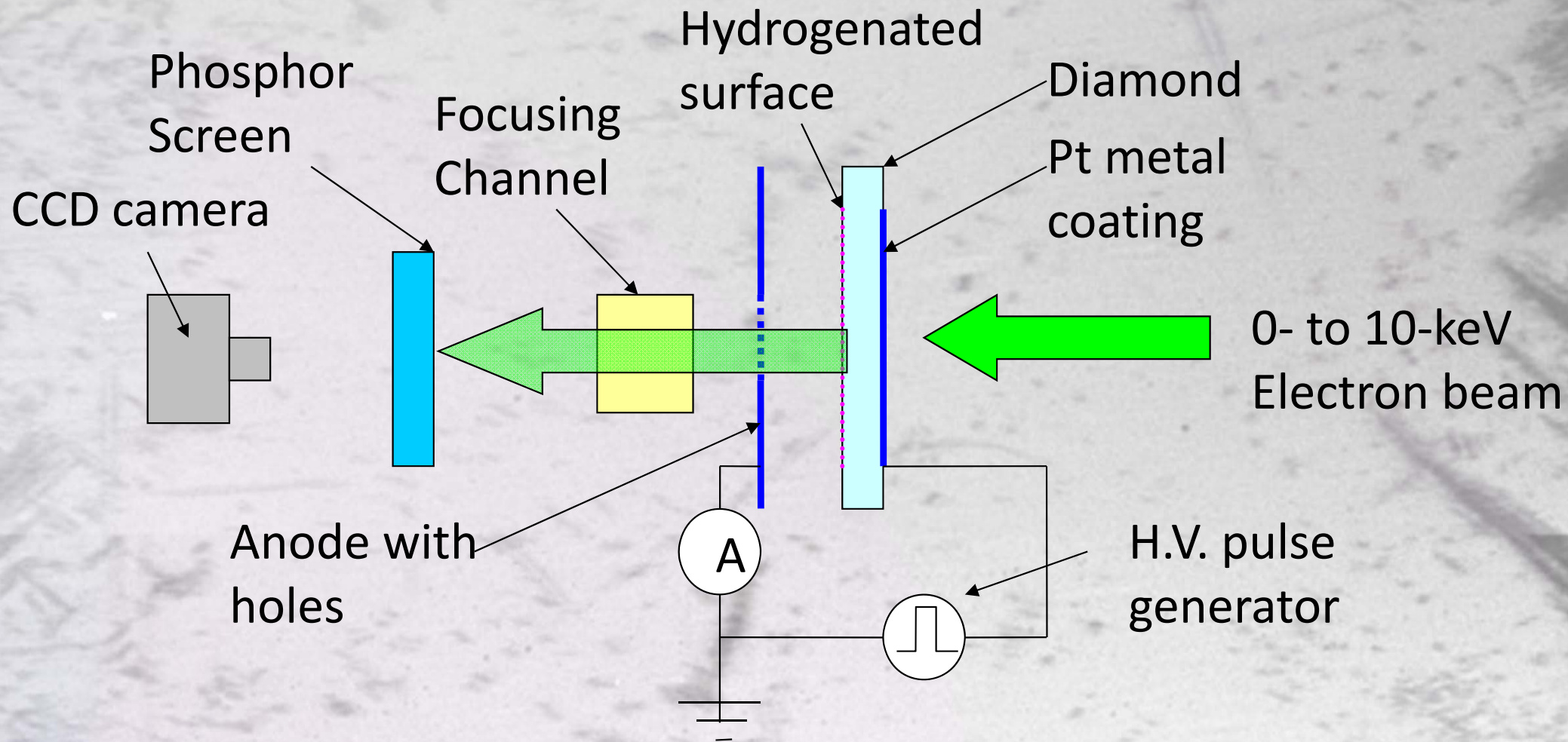
Advantages

Secondary current can be **>300x** primary current

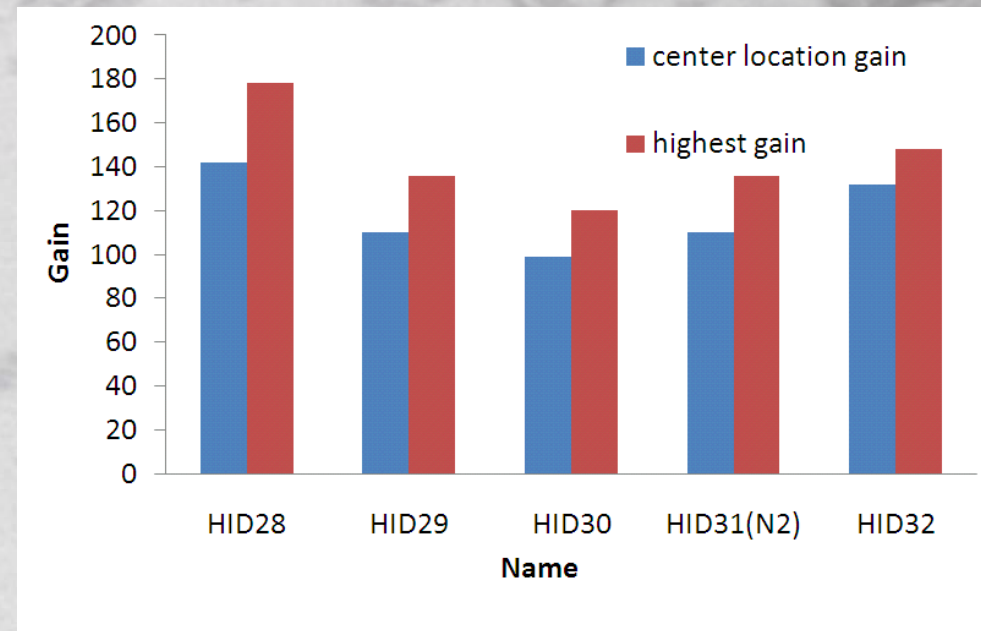
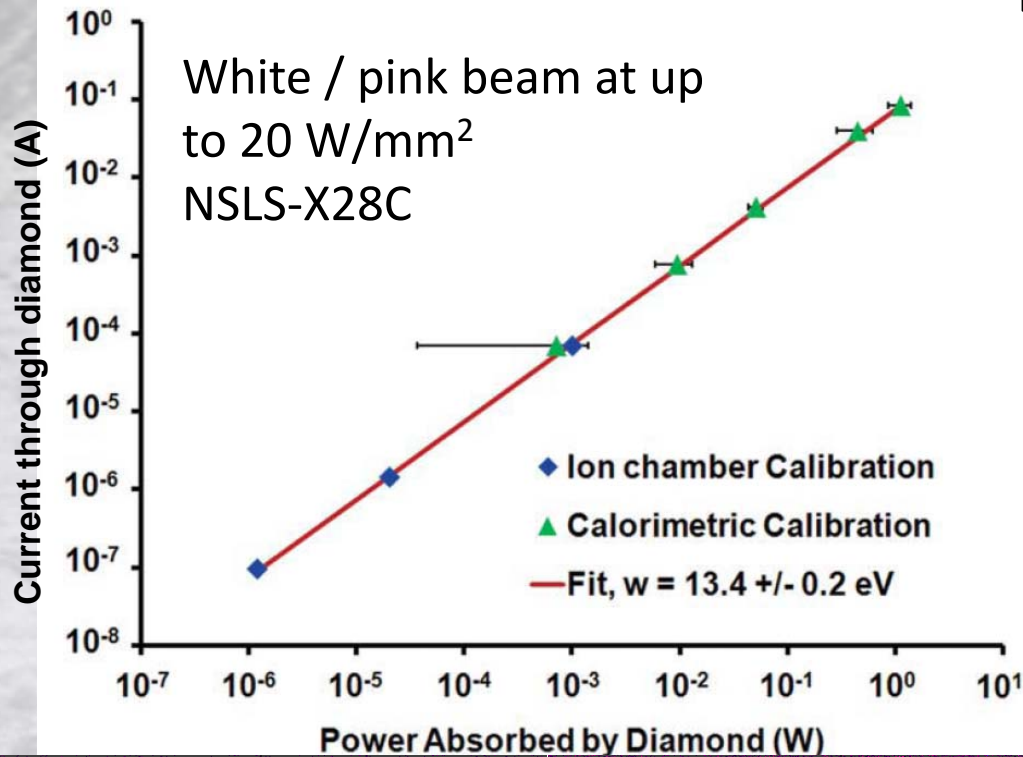
Diamond acts as vacuum barrier

e^- thermalize to near conduction-band minimum

Diamond Amplifier Setup



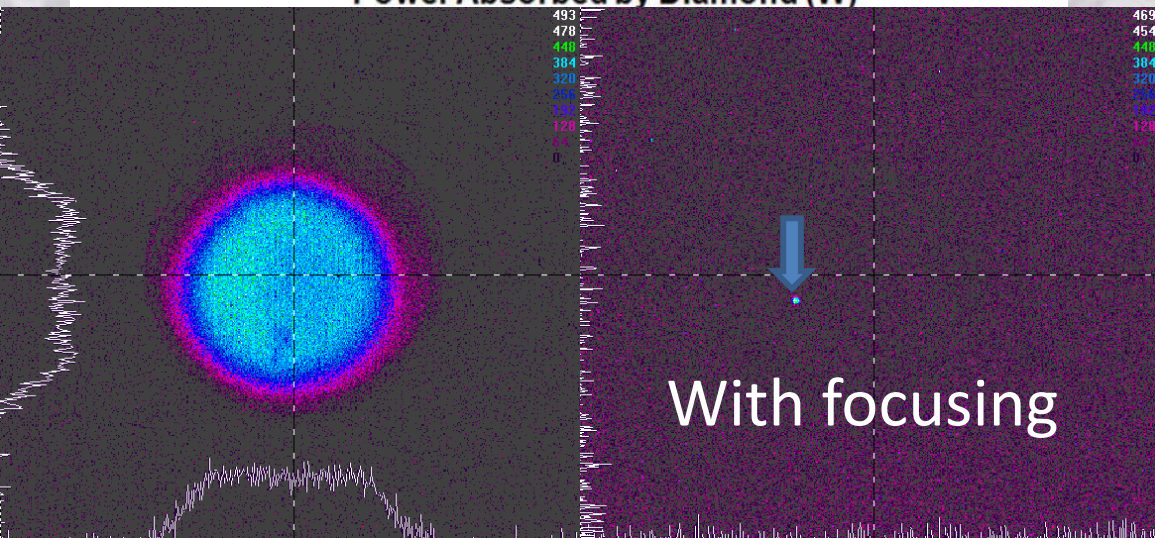
Diamond Amplifier Results



Demonstrated emission and gain of >100 for 7 keV primaries

Emitting ~60% of secondaries

X-ray photons have been used to generate current densities in excess of 20 A/cm² with no deviation from response linearity

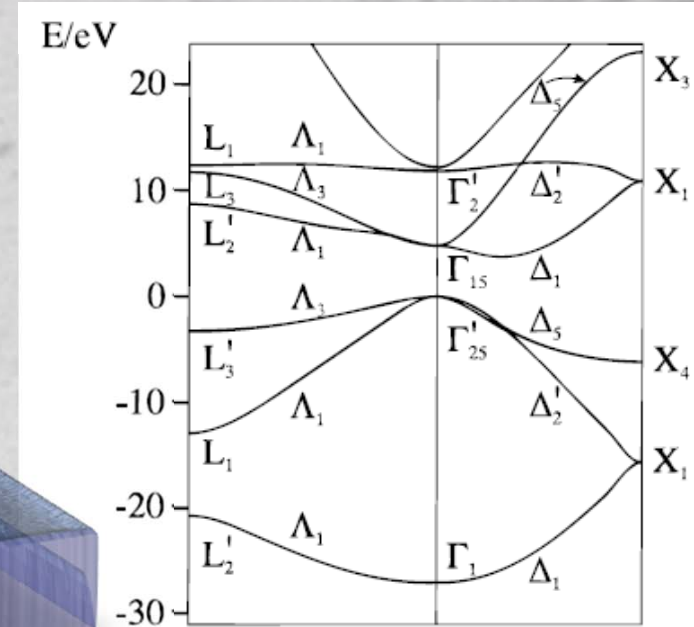
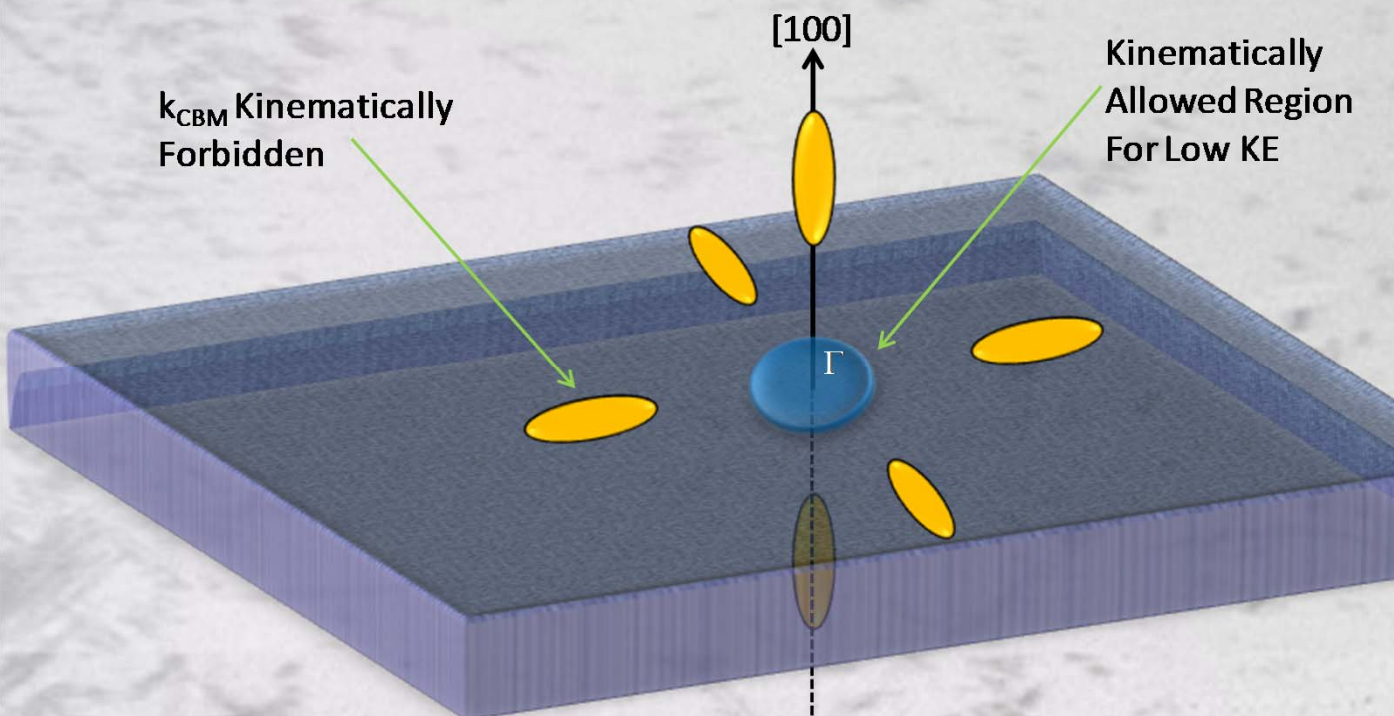


X. Chang et al., Phys. Rev. Lett. **105**, 164801 (2010)

J. Bohon, E. Muller and J. Smedley, J. Synchrotron Rad. **17**, 711-718 (2010)

Why Does Diamond Emit?

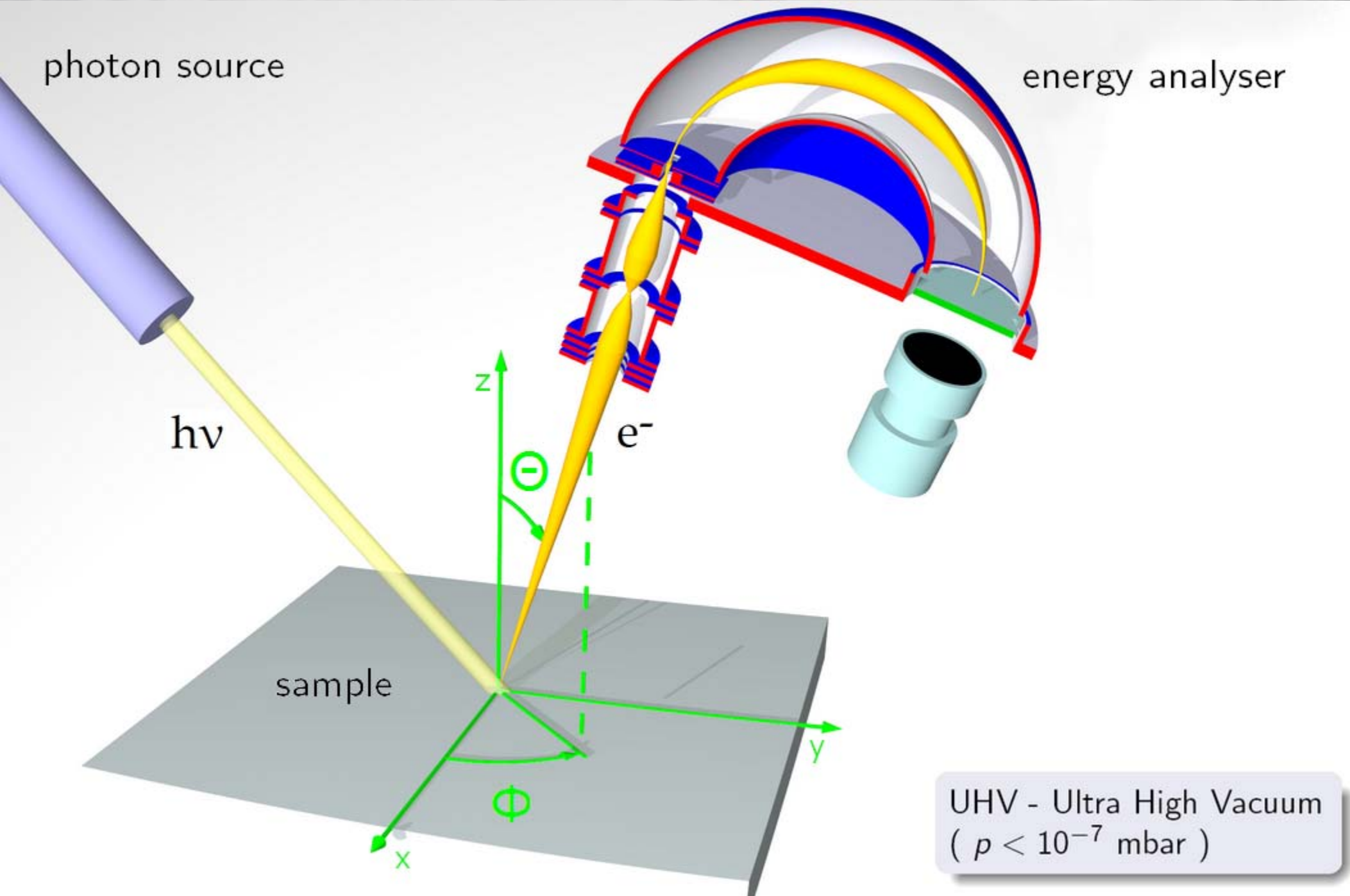
Projection of k-space onto [100] Surface



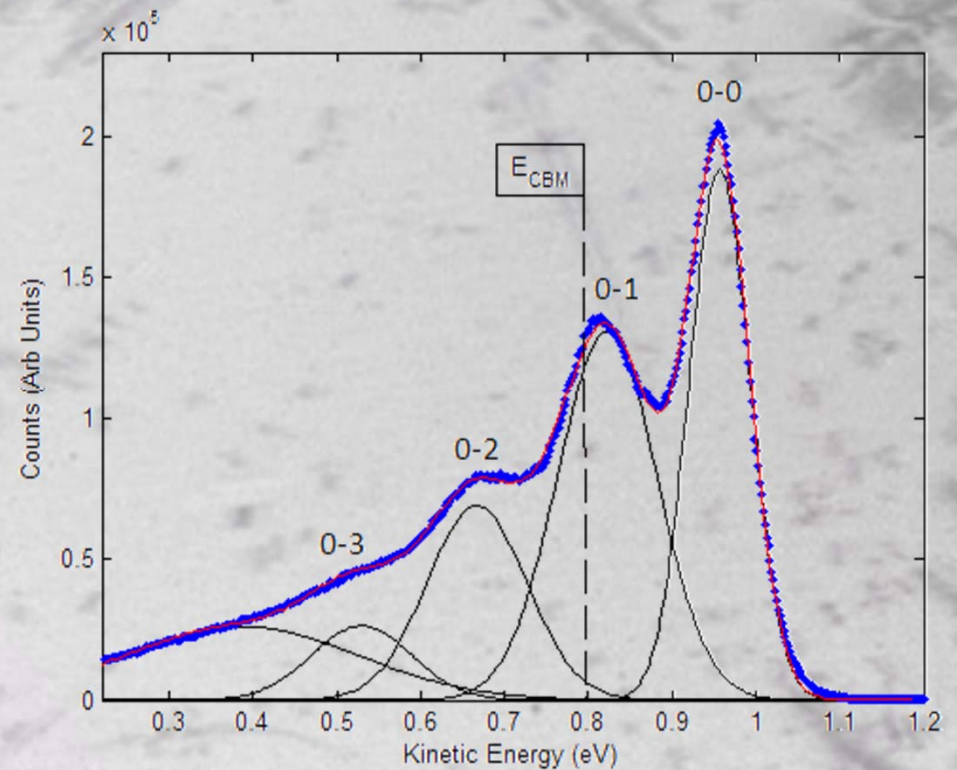
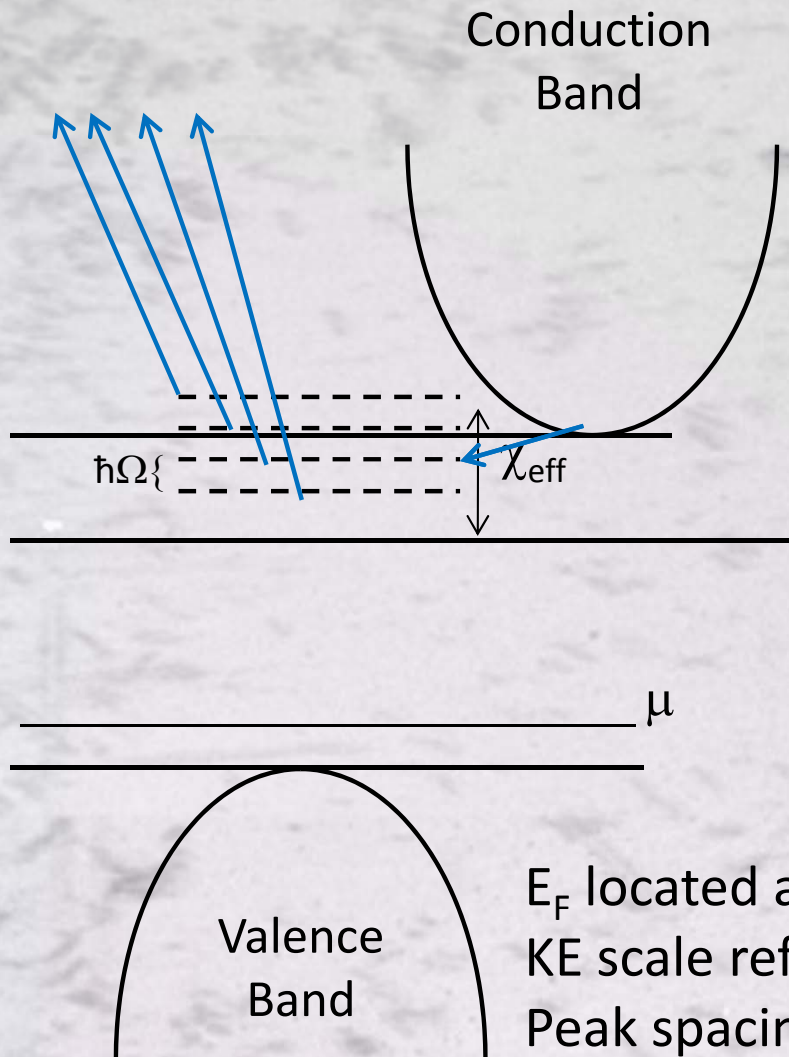
J. Phys. Chem., Vol. 100, No. 26, 1996

Hydrogen termination causes diamond to have a work function ~ 1 eV lower than its band gap **but** the band gap is indirect
Thus even electrons with energy 1 eV above the conduction band minimum are not in a momentum state capable of emission
This is the crux of the problem for Negative Electron Affinity Diamond

Angle-Resolved Photoemission Spectroscopy



6 eV Laser ARPES



E_F located at 1.662 eV according to Au reference
 KE scale referenced to E_{vac} for NEA material; NEA = -0.955 eV
 Peak spacing 142 ± 5 meV, consistent with the 145 meV
 energy of optical phonon which connects Γ to Δ

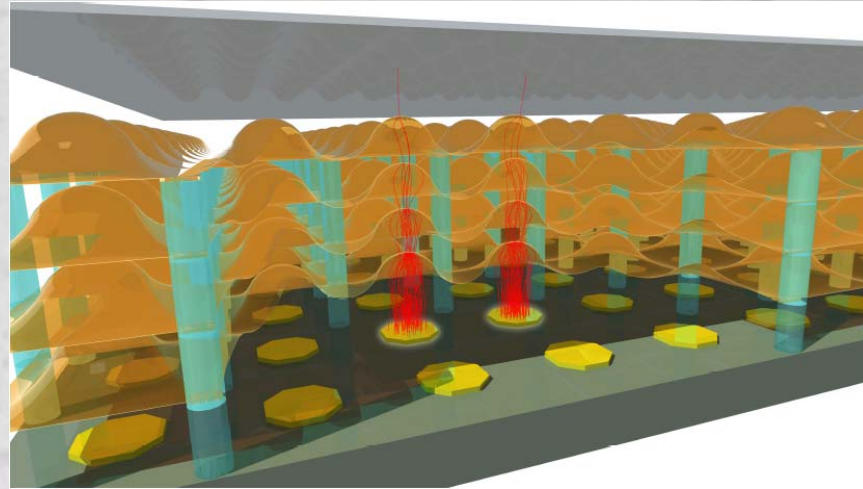
Functional Aspects of Topsy

“Timed Photon Counter”=>TiPC=>Topsy

Photocathode:

High QE important
but

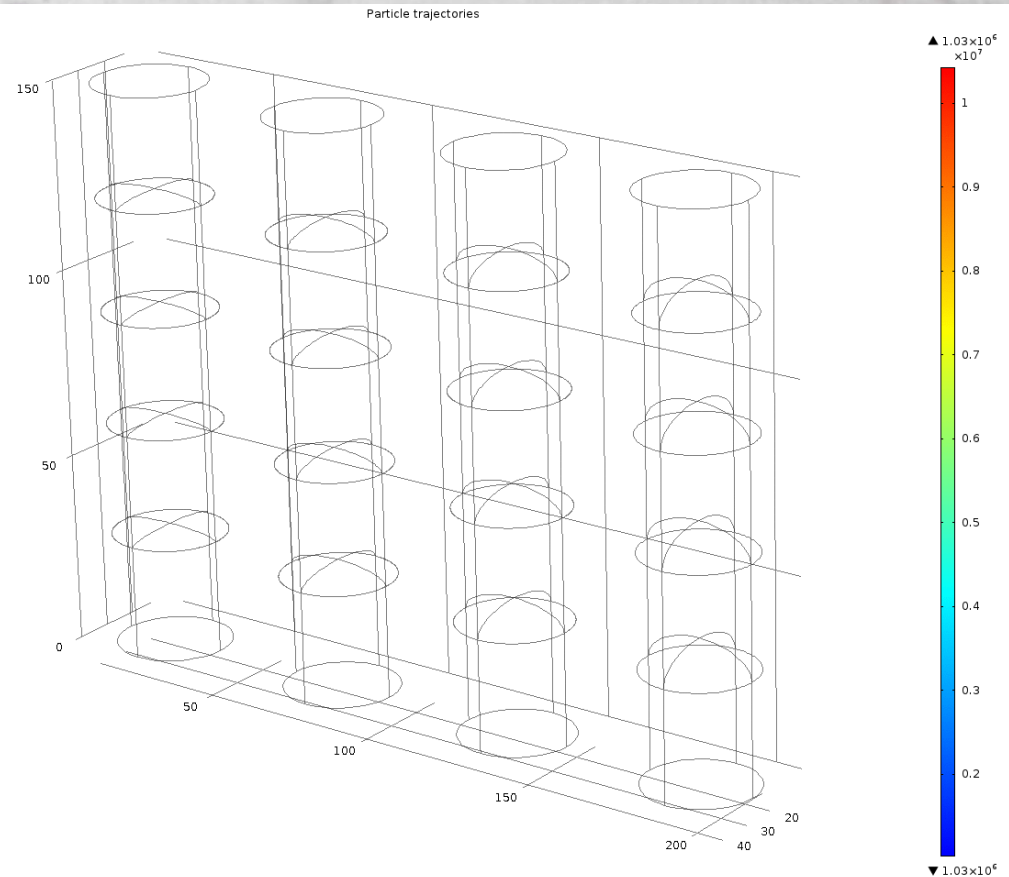
Must tolerate 3-7 V/ μm
with minimal dark cts



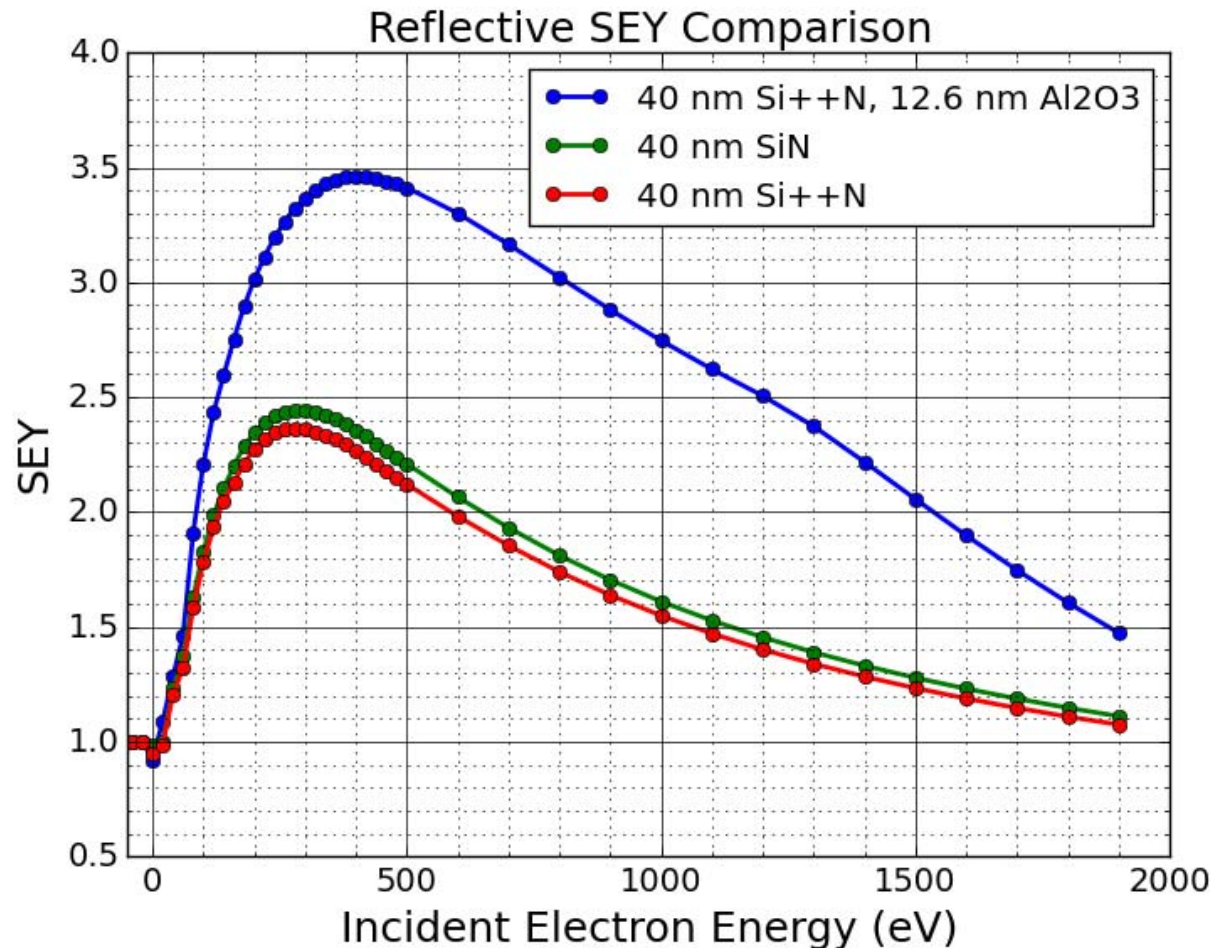
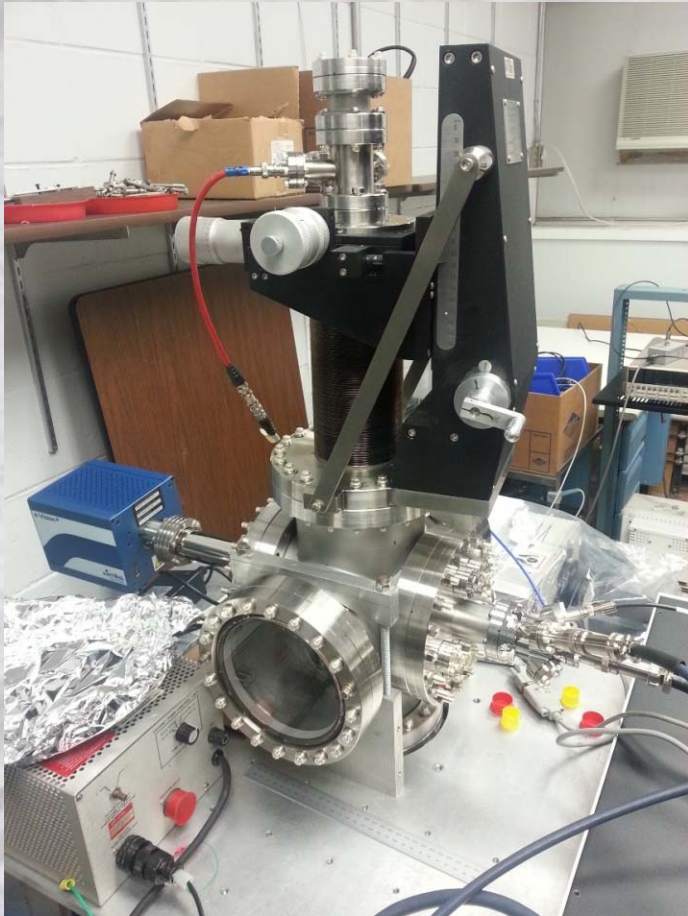
Dynodes:

SEY will determine
viability of device and
number of dynodes

Surface treatment and
processing optimization
required



Dynode Testing for Tispy (DyTest)



UHV system, with electron gun and optical port for QE/workfunction measurement
Load multiple samples and measure secondary electron yield in reflection and transmission mode
In-situ heating and surface treatment (Cs evaporation)

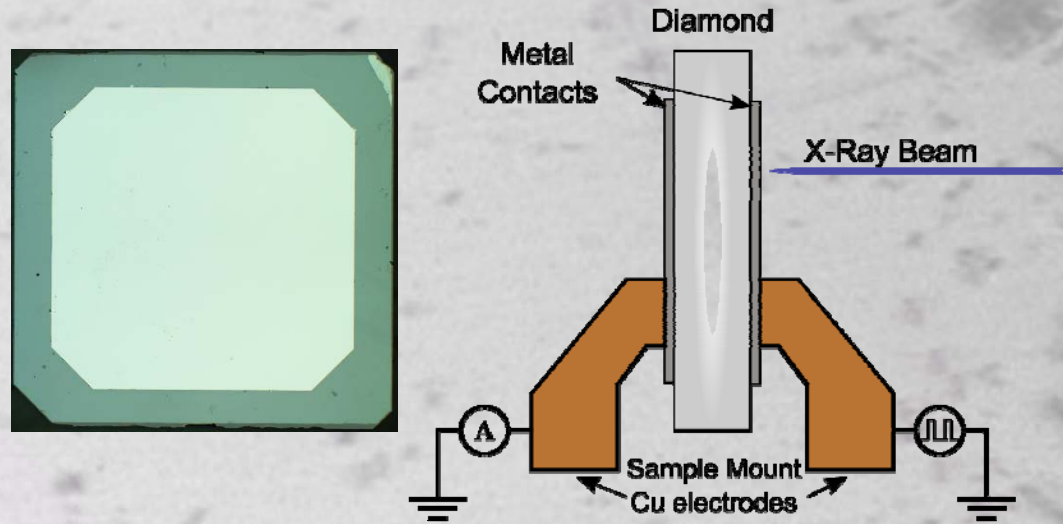
Diamond as a X-ray sensor

Diamond Advantages:

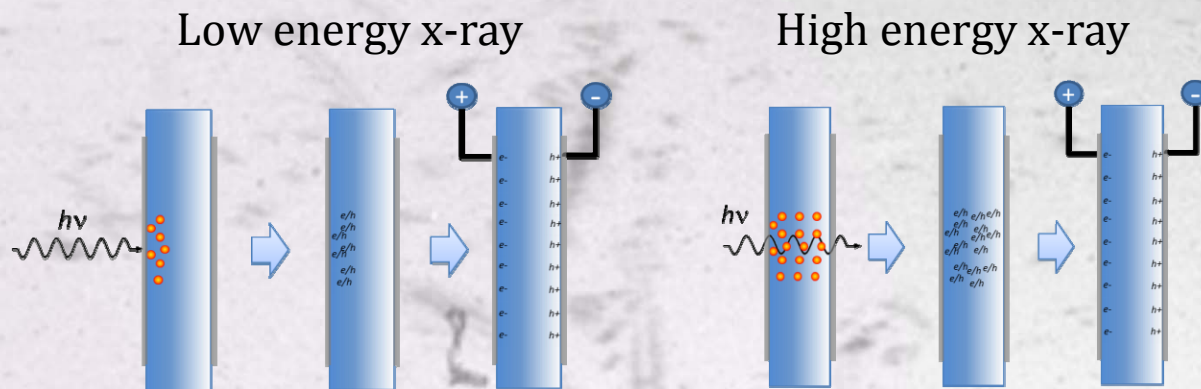
- Low X-ray Absorption
- High Thermal Conductivity
- Mechanical Strength
- Radiation Hardness
- Indirect bandgap

Sample Information:

- Electrical grade CVD single crystal diamond
- (100) surface orientation
- ~1 ppb nitrogen impurity
- Typical size: 4mm x 4mm x 50 μ m



X-ray generated charge carriers



Electron hole pairs created near incident electrode: must move entire thickness of the diamond

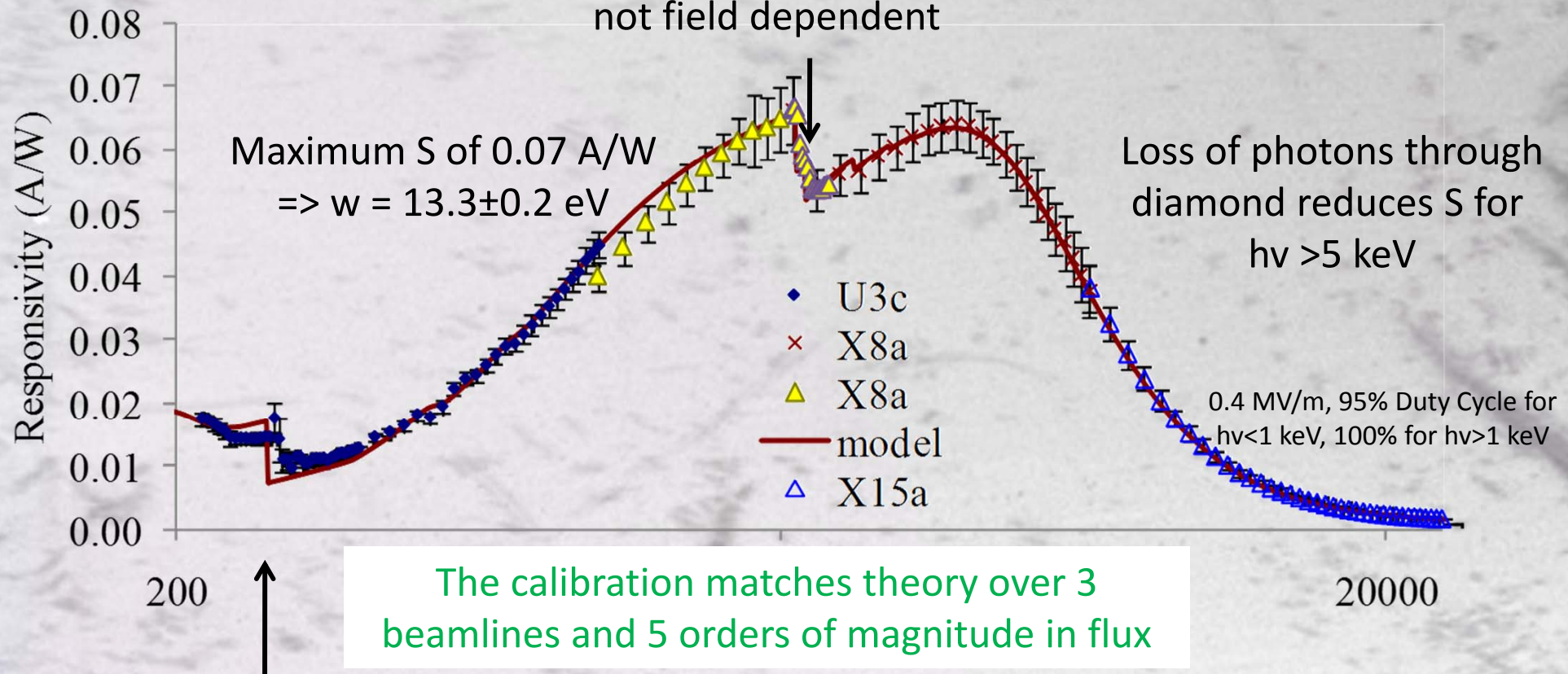
Electron hole pairs created throughout the thickness creating a column of electron-hole pairs

Responsivity vs Photon Energy

$$S = \frac{1}{w} e^{-t_{\text{metal}}/\lambda_{\text{metal}}} \left(1 - e^{-t_{\text{dia}}/\lambda_{\text{dia}}}\right) CE[\nu, F]$$

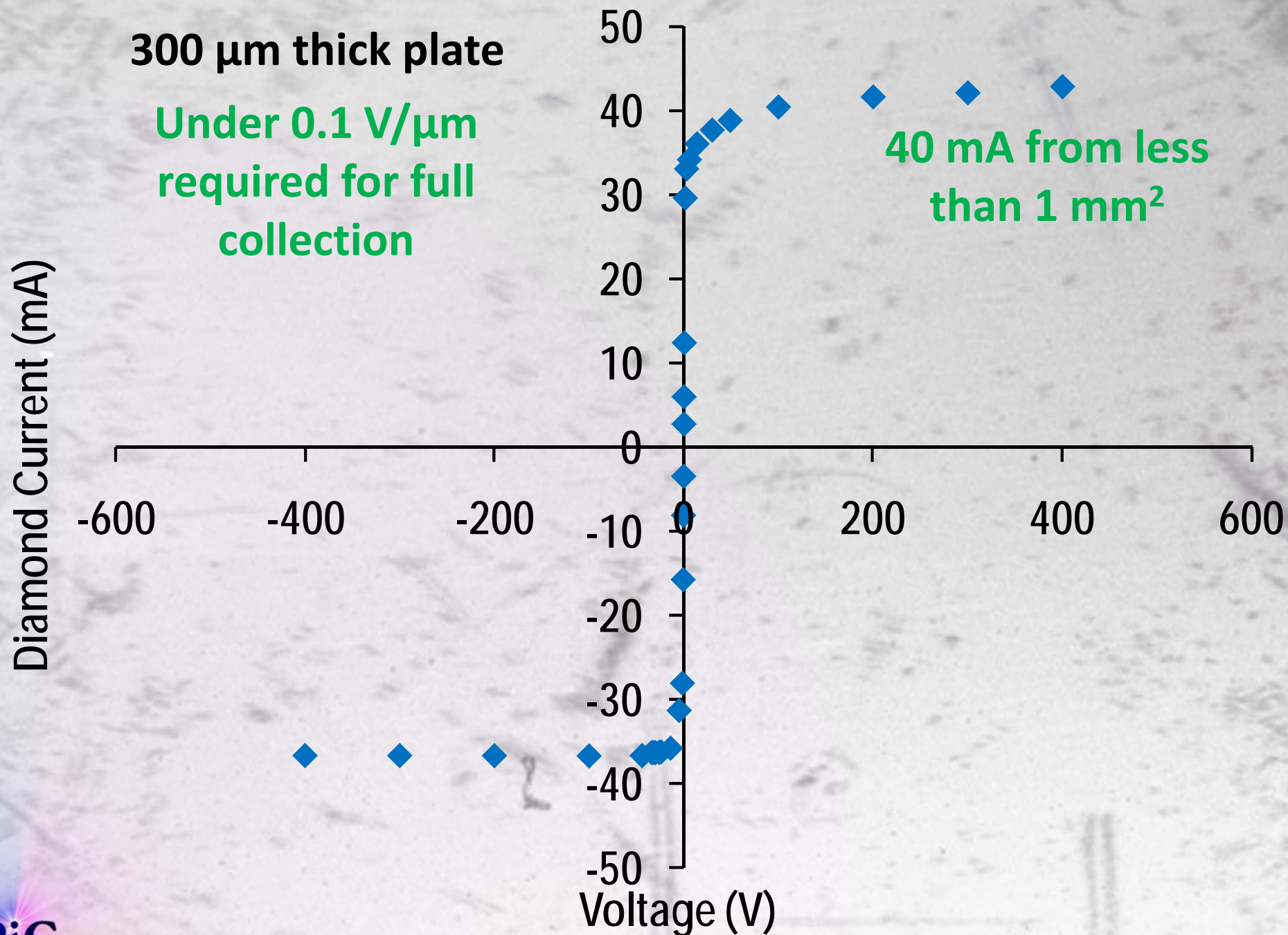
Platinum M edge feature due to loss of photons absorbed by incident contact

not field dependent

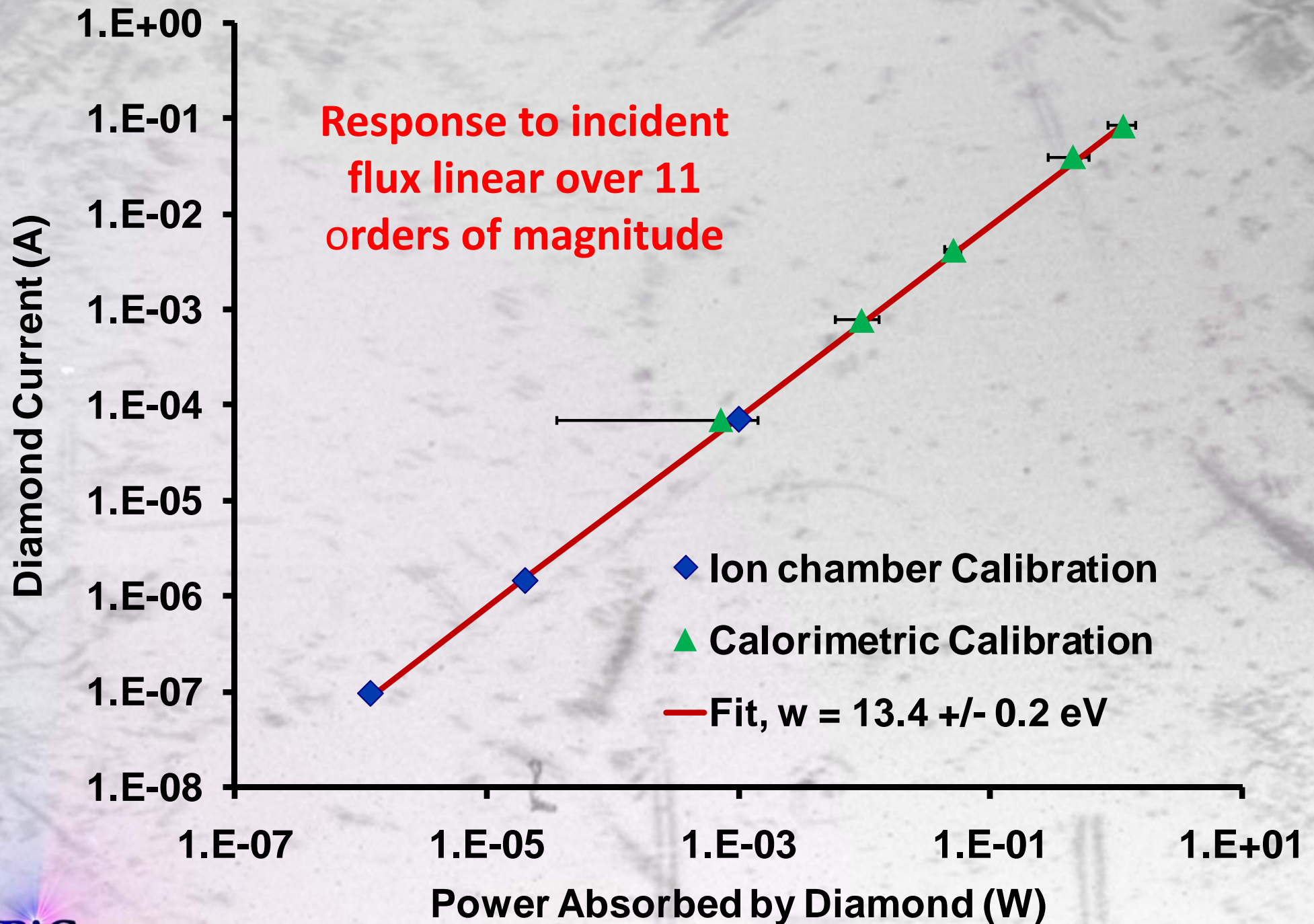


C K edge feature is field dependent, caused by incomplete carrier collection for carriers produced near incident electrode – electrons diffuse into incident contact and are lost

Response vs Bias



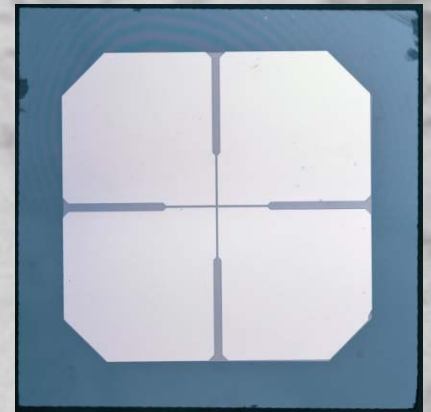
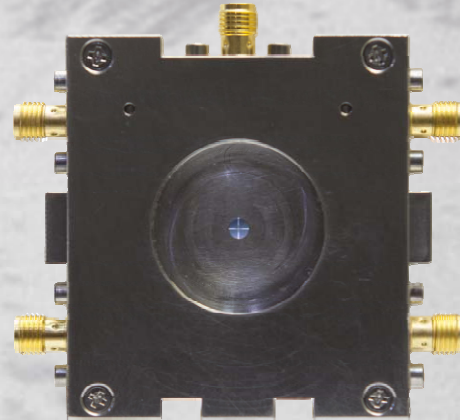
High Flux Response



Diamond Beam Position Monitors

❖ Circuit Board Mounted

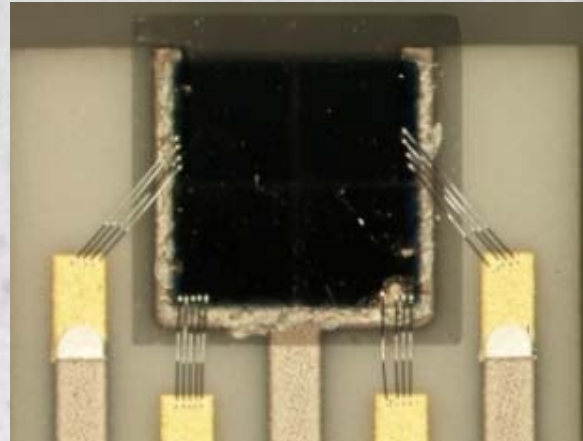
- ❖ Pt metallization
- ❖ wire-bonded electrodes
- ❖ SMA/LEMO connectors



❖ Application specific –

X-Ray fluorescence (X27)

- ❖ Ag diamond metallization
- ❖ Ceramic board
- ❖ 1 cm wide (compact)
- ❖ Ag traces



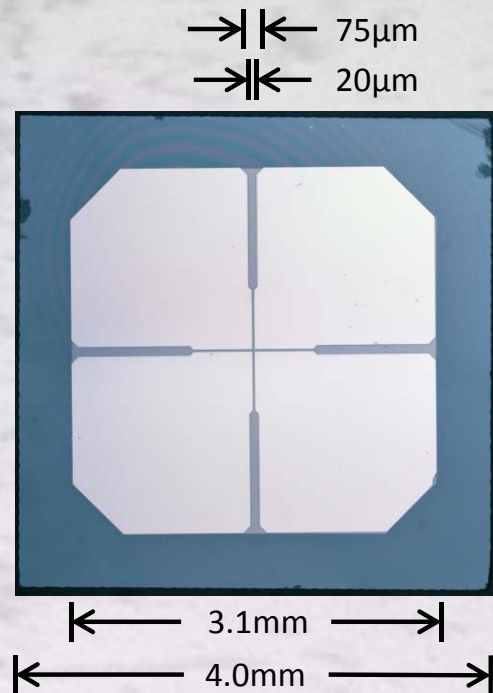
❖ White BPM (X25)

- ❖ Mini-gap undulator
- ❖ ~100W incident power
- ❖ Large beam



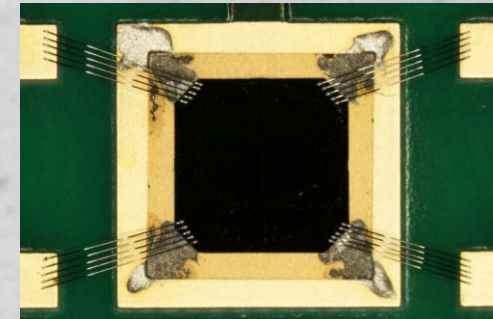
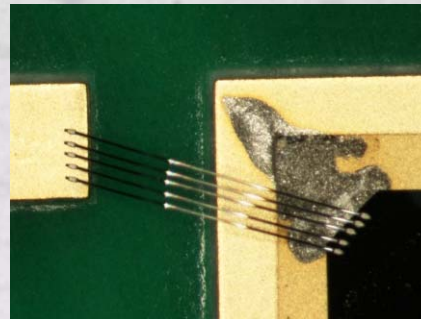
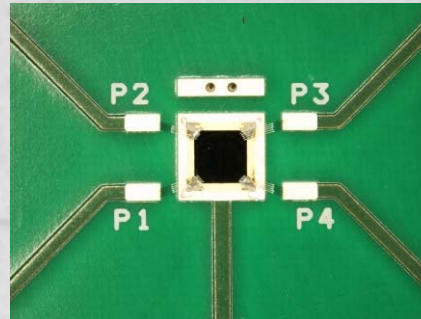
Fabrication

Lithography @ CFN



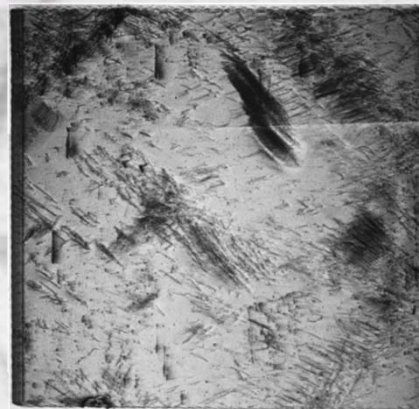
Electronic grade single crystal
(100) diamond
30-50 μm thick
20 μm street over a 1mm
center region
Metalization: 25 nm Pt

Wire Bonding - Instrumentation



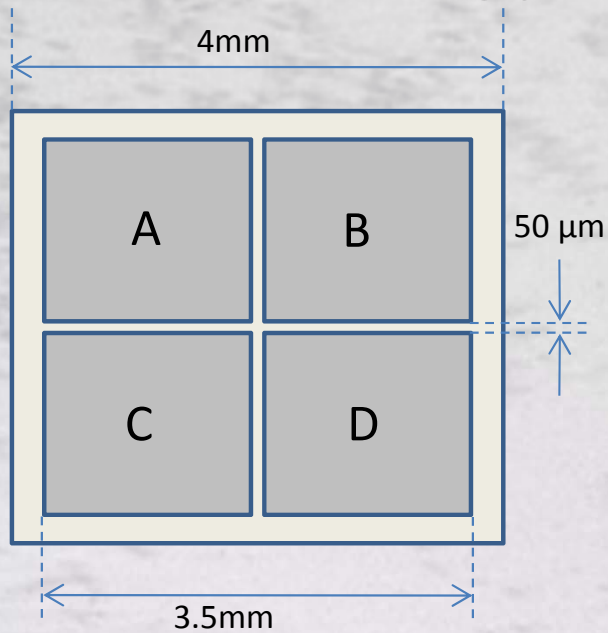
25 μm aluminum
wirebonds
5 bonds per pad
Conductive epoxy for
backside/bias contacts

Topography – NSLS/CHESS

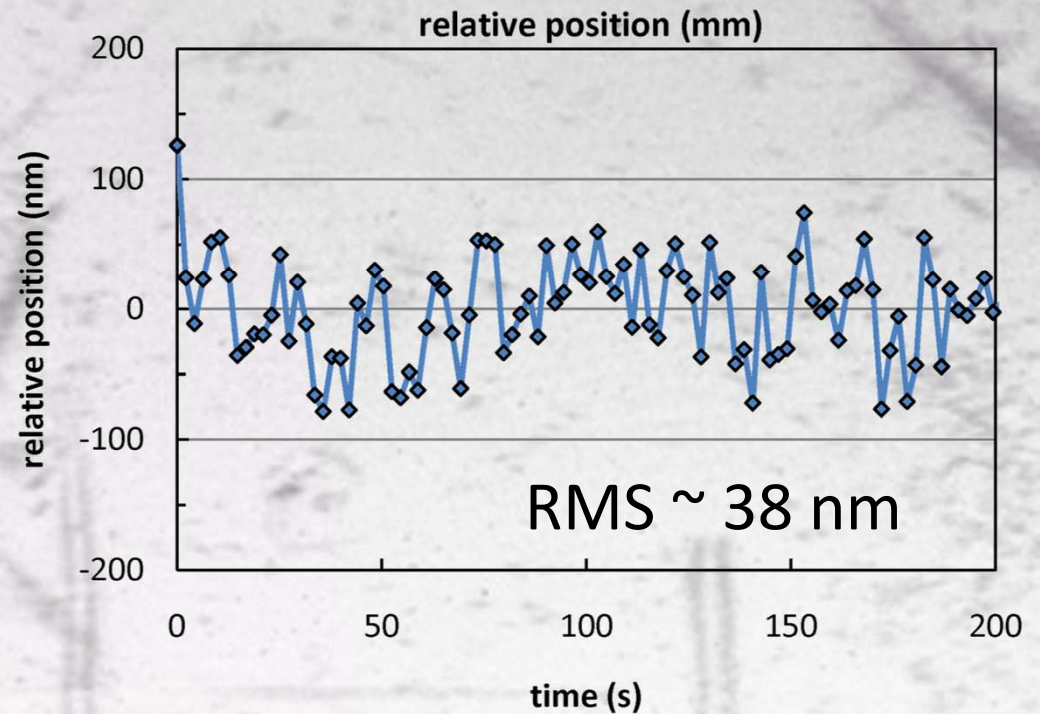
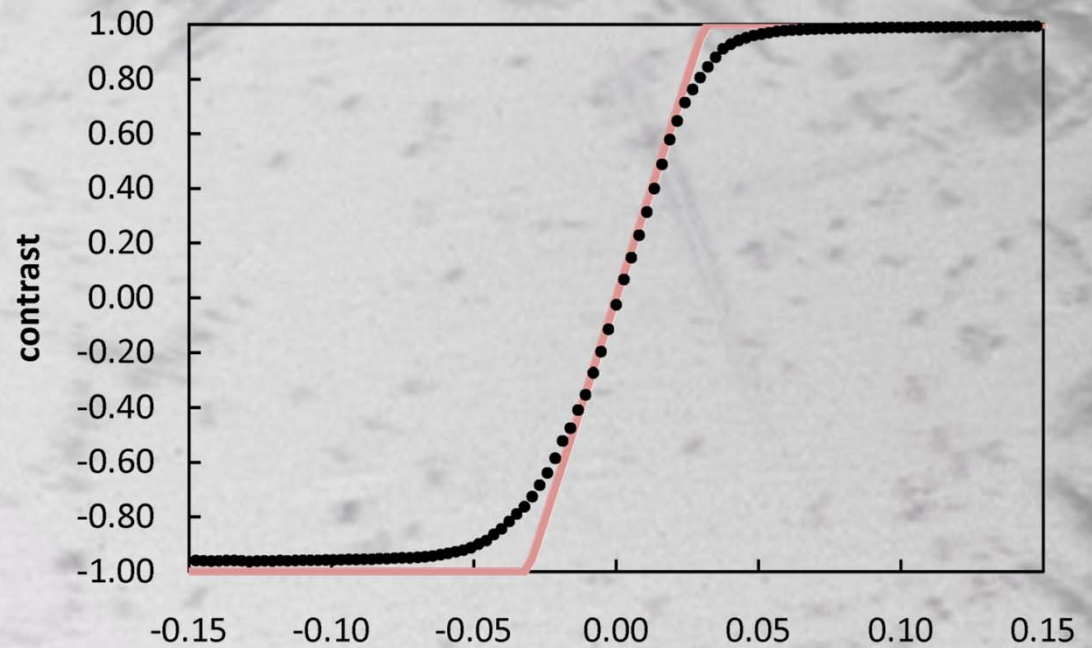
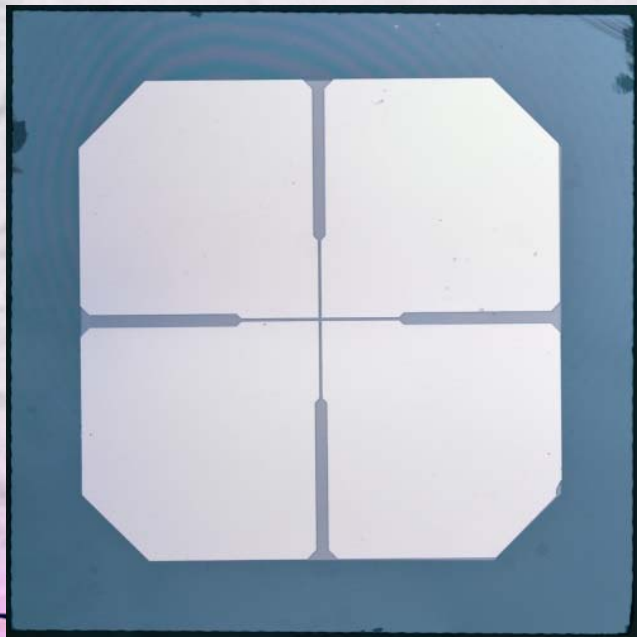


White beam topography
Prior to slicing

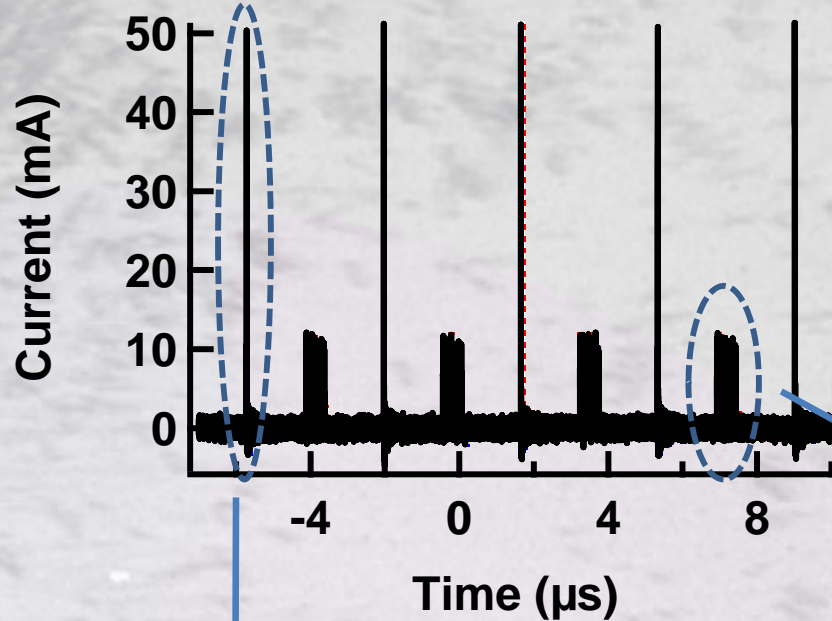
Beam Position Monitors



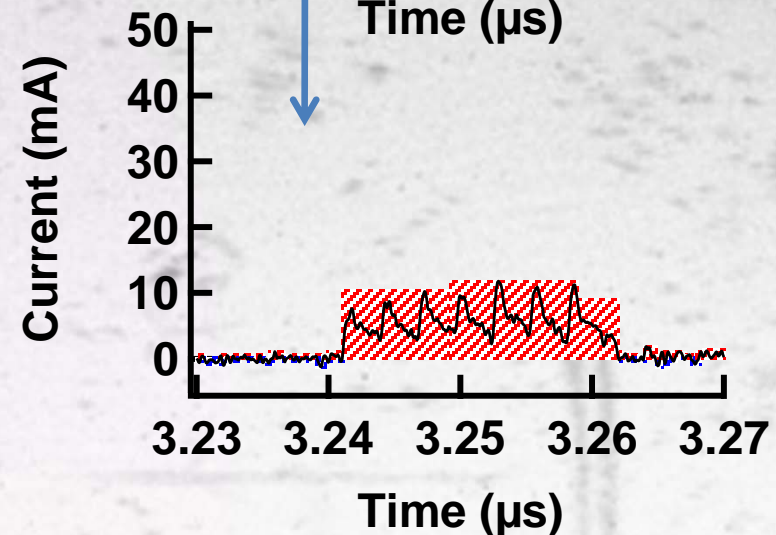
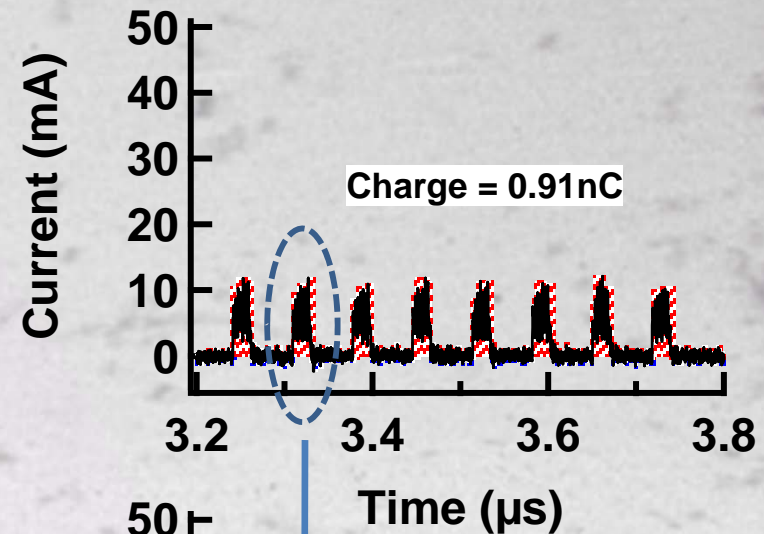
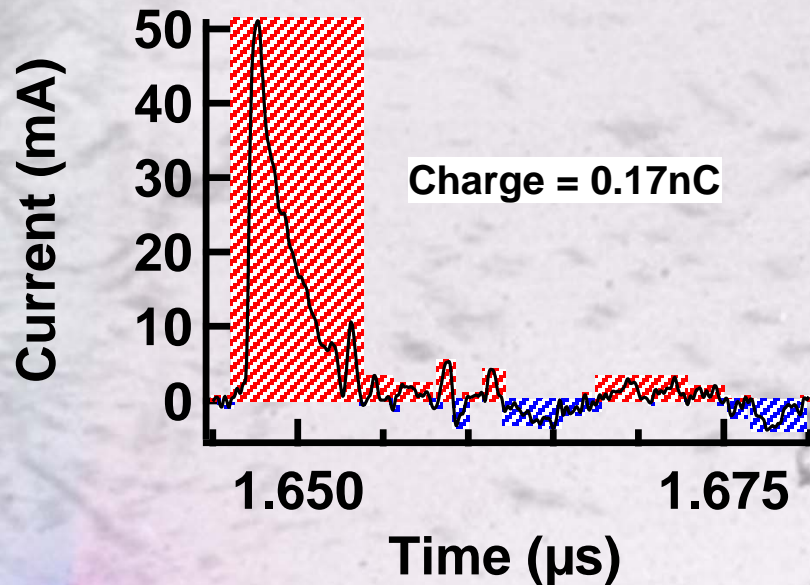
$$X = G_x \frac{(I_B + I_D) - (I_A + I_C)}{I_A + I_B + I_C + I_D}$$



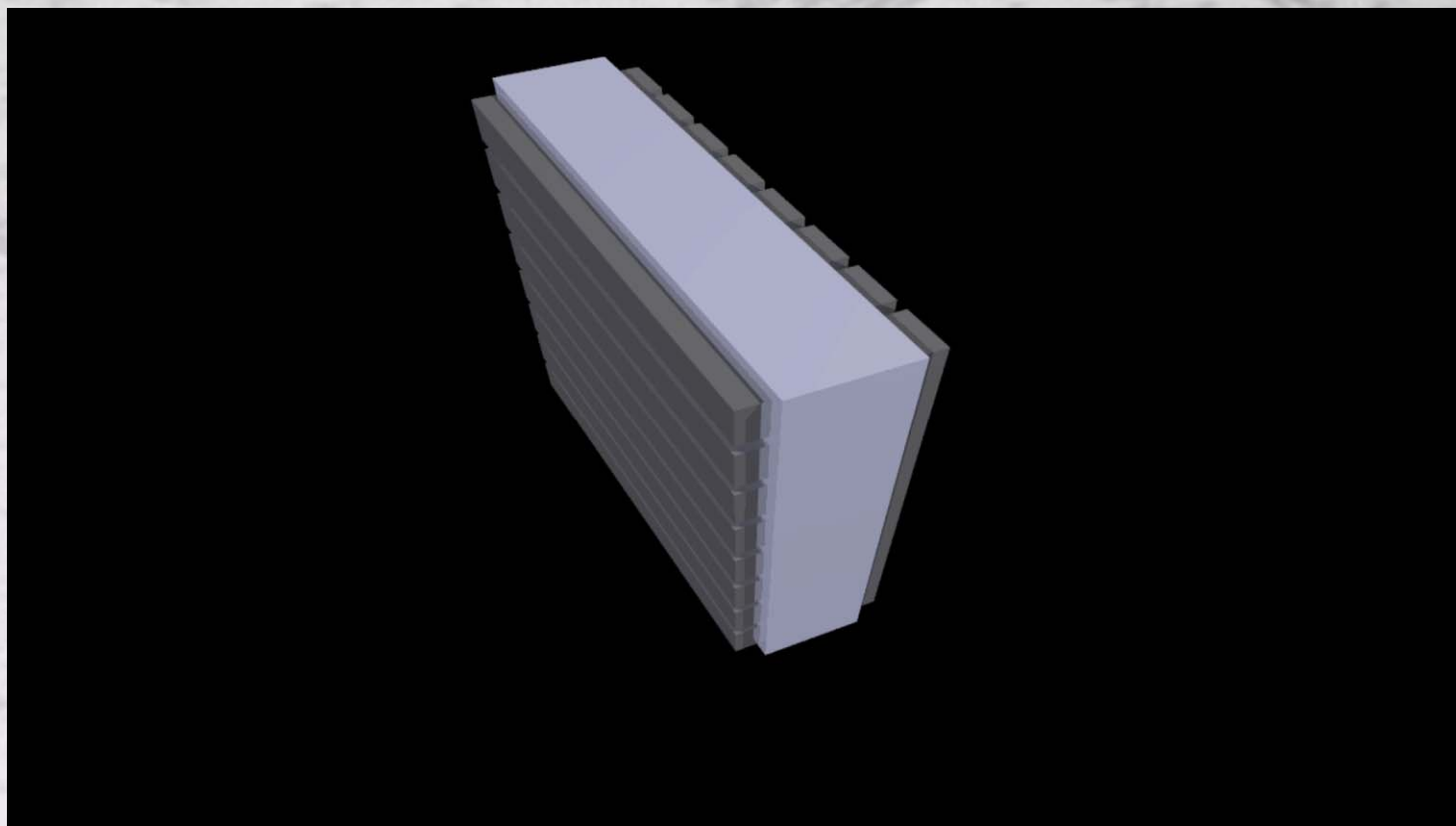
Pulse Mode Beam Position 11-ID-D, APS



- Ring mode “hybrid fill, top up”.
- 102mA total, 16mA in first bunch, 86mA in remaining pulse train.
- Separated by 1.594 μs
- Ratio of ring currents matches very closely to measured charge ratio
- *Current Ratio:* $86\text{mA}/16\text{mA} = 5.38$
- *Measured Q Ratio:* $0.91\text{nC}/0.17\text{nC} = 5.35$



Pixelated Diamond Window



readout animation

Pixels are created by metalizing one side of the diamond with horizontal stripes and the other with vertical stripes. As the x-rays pass through the diamond, the induced current is collected in each vertical stripe, while the bias is applied to individual stripes on the other side. This bias is cycled, allowing readout of one line of “pixels” at a time.

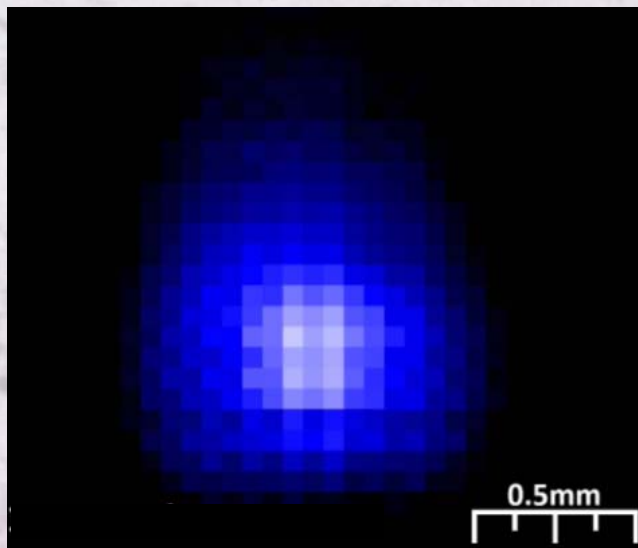
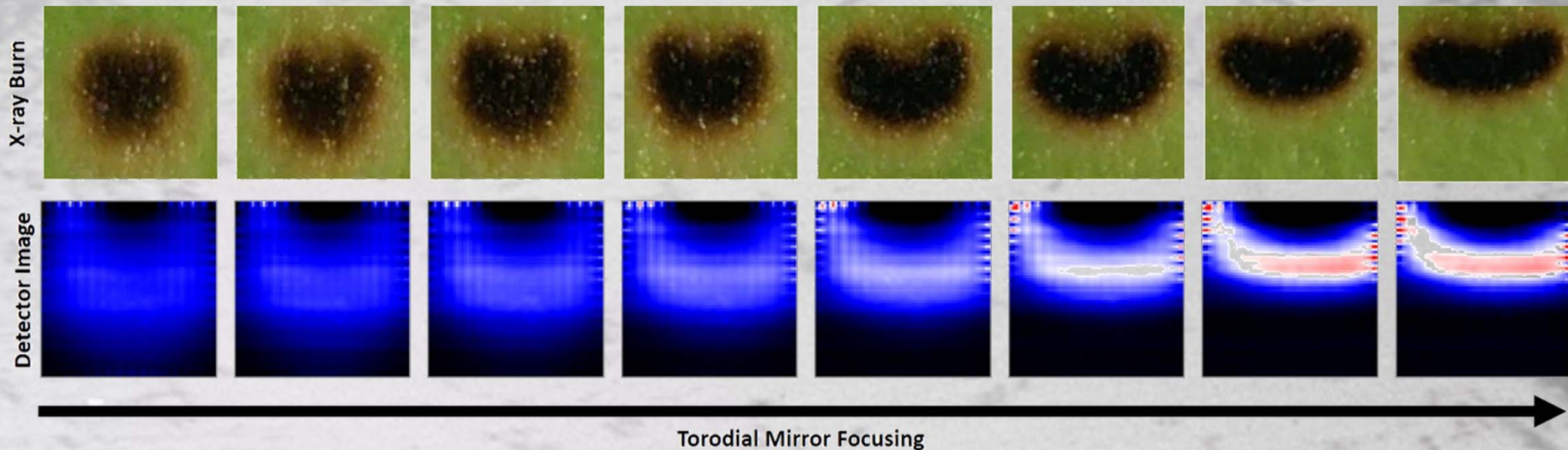
Image Readout

- 32 x 32 stripes, yielding 1024 pixels
- Only one row is active at a time minimizing ohmic heat generation.
- Project goal of real time imaging at 1 Hz, currently at 32 Hz
- Up to ~10mA per pixel

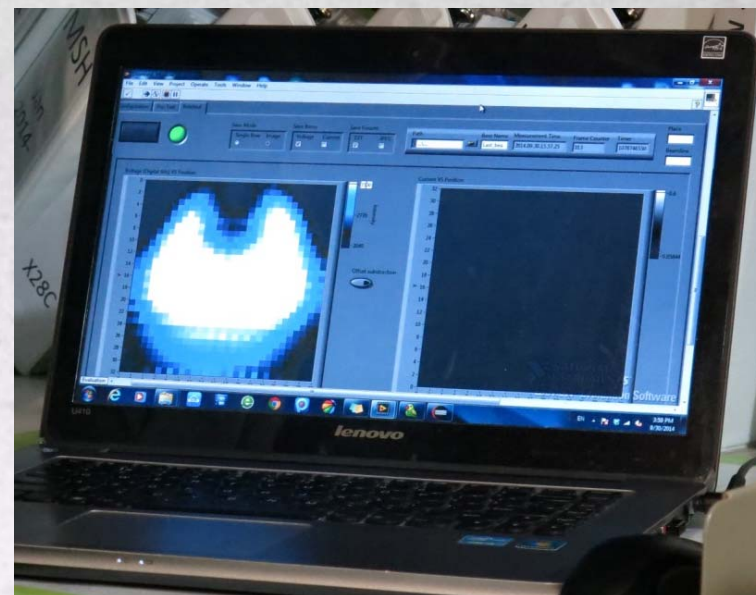
Window Fabrication

- The diamond sensor will be brazed to a stainless steel vacuum flange.
- The diamond and electronic interconnects will be protected by a metal mask.
- Heat dissipation provided by water cooling.

Beam Imaging

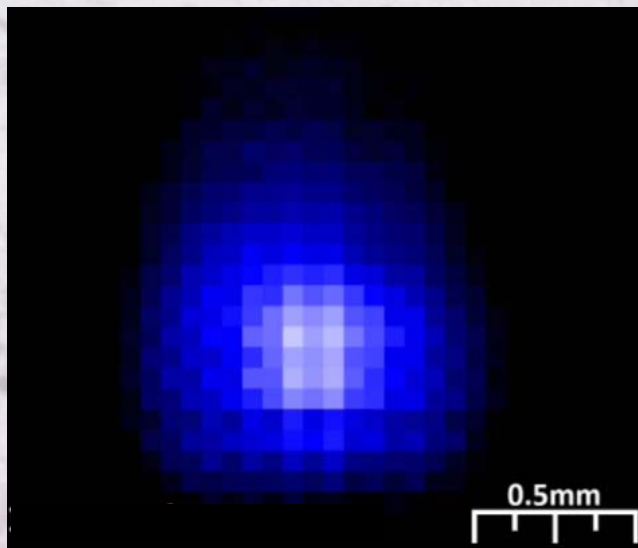
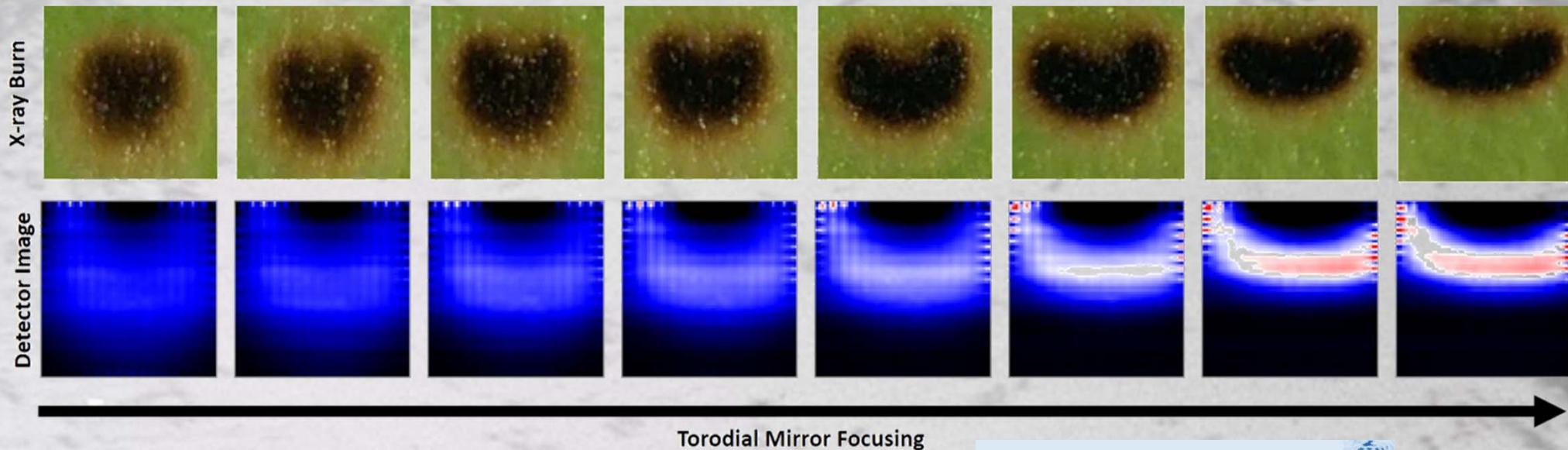


CHES G3 Beam

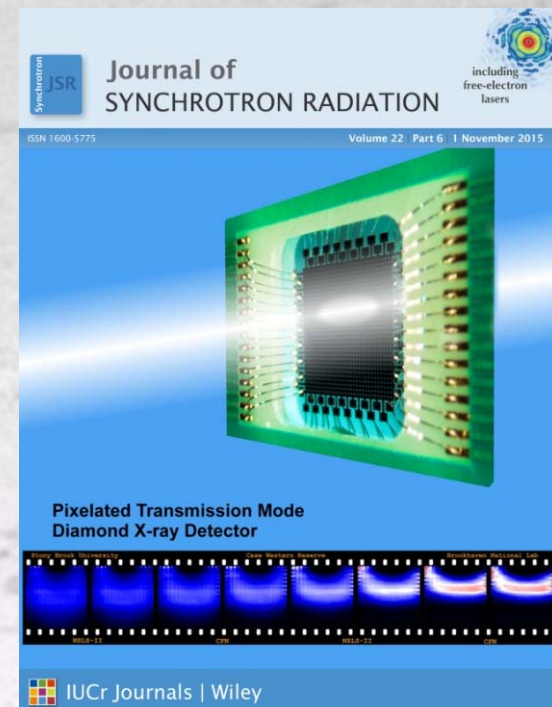


NSLS X28C Beam

Beam Imaging

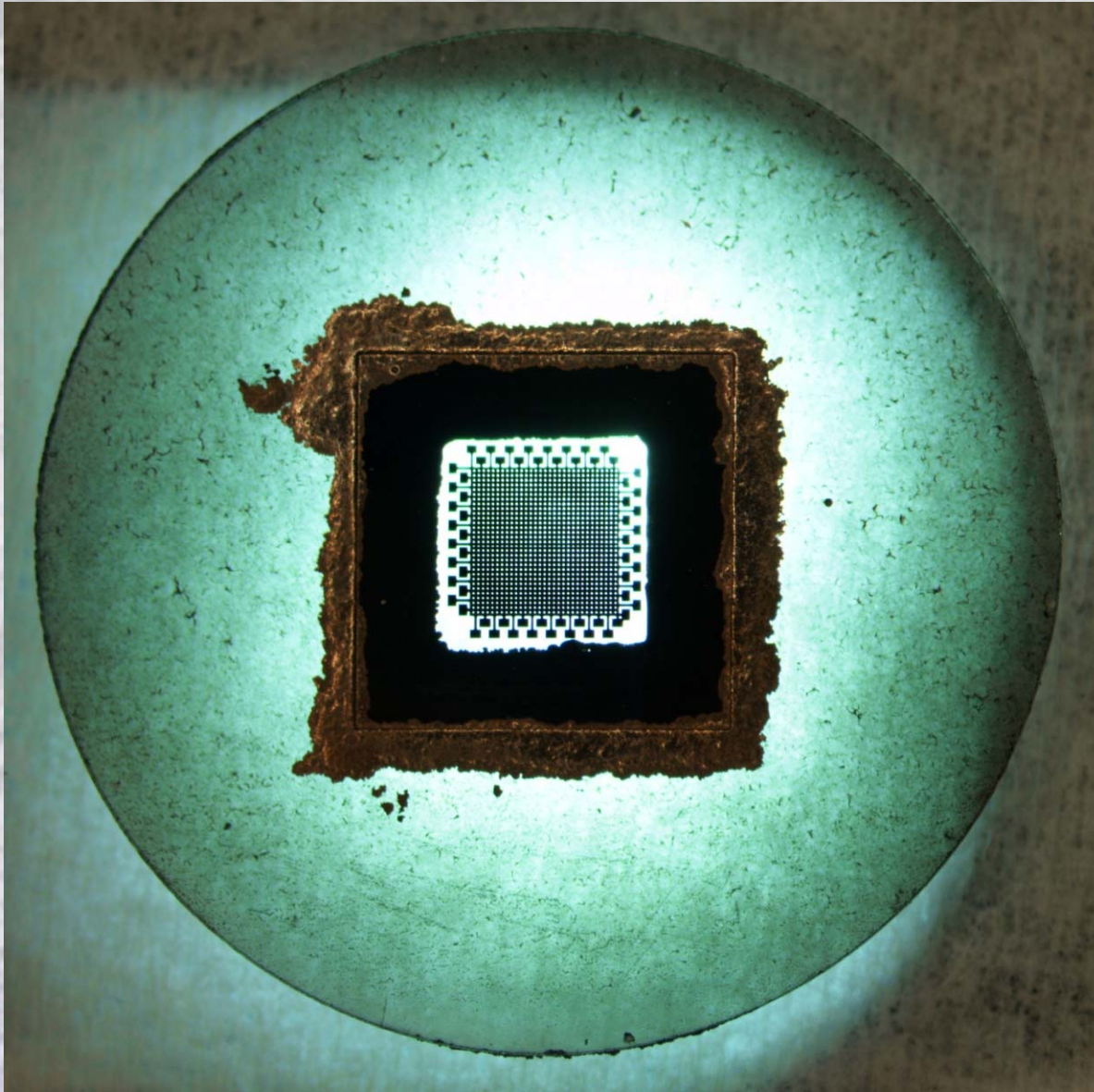


CHES G3 Beam



Zhou et al. (2015) JSR 22 :1396 (cover article)

Brazing the Way to the Instrumented Window



Single Crystal Diamond

- Laser cut and polished by Applied Diamond
- **4.7x4.7x0.054 mm³**

Lithographically patterned

- 60 μm pixels, 2x2 mm² active area
- Platinum metallization

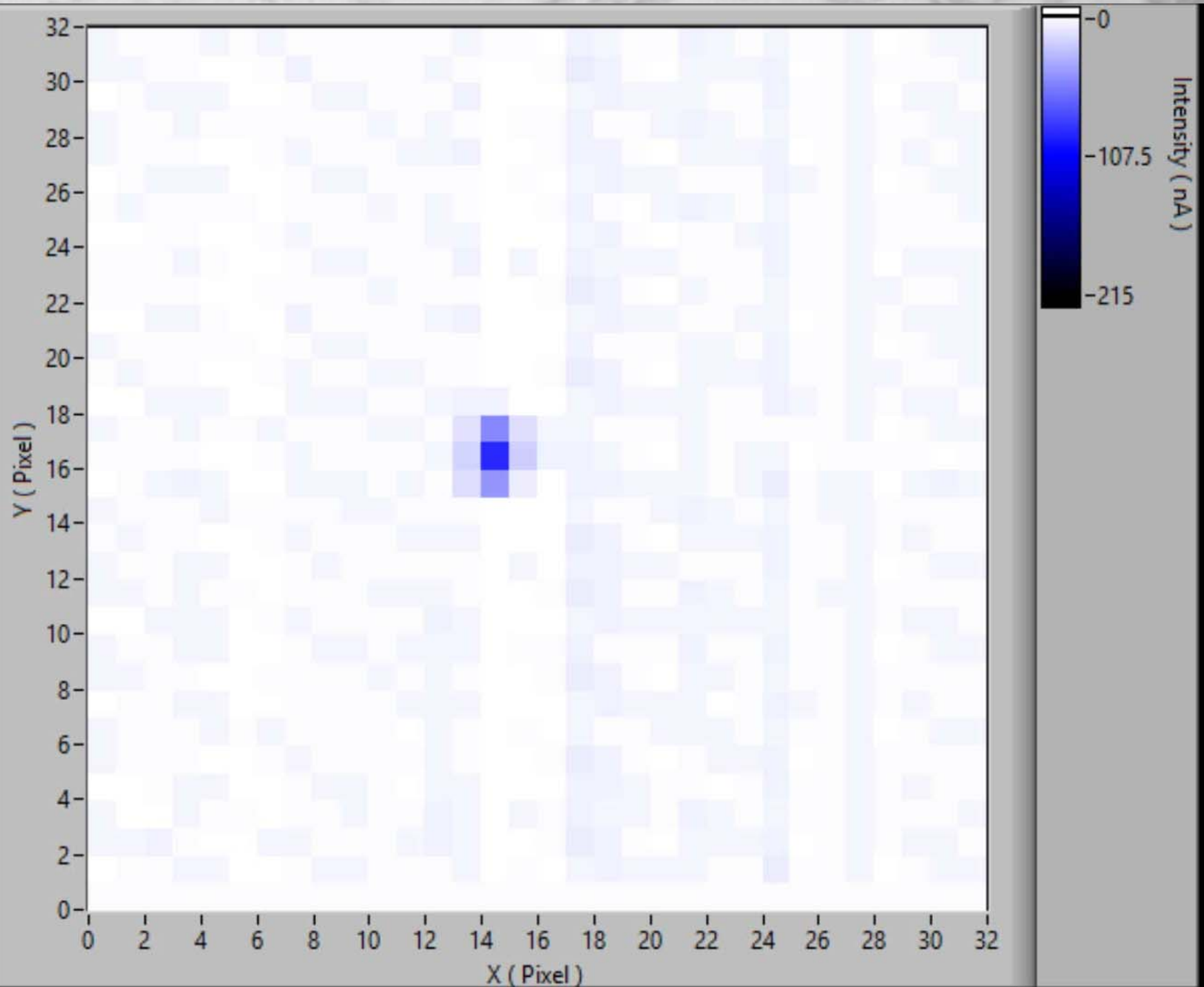
Brazed by Applied Diamond

- 13 mm diameter polycrystalline diamond
- Laser cut 3.3 mm square
- Brazed w/o compromising metallization

Custom boards

- Wirebonded front and back to individual circuit boards as in final device

Brazed Detector Test at CHESS

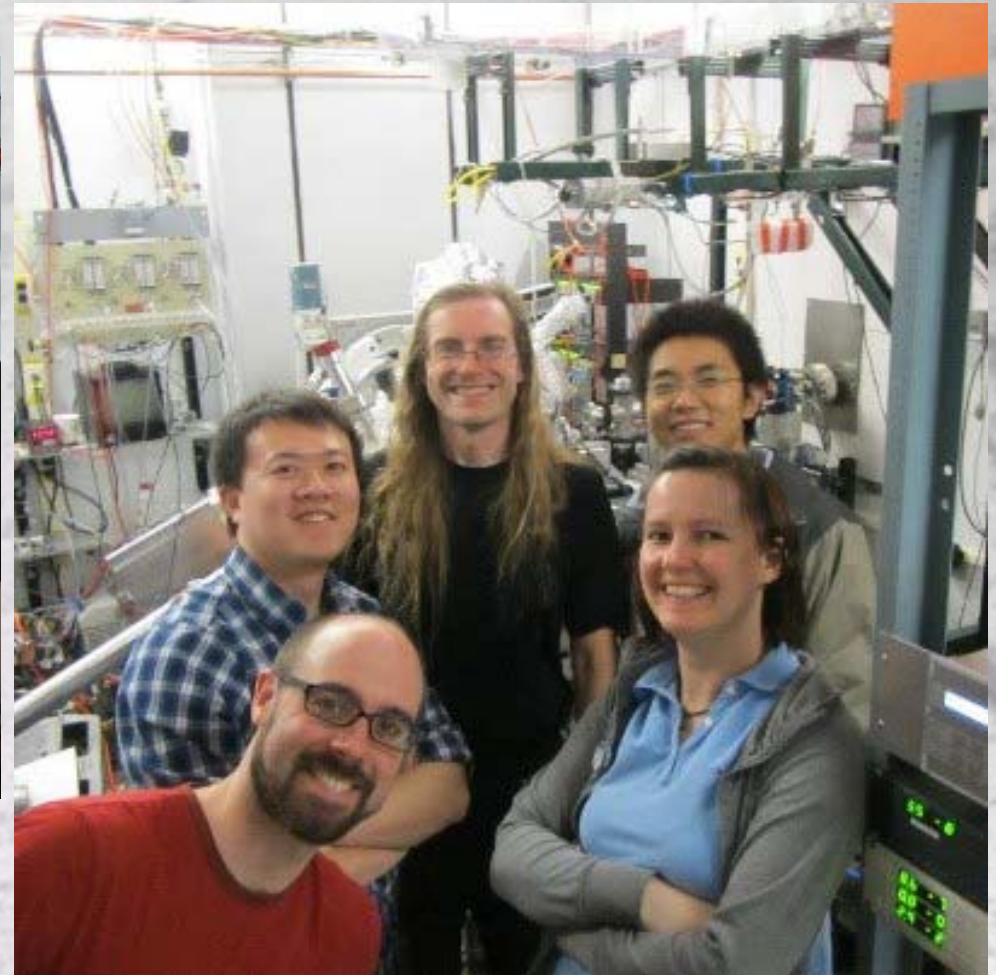
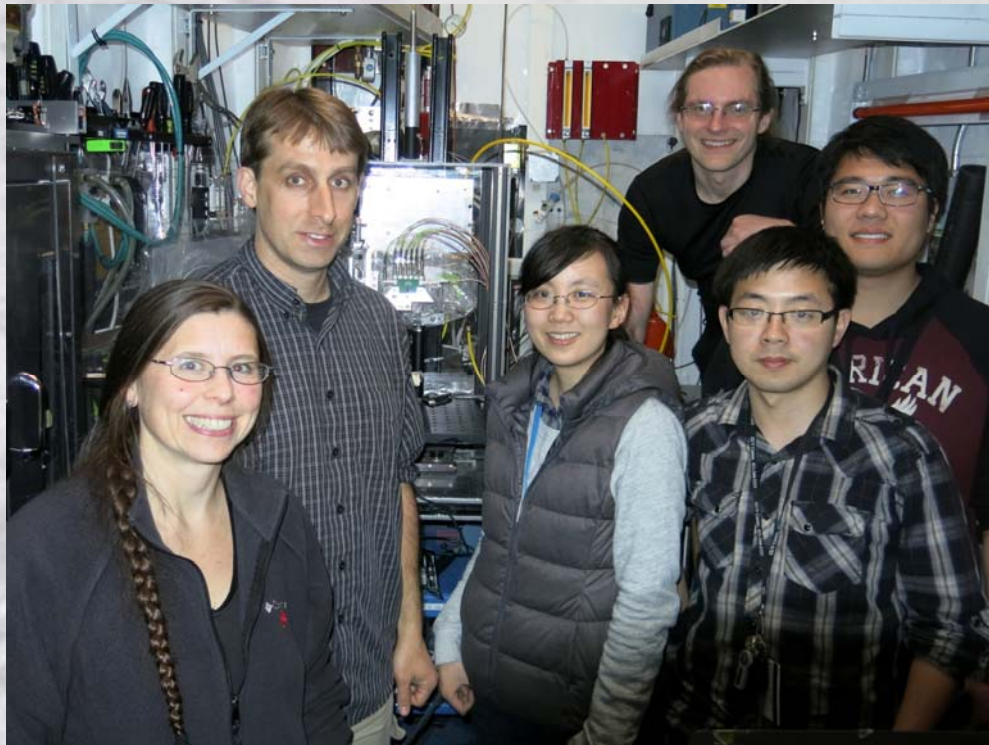


Conclusions

- From Photocathodes to X-ray diagnostics, we can use our tools to build better ones
- Alkali Antimonide cathodes
 - Peak QE of 35% and a green QE of 7.5% have been achieved
 - We can optimize cathodes for structure as well as QE
 - Traditional cathodes are *very* rough... but we are learning to make them smoother
 - Sputter growth may open new opportunities for this material
- Secondary yield
 - Diamond, when operated as an active drift device with NEA, has a SEY of >100
 - SiN with ALD Alumina coating can achieve SEY of 3.5 in “diffusion” mode
- DiamondDetectors
 - Flux linearity demonstrated over ***11 orders of magnitude***
 - Position resolution of better than 50nm, and single bunch flux and position have been achieved
 - 50 devices delivered or on order world wide (APS, CHESS, Diamond, NSLS-II)
 - 1k Pixel beam imaging system demonstrated for both white and monochromatic beams

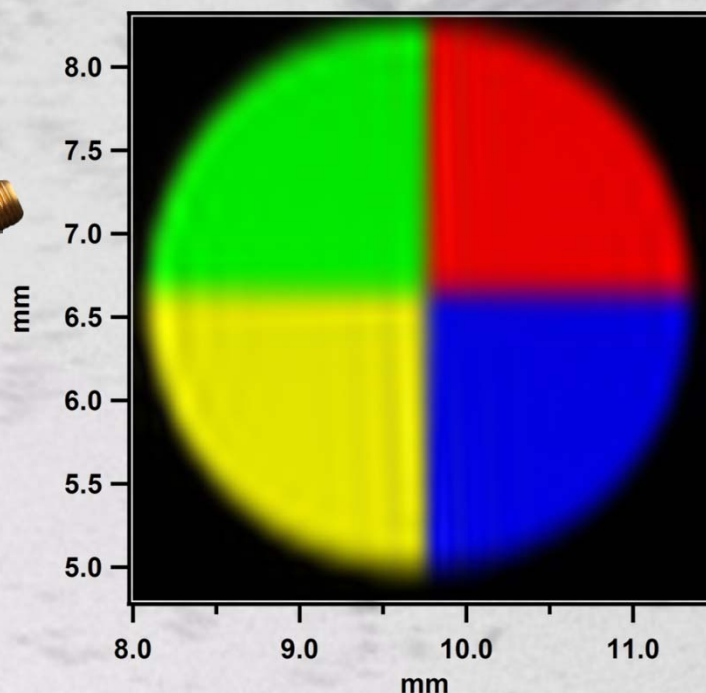
Thank you!

ELECTRON PHOTON INSTRUMENTATION CENTER



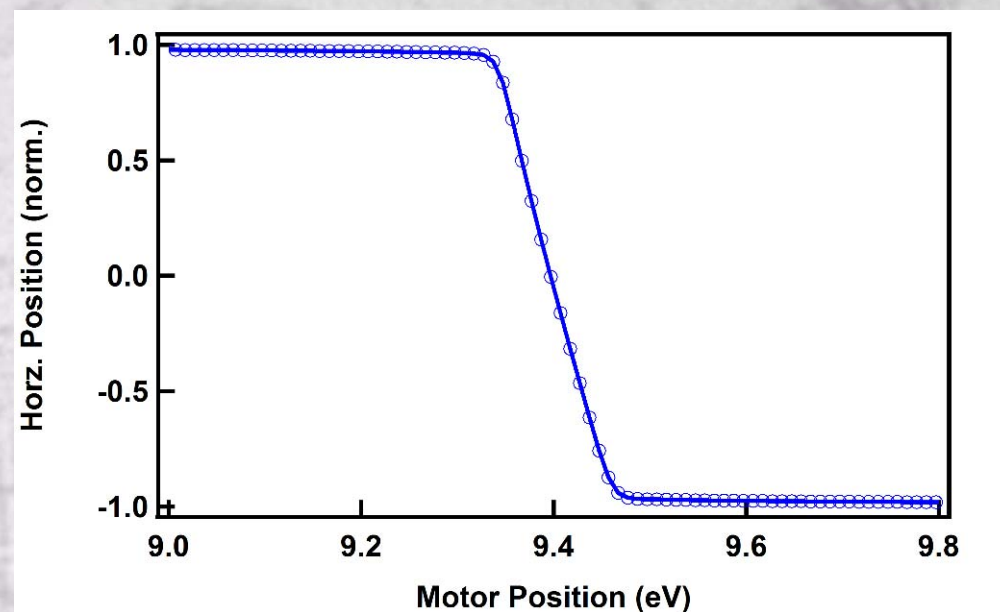
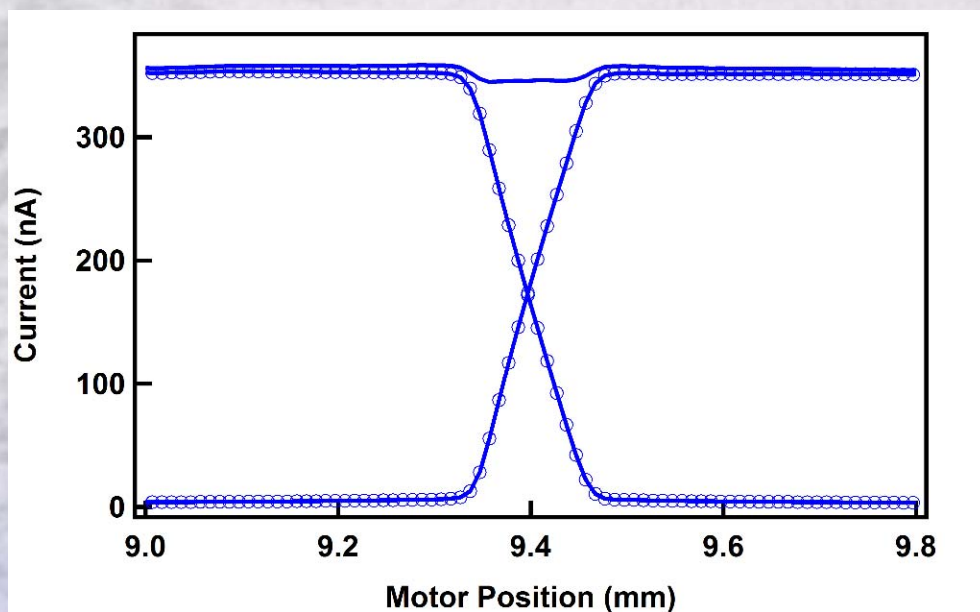
Thanks for your attention!

- Thanks to K. Attenkofer, J. Mead, W. Ding, T. Zhou, M. Maggipinto, A. Della Penna, T. Rao, S. Schubert, M. Ruiz Osés, J. Xie, J. Wang, H. Padmore, E. M. Muller, J. Bohon, J. Mead, M. Gaowei, A. Héroux, L. Berman, M. Sullivan, R. Beuttenmuller, J. Jordan-Sweet, J. Keister, A. Sumant, E. DiMasi, J. Walsh, B. Raghothamachar, J. Distel, K. Vetter, G. DeGeronimo, B. Dong, D. Dimitrov, D. Pinelli, J. Skinner, M. Cowan, S. Ross, R. Tappero, B. Ravel, C. Jaye, D. Fischer, M. Lu, F. Camino, D. Abel, I. Ben-Zvi, T. Vecchione, X. Liang, J. Rameau, P. Johnson, J. Sinshiemer, **H. van der Graff and the MEMBrane collaboration**
- Beamlines (and staff): U2A, U2B, U3C, U7A, U13, X3B, X6B, X8A, X15A, X16C, X19C, X20A&C, X21, X23, X24, X25, X28C & APS ID 11D & CHESS G3
- DOE Office of Science – Basic Energy Science and High-Energy Physics, NSF IDBR Program

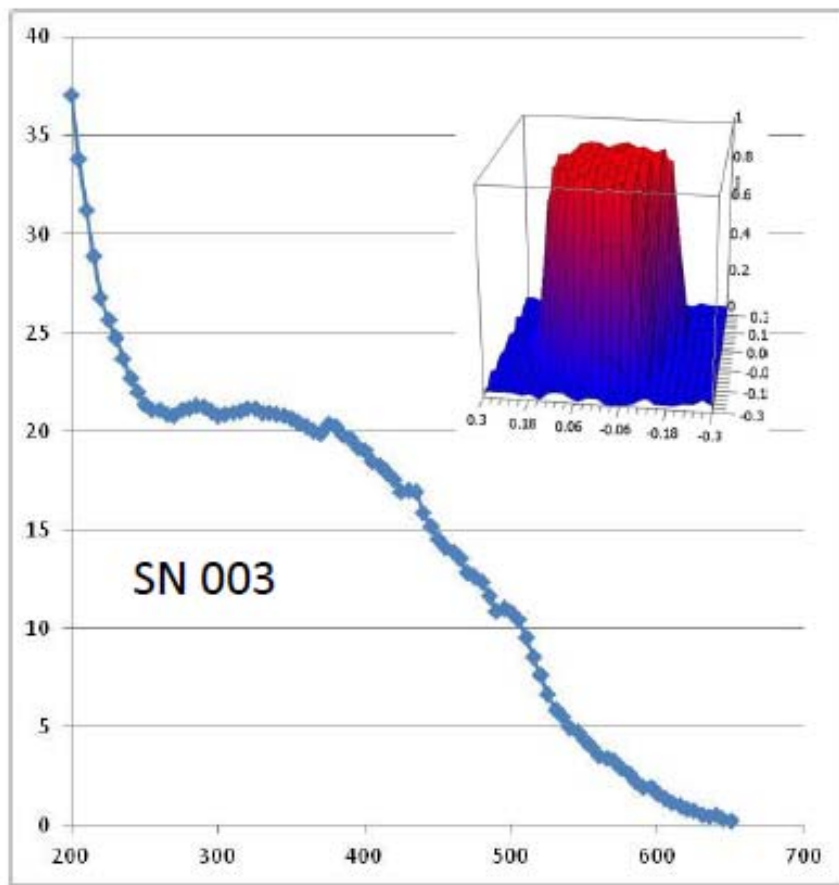


Quad detectors for NYSBC

- 2 quad detectors (65 μ m and 80 μ m thick)
- 3.6mm x 3.6mm x 30nm Pt contacts, 20 μ m streets
- High thermal conductivity ceramic circuit board (Beryllia)
- Integrated vacuum seal
- Operating voltage 10V.
- Self-aligning defractometer



Sealed Capsule Photocathodes

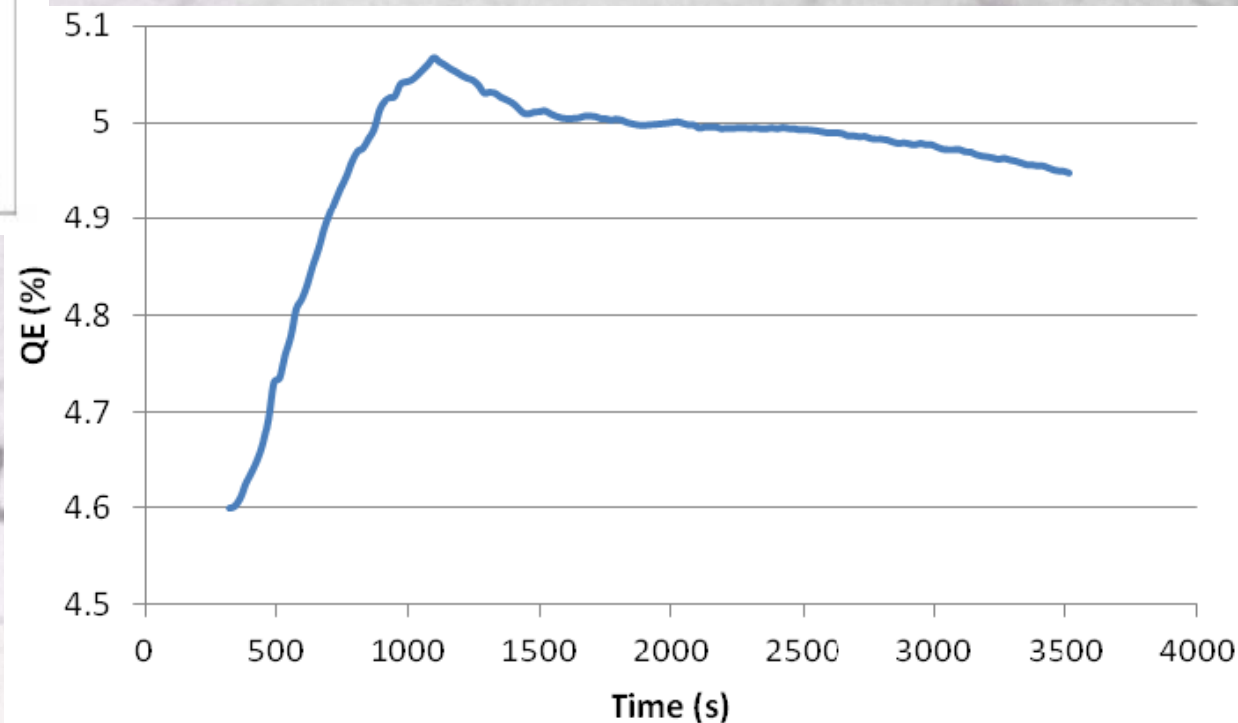


Photonis USA, using detector growth process

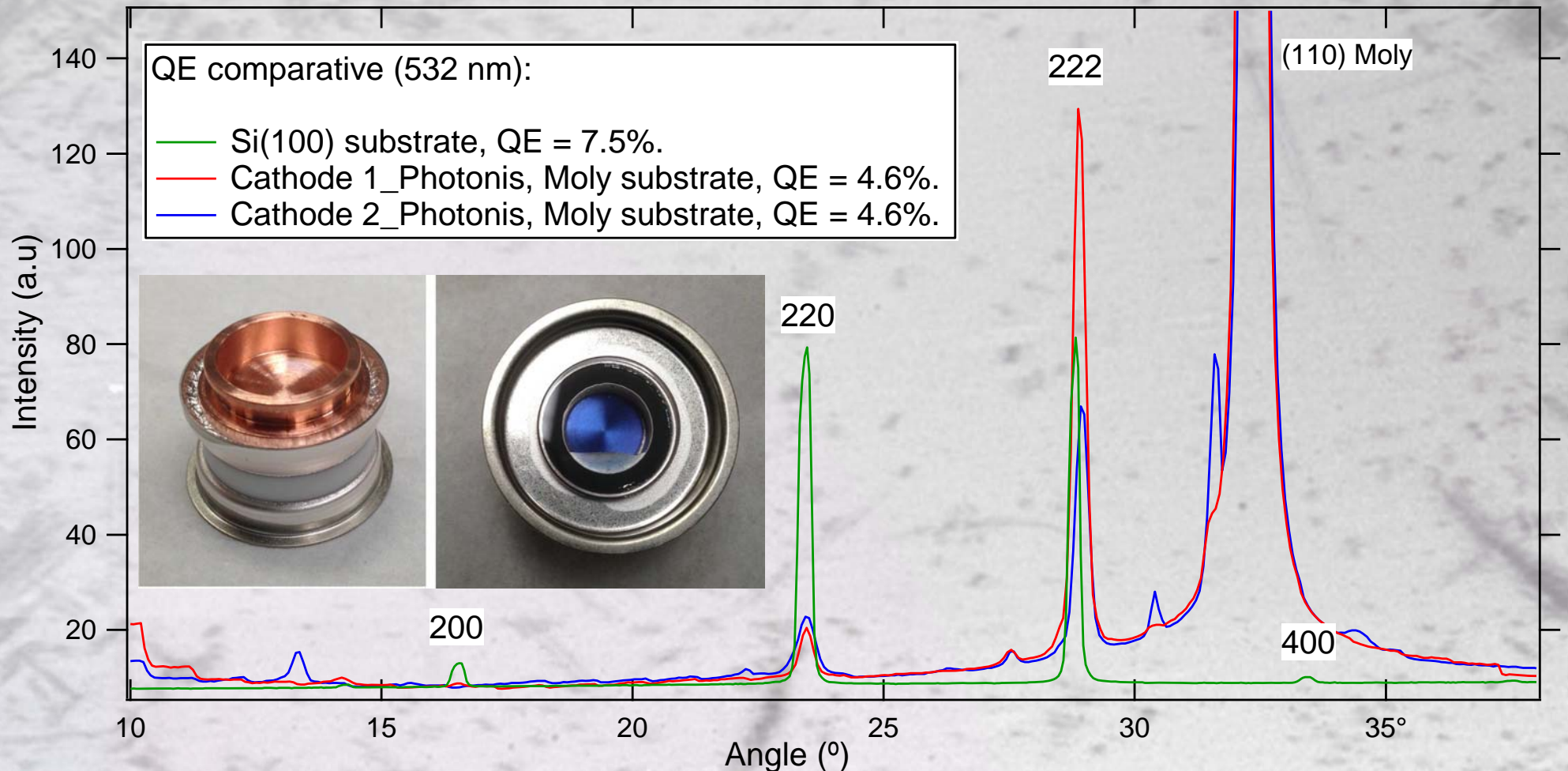
Shelf life of months at least

NaK_2Sb available

QE drops during heating to remove cap, but recovers



Sealed Capsule Photocathodes

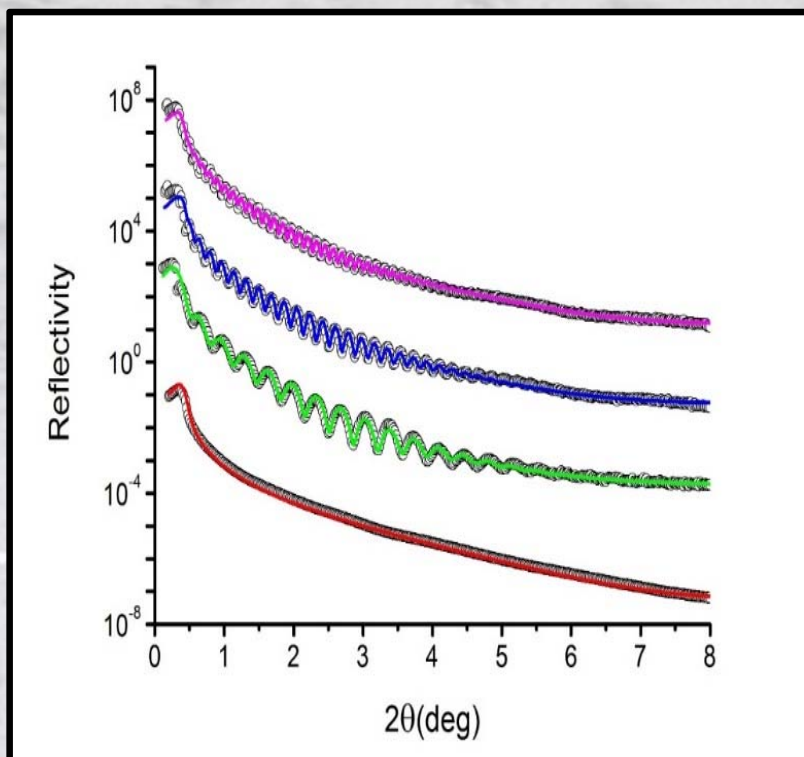


Comparison to Photonis commercial PMT cathode

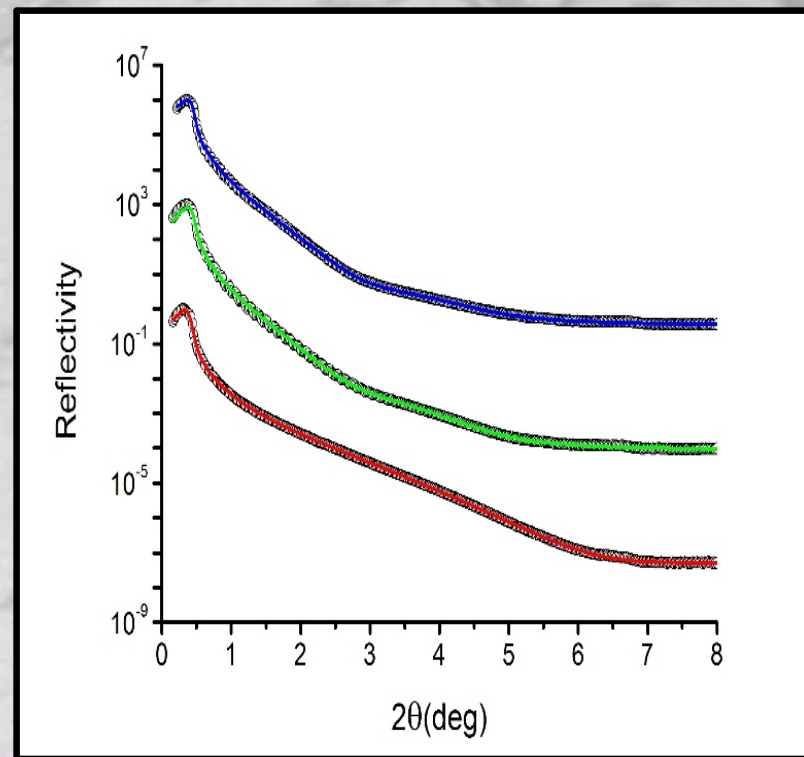
Similar texture (222 surface normal preferred)

Broader peaks imply smaller grain size

(50 nm for BNL cathode, 39 nm for Photonis cathode)



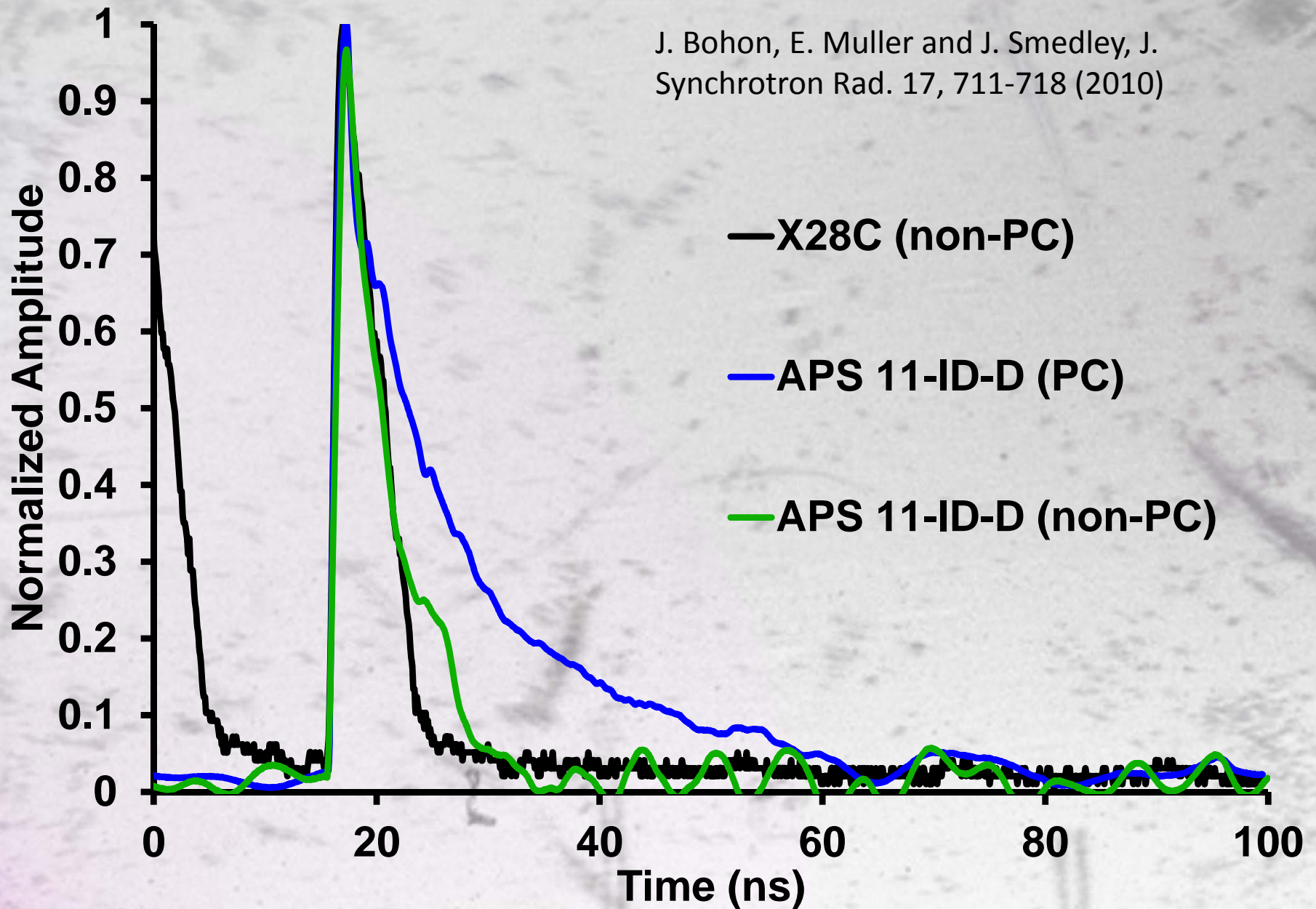
layer	Roughness(Å)	Thickness(Å)
3 rd layer	6.87 (-0.17, 0.19)	512 (-1.17, 1.30)
2 nd layer	6.20 (-0.19, 0.33)	336 (-1.35, 1.04)
1 st layer	6.05 (-0.23, 0.18)	178 (-0.54, 0.47)
Substrate (MgO)	2.43 (-, -)	



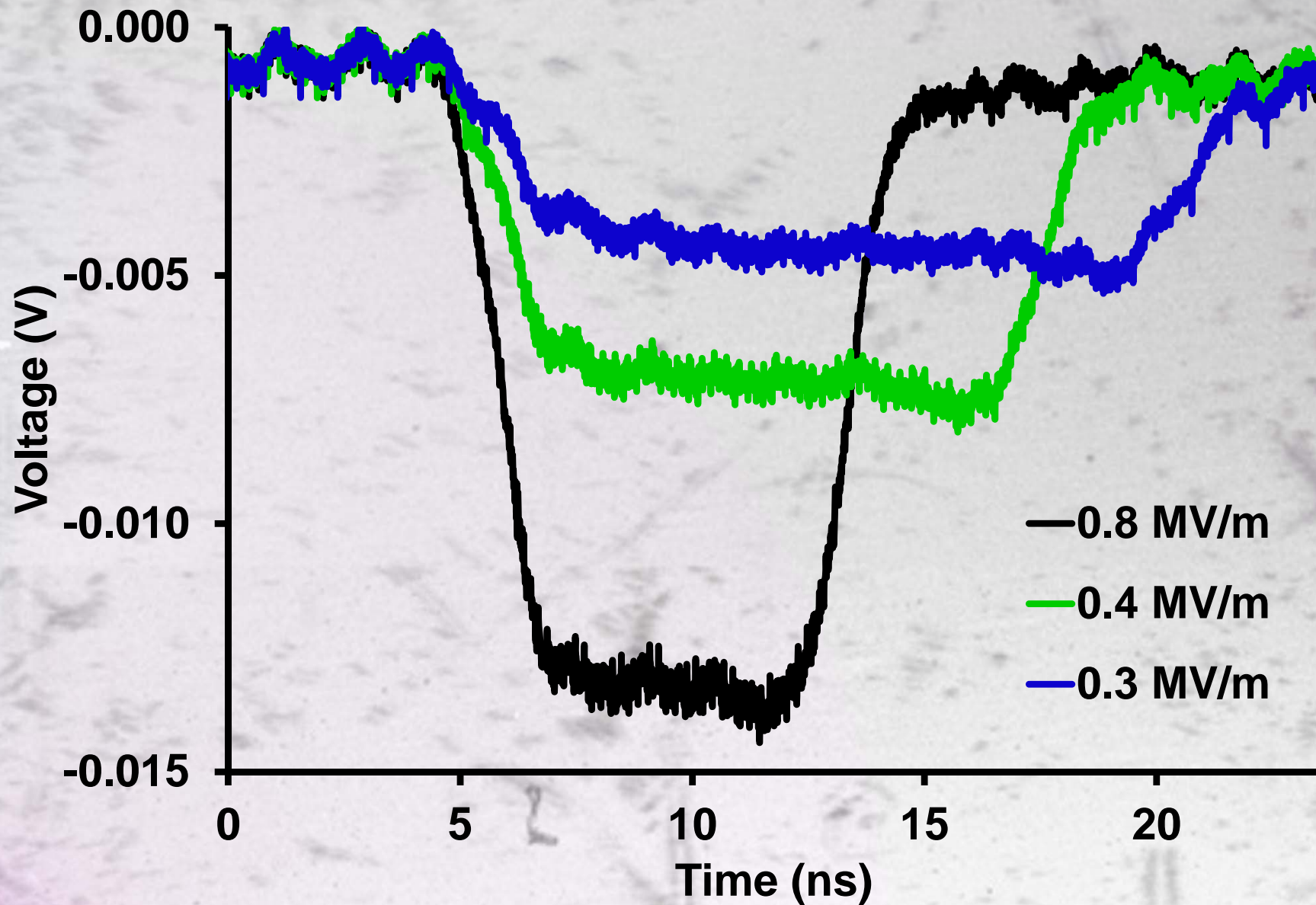
layer	Roughness(Å)	Thickness(Å)
After Cs	7.56 (-0.20, 0.13)	776.0 (-75.7, 71.0)
1 st layer	8.21 (-0.068, 0.13)	555.4 (-2.6, 3.3)
Substrate (MgO)	3.93 (-0.03, 0.03)	

Temporal Response, Hard X-rays

J. Bohon, E. Muller and J. Smedley, J.
Synchrotron Rad. 17, 711-718 (2010)



Temporal Response, Soft X-rays



What do we want out of an electron source?

- The electron beam properties determine the photon beam properties
 - Pulse duration, degree of coherence, flux
- In all light sources through 3rd generation, the phase space is determined by the ring

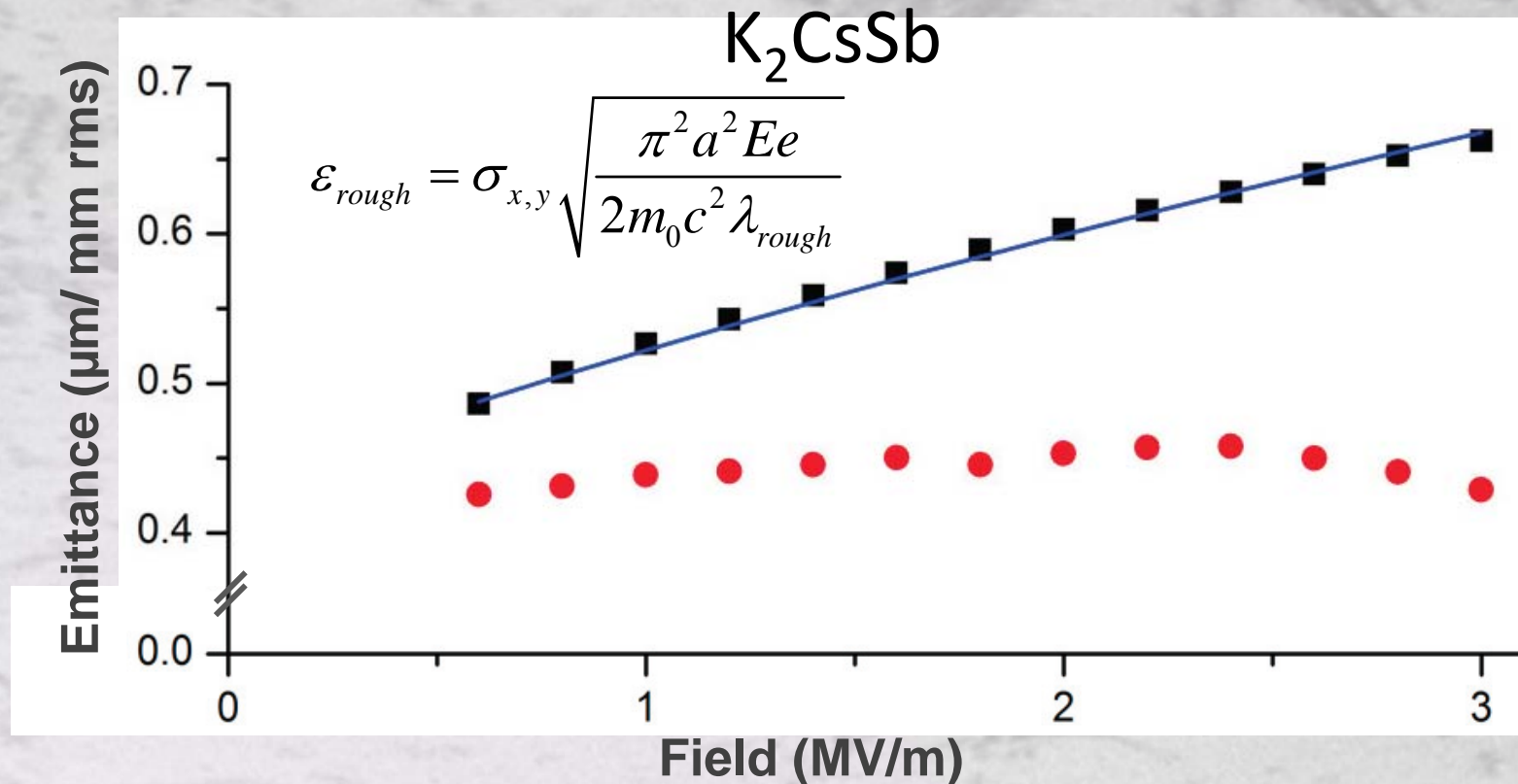


- In 4th generation sources (LCLS, XFEL, NGLS), this will change
 - the electron source will determine the beam properties
- The highest brightness sources available are photoinjectors, which use a laser on a photocathode to control the spatial and temporal profile of the emitted electron beam

What do we want out of photocathode?

- High Brightness: $B = \frac{N_e}{\varepsilon_{nx}\varepsilon_{ny}\varepsilon_{nz}}$
 - large number of electrons in a small volume of phase space
 - Low Emittance: $\varepsilon_n = \sigma_x \sqrt{\frac{\hbar\omega - \phi_{eff}}{3mc^2}}$
 - Determines the electron energy required for an X-FEL at a given wavelength $\varepsilon \approx \frac{\lambda}{4\pi} \Rightarrow \frac{\varepsilon_n}{\beta\gamma} \approx \frac{\lambda}{4\pi}$
 - High Quantum Efficiency
 - High Average Current
 - Long Operational Lifetime
 - Chemical Contamination
 - Ion back bombardment
 - Sub-ps response time
- The optimal cathode is still a work in progress*
- It is becoming increasingly clear that material parameters such as texture and surface roughness may play an important role*

Effects of roughness seen in the emittance of thick multilayer



Thin films grown at high rate give ~ expected emittance (very low field dependence)

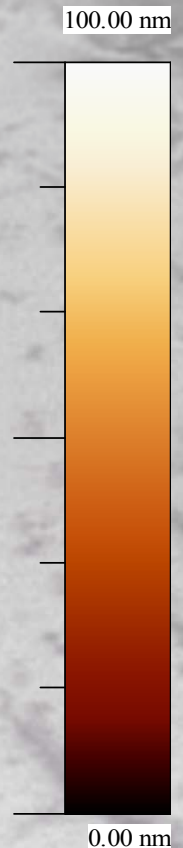
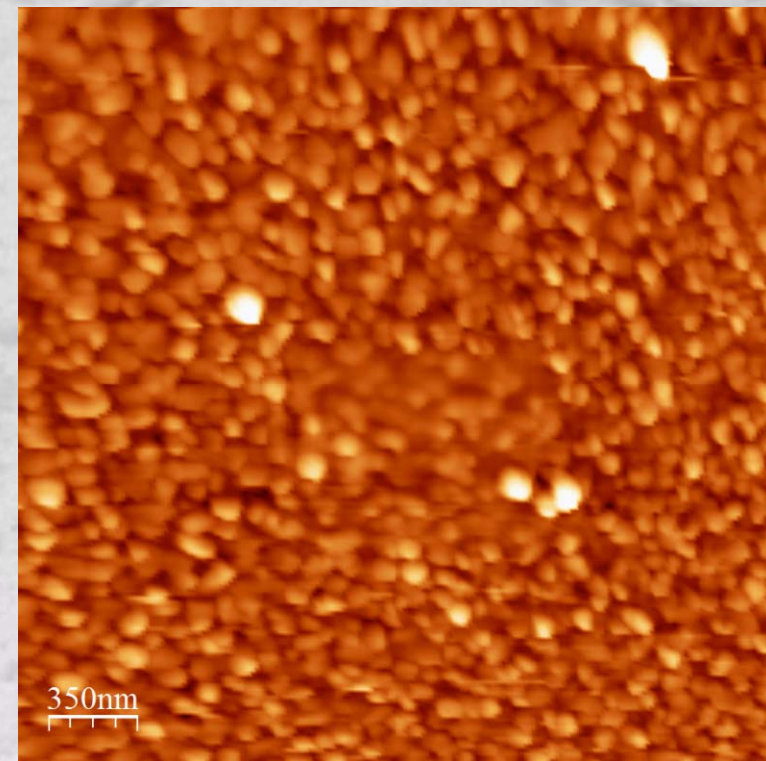
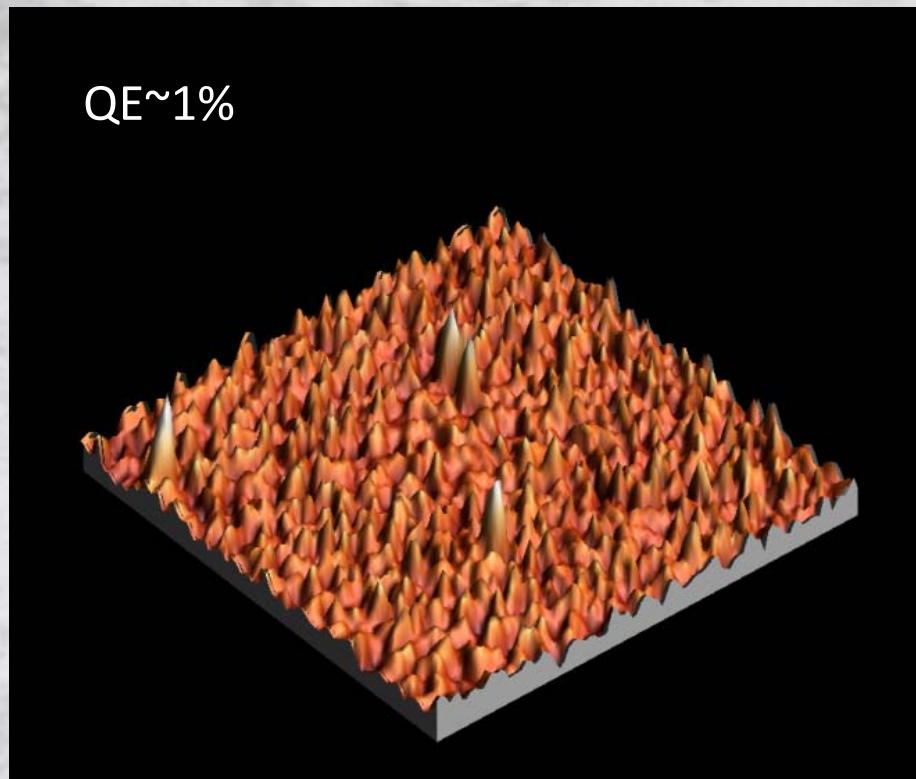
Films grown in a multilayered manner were shown to give higher QE but showed marked emittance growth with field

Can be explained by invoking a simple roughness model.

Fitting gave reasonable roughness parameters, confirmed by in vacuum AFM

Roughness in high gradient guns looks to be an issue based on current in-situ measurements of cathode surfaces

in-situ AFM on cathode at CFN



10 nm Antimony film evaporated at room temperature

Potassium and Cs added by monitoring QE

Should result in a 50 nm thick final film

Observed **25 nm** RMS roughness, with a 100 nm spatial period

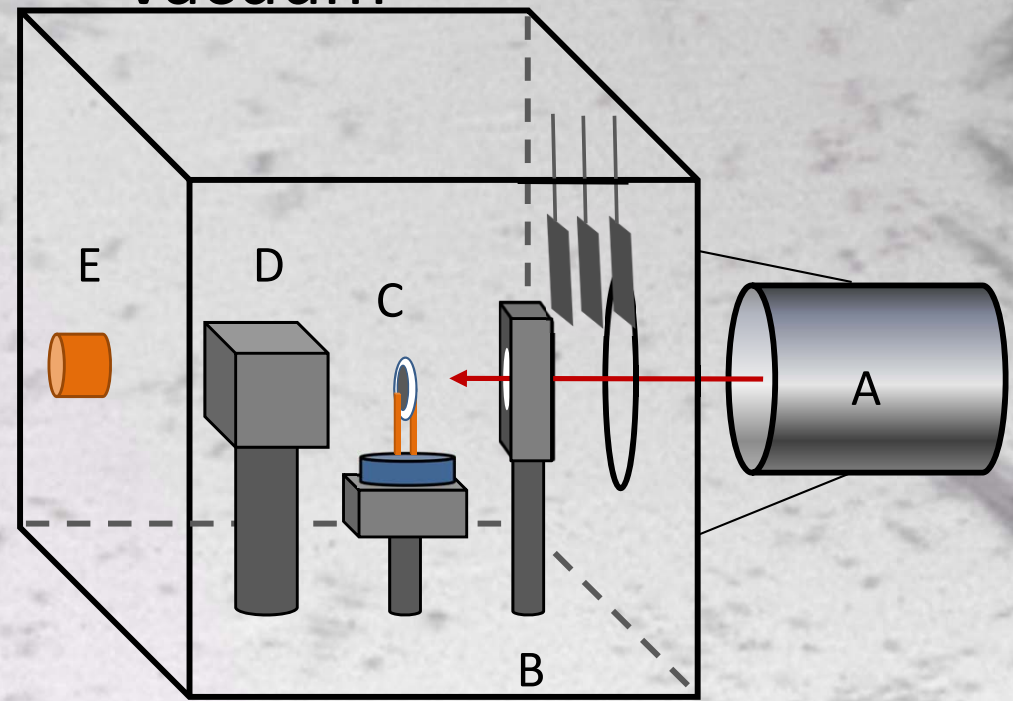
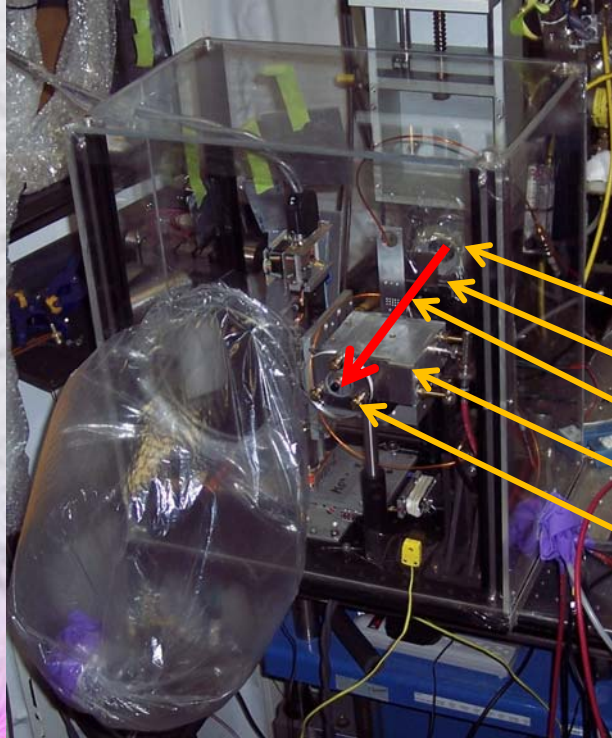
Nano-pillars of uniform height – consistent with XRR and GISAXS

Likely the source of the Field dependence of the intrinsic emittance

S. G. Schubert, et al, APL Mater. **1**, 032119 (2013)

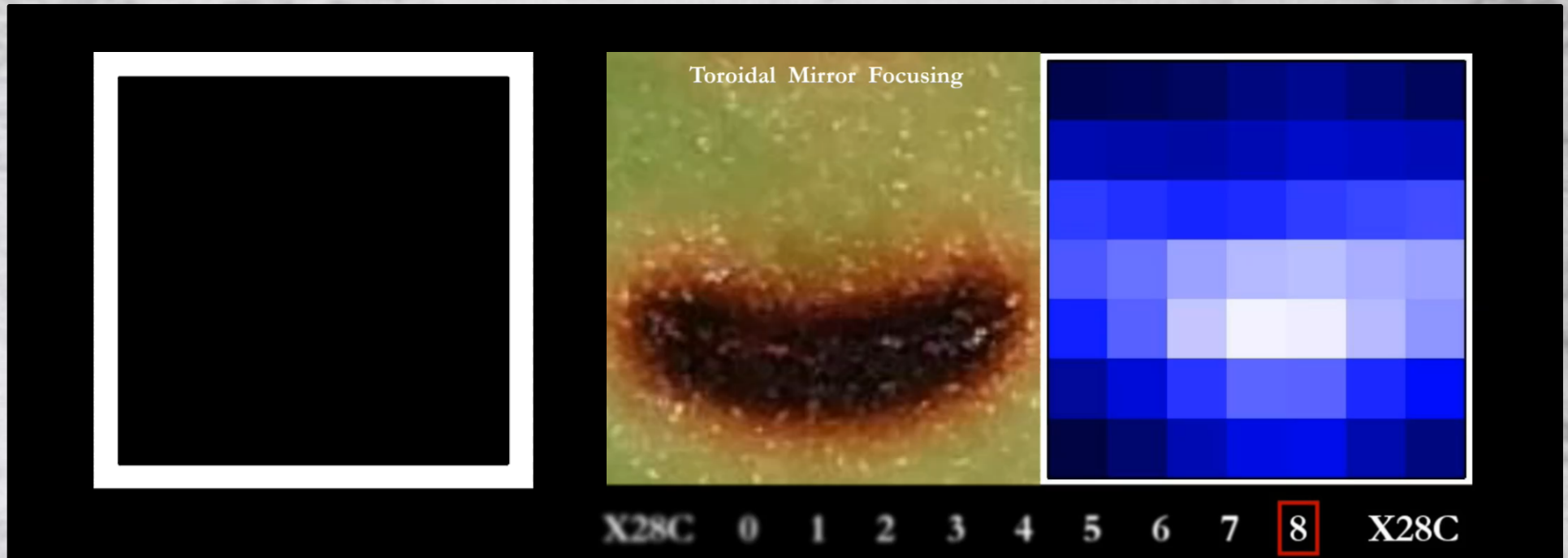
Experimental Setup

- Monochromatic beam tests demonstrate flux linearity from 100 pW to 10 μ W
- Reach >10 W ($>3\text{kW}/\text{cm}^2$) with focused white beam
- Calorimeter, Diode and Ion Chamber
- Nitrogen Enclosure or Vacuum

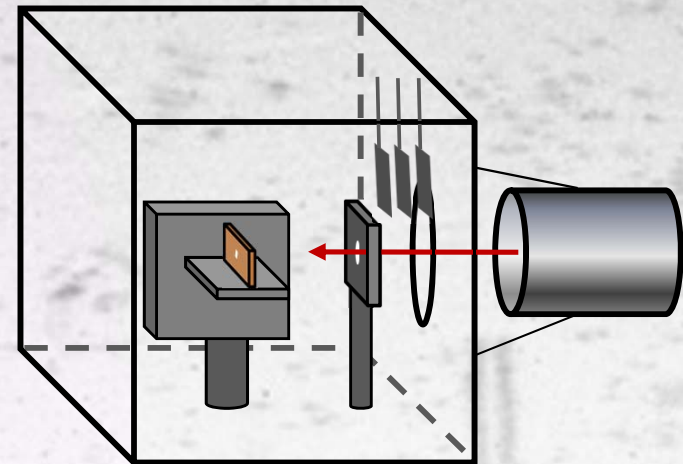
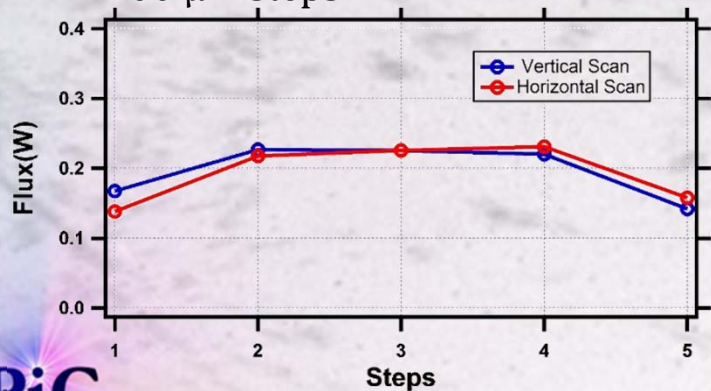


- X-ray port (A)
- Beam defining aperture (B)
- Diamond Detector (C)
- Ion Chamber or Diode (D)
- Calorimeter (E)

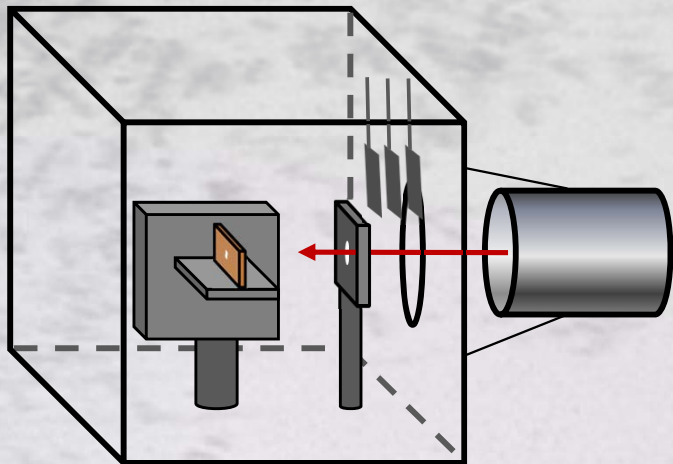
X28C – motion and focusing tests



- Detector Bias: 8V
- Circular aperture 1.6 mm in diameter.
- Scanned horizontally and vertically in 200 μm steps

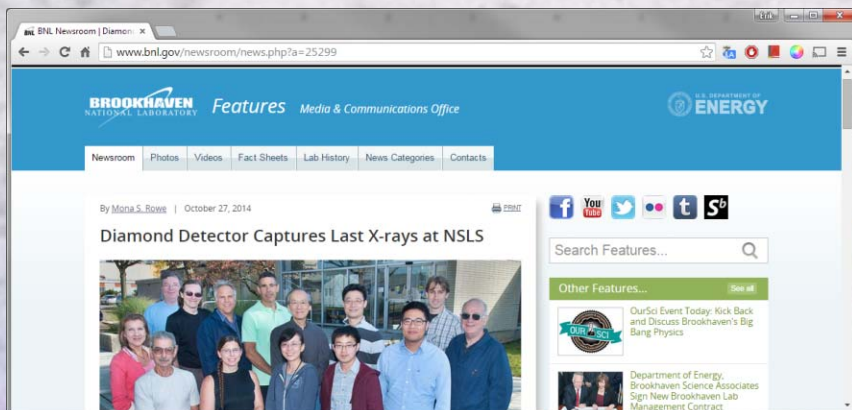


Imaging Testing at X28C



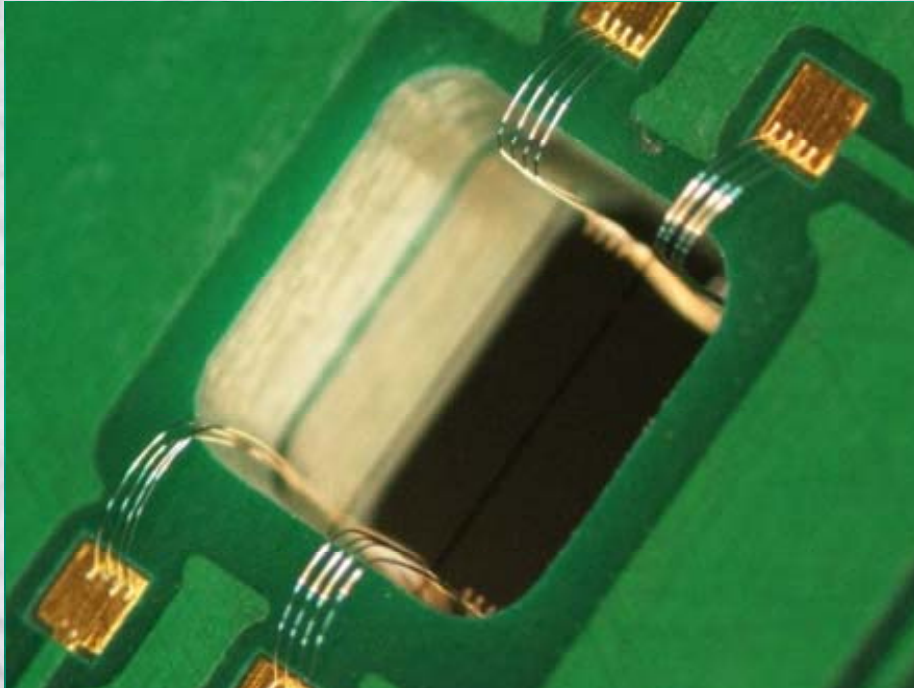
Test Setup

- Detector mounted on x-z stage.
- Pinhole to define beam size
- Filters to change X-ray flux
- Nitrogen enclosure to avoid ozone depletion of contacts



<http://www.bnl.gov/newsroom/news.php?a=25299>

Pixelated Diamond X-ray Detectors



Early Prototypes

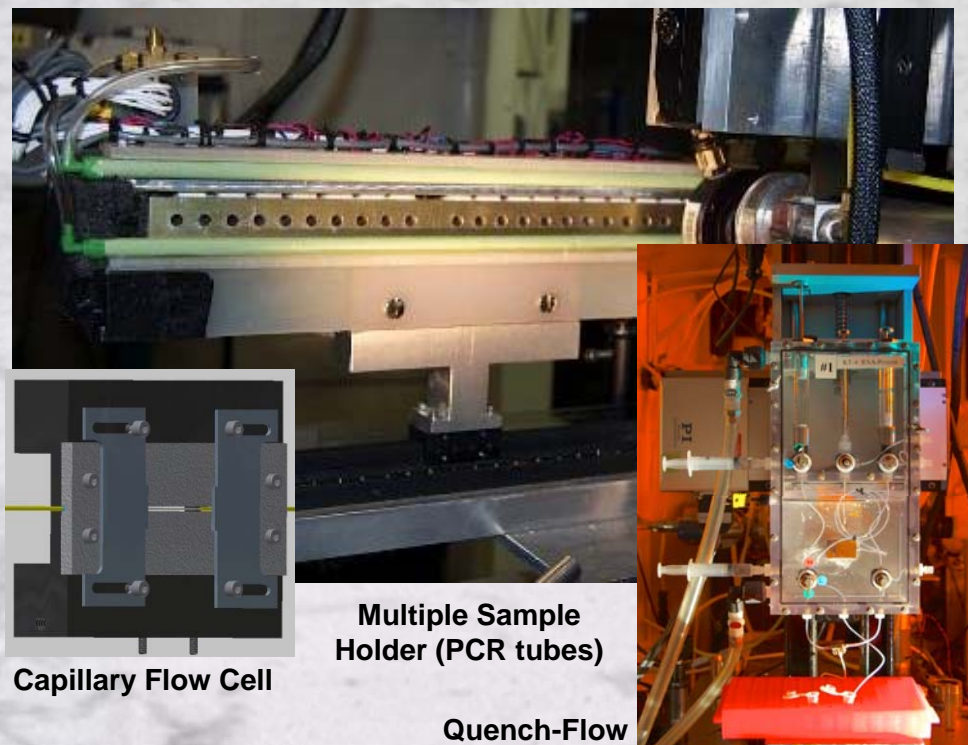
- 16 Pixels – 4 strips each side, 1mm wide
- Standard Pt metallization, Al wirebonds
- Circuit board design, device assembly and wire bonding done at the Instrumentation Division
- Validated concept measuring both position, morphology and flux

Current Prototypes

- Two devices – one using an Element Six diamond and one a IIA Technologies'
- 1024 Pixels – 32 strips each side, pitch: 60 μm and 100 μm
- Diamond thickness: 50 μm
- Full image readout at video rate (limited by USB 2.0 transfer speeds).
- Fully calibrated position, flux and beam shape monitor

Diamond Instrumented Window

Development of a diamond window which will provide position, flux and morphology of high flux x-ray beams while simultaneously acting as the vacuum-air interface



Major Challenges for high flux beamlines

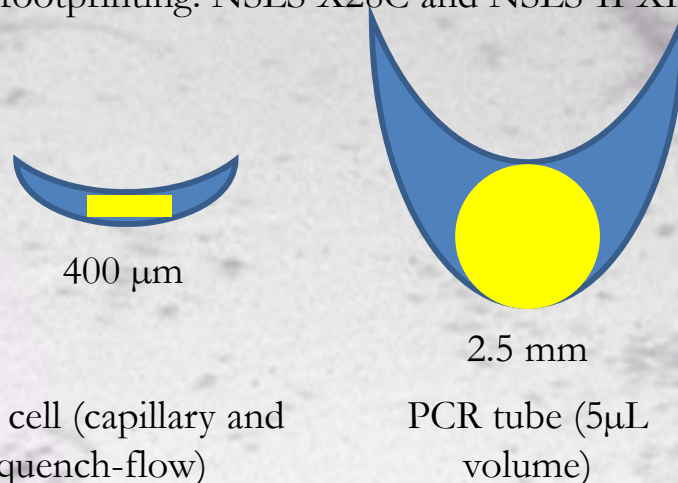
- Heat load management in optics (including Be windows)
- Real-time volumetric measurement of beam properties such as flux, position, and morphology

The beam optimization capabilities of this device will be useful for almost every synchrotron technique!

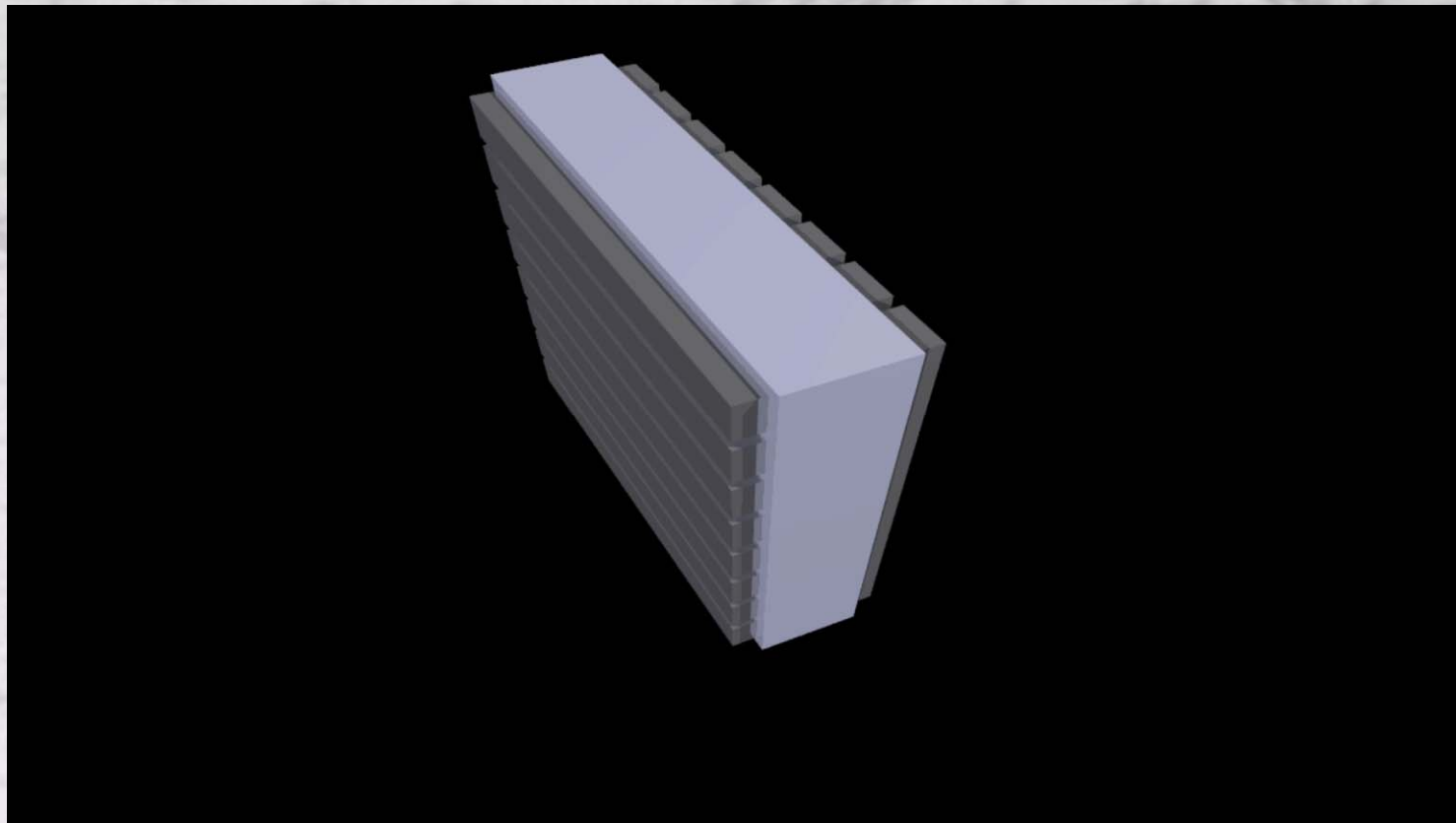
X-ray Footprinting (XFP) at NSLS-II

- Structural biology: X-ray Footprinting for *In Vitro* and *In Vivo* Structural Studies of Biological Macromolecules
- Focused white beam (Expected incident x-ray power: $\sim 100\text{W}$)
- Variety of beam sizes/shapes needed
- Feedback and control systems for optical elements (toroidal focusing mirror) or sample positioning stages

Target Morphologies for the current target application (x-ray footprinting: NSLS X28C and NSLS-II XFP)



Pixelated Diamond Window



readout animation

Pixels are created by metalizing one side of the diamond with horizontal stripes and the other with vertical stripes. As the x-rays pass through the diamond, the induced current is collected in each vertical stripe, while the bias is applied to individual stripes on the other side. This bias is cycled, allowing readout of one line of “pixels” at a time.

Image Readout

- 32 x 32 stripes, yielding 1024 pixels
- Only one row is active at a time minimizing ohmic heat generation.
- Project goal of real time imaging at 1 Hz, currently at 32 Hz
- Up to ~10mA per pixel

Window Fabrication

- The diamond sensor will be brazed to a stainless steel vacuum flange.
- The diamond and electronic interconnects will be protected by a metal mask.
- Heat dissipation provided by water cooling.